

THESIS ON CHEMISTRY AND CHEMICAL ENGINEERING G39

**Role of Specifically Interacting
Solvents in Solvent Swelling of
Kukersite Oil Shale Kerogen**

JELENA HRULJOVA

TUT
PRESS

TALLINN UNIVERSITY OF TECHNOLOGY
Faculty of Chemical and Materials Technology
Department of Chemical Engineering

This dissertation was accepted for the defence of the degree of Doctor of Philosophy in Chemistry and Materials Technology on April 29, 2014

Supervisor: Professor Vahur Oja, Department of Chemical Engineering,
Tallinn University of Technology, Estonia

Opponents: Professor Emeritus Olev Träss, University of Toronto, Canada
Dr. Petri Uusi-Kyyny, Aalto University, Finland

Defence of the thesis: June 17, 2014
Lecture hall VIa-201
Tallinn University of Technology, Ehitajate tee 5, Tallinn

Declaration:

Hereby I declare that this doctoral thesis, my original investigation and achievement, submitted for the doctoral degree at Tallinn University of Technology has not been submitted for doctoral or equivalent academic degree.

Jelena Hruljova



European Union
European Social Fund



Investing in your future

This work has been partially supported by graduate school „Functional materials and technologies“ receiving funding from the European Social Fund under project 1.2.0401.09-0079 in Estonia.

Copyright: Jelena Hruljova, 2014
ISSN 1406-4774
ISBN 978-9949-23-636-7 (publication)
ISBN 978-9949-23-637-4 (PDF)

KEEMIA JA KEEMIASTEHNIKA G39

**Spetsiifiliste vastasmõjudega
lahustite roll kukersiitse põlevkivi
kerogeeni pundumises**

JELENA HRULJOVA

TABLE OF CONTENTS

LIST OF PUBLICATIONS	7
THE AUTHOR'S CONTRIBUTION TO THE PUBLICATIONS	8
INTRODUCTION.....	9
LIST OF ABBREVIATIONS AND SYMBOLS.....	11
1. LITERATURE REVIEW	12
1.1. Oil shale.....	12
1.2. Solvent swelling studies on solid fossil fuels	13
1.2.1. Review of solvent swelling studies on solid fossil fuels	14
1.2.2. Solvent swelling techniques	19
1.2.3. Approaches to the presentation of solvent swelling experimental results.....	20
1.3. DSC in polymer solvent swelling studies.....	21
1.4. DSC application in solid fossil fuel studies.....	23
2. EXPERIMENTAL SECTION	25
2.1. Oil shale samples.....	25
2.1.1. Raw Kukersite oil shale sample	25
2.1.2. Concentrated Kukersite oil shale kerogen sample.....	26
2.1.3. Dictyonema oil shale sample.....	26
2.2. Solvents	26
2.3. Volumetric solvent swelling method.....	28
2.3.1. Basic volumetric solvent swelling procedure.....	29
2.3.2. Swelling in binary solvent mixtures	30
2.4. Swelling extent determination using the DSC-based method	30
2.4.1. Sample preparation.....	31
2.4.2. Experimental procedure.....	31
2.4.3. Methodological background and evaluation.....	32
2.5. GC analysis of supernatant over a swollen kerogen sample	37
3. RESULTS AND DISCUSSION	38
3.1. Oil shale kerogen swelling in pure single solvent	39

3.2. Swelling in binary solvent mixtures over the entire concentration range	43
3.3. The impact of specifically interacting solvent on preswollen kerogen sample.....	45
4. CONCLUSIONS.....	47
REFERENCES.....	49
ACKNOWLEDGEMENTS	56
ABSTRACT.....	57
KOKKUVÕTE.....	59
APPENDIX A: PUBLICATIONS	61
ARTICLE I.....	63
ARTICLE II	71
ARTICLE III.....	85
ARTICLE IV.....	93
ARTICLE V.....	103
APPENDIX B: CURRICULUM VITAE.....	117

LIST OF PUBLICATIONS

Article I:

Savest, N.; **Hruljova, J.**; Oja, V. (2009). Characterization of thermally pretreated Kukersite oil shale using the solvent-swelling technique. – *Energy & Fuels*, 23 (12), 5972–5977.

Article II:

Kilk, K.; Savest, N.; **Hruljova, J.**; Tearo, E.; Kamenev, S.; Oja, V. (2010). Solvent swelling of Dictyonema oil shale. – *Oil Shale*, 27 (1), 26–36.

Article III:

Hruljova, J.; Savest, N.; Oja, V.; Suuberg, E. M. (2013). Kukersite oil shale kerogen solvent swelling in binary mixtures. – *Fuel*, 105, 77–82.

Article IV:

Hruljova, J.; Järvik, O.; Oja, V. (2014) Application of differential scanning calorimetry to study solvent swelling of Kukersite oil shale macromolecular organic matter: A comparison with the fine-grained sample volumetric swelling method. – *Energy & Fuels*, 28 (2), 840–847.

Article V:

Hruljova, J.; Savest, N.; Yanchilin, A.; Oja, V.; Suuberg, E. M. Kukersite oil shale macromolecular organic matter solvent swelling in binary mixtures: impact of specifically interacting solvents. – *Oil Shale*. *Accepted for publication*.

THE AUTHOR'S CONTRIBUTION TO THE PUBLICATIONS

Article I:

Carried out experiments and participated in data processing and results analysis: studies on thermally non-treated samples.

Article II:

Carried out experimental and data processing tasks: studies on non-acid-treated samples.

Article III:

Carried out major aspects of the experimental and data processing tasks and participated in the analysis and discussion of results.

Article IV:

Developed the experimental procedure, carried out experimental and data processing tasks, and assumed a major role in data analysis and article-writing responsibilities.

Article V:

Carried out a major portion of the experimental and data processing work and participated in the analysis and discussion of results.

INTRODUCTION

While the oil shale development industry was previously rather specific to Estonia, international interest in oil shale has increased in recent decades. In Estonia, oil shale is used as a strategic resource for ensuring the energy security of the country. The material provides a source of shale oil and is primarily used to fuel power stations. Kukersite – an Estonian variety of oil shale of industrial interest – is the main object of this research.

Considerable data on oil shale composition, structure, pyrolysis and combustion processes are available in the existing literature. Oil shale is a sedimentary rock consisting of tightly bound minerals and organic materials. The organic matter within oil shale is of particular research interest because it acts as the source of electric, shale oil and chemical industry production. The organic component of oil shale primarily consists of a macromolecular, cross-linked network called kerogen. In addition to other methods, solvent swelling technique has been successfully applied to characterize the macromolecular structure of kerogen from different oil shale deposits across the globe. Solvent swelling experiments allow one to expose kerogen structural changes that occur during maturation and to reveal cross-linking and relaxation processes that emerge during thermal kerogen treatments. Solvent swelling data can be used to determine kerogen solubility parameters and number average molecular weights between cross-links. The latter is a required input parameter for the coal devolatilization model: Functional Group – Depolymerization, Vaporization and Crosslinking model, FG-DVC model (Solomon *et al.*, 1988). This model may potentially be used to modify the oil shale industry.

A prevalent experimental method applied in solid fossil fuel (i.e., oil shale and coal) studies is Green's volumetric solvent swelling method (Green *et al.*, 1984^a), which has proven to be a useful technique for characterizing swelling behavior of fossil fuels. The method involves measuring solvent-induced volume changes in fine-grained samples that are packed into a test tube through centrifugation. The primary disadvantage of this method is that information on possible changes in void volume fractions within the sample bed is not provided during the experiment, and this may lead to quantitatively inaccurate results.

The ongoing study of solvent swelling of Estonian oil shales began in 2006, and the present work represents the second part of this extensive research project. The first phase of the research (Savest, 2010) was largely focused on characterizing structural changes that occur in the kerogen structure under low temperature treatments. Several fundamental questions surrounding Kukersite kerogen solvent swelling principles were, however, not studied in detail. It was found that solvents that can act as electron donors and form hydrogen bonds are more effective swelling agents than other solvents, but the impact of these specific solvent–kerogen interactions was not thoroughly studied. Though valuable qualitative results on Kukersite kerogen cross-link density changes during heat treatments were obtained, the value of the kerogen number average molecular

weight between cross-links estimated via the classical Flory-Rehner and Kovac models (Flory, 1953; Kovac, 1978) using solvent swelling data appeared to be unreasonably low.

Thus, in the present research, in addition to the volumetric test-tube method, a differential scanning calorimetry-based (DSC-based) method was applied. The latter method allowed for an evaluation of the potential effect of void volume fraction change, that may be associated with the common solvent swelling procedure mentioned above, on swelling results. The latter method also yielded more accurate quantitative results. Two methods for the determination of swelling extent (classical volumetric and DSC-based) were used to obtain the most reliable results.

The primary aim of this research was to evaluate the swelling potential of Kukersite kerogen by studying the role of specifically interacting (hydrogen-bonding) solvents. Specifically interacting solvents are examined in detail as they appear to significantly influence Kukersite kerogen swelling and, as a consequence, the estimated kerogen number average molecular weight between cross-links as well.

LIST OF ABBREVIATIONS AND SYMBOLS

AN	Gutmann electron acceptor number
DMF	N,N-dimethylformamide
DN	Gutmann electron donor number
DSC	differential scanning calorimetry
MEK	methyl ethyl ketone
NMP	N-methyl-2-pyrrolidone
PDMS	poly(dimethyl siloxane)
PEA	poly(ethyl acrylate)
TGA	thermogravimetric analysis
h_i	the initial height of the centrifuged dry kerogen sample in a test tube
h_f	the final height of the centrifuged swollen kerogen sample in a test tube
Q	volumetric swelling ratio
Q_{dmmf}	volumetric swelling ratio on dry mineral matter free basis
M_c	number average molecular weights between cross-links
δ	Hildebrand or total solubility parameter

1. LITERATURE REVIEW

1.1. Oil shale

Oil shale is a sedimentary rock consisting of organic and mineral materials. According to one of the latest classifications, oil shale is a solid sedimentary fossil fuel of 50–90% ash content that produces oil yields of 50–250 L/ton (Alpern and Lemos de Sousa, 2002). The major component of the organic portion of oil shale is kerogen – cross-linked macromolecular organic matter that is insoluble in common organic solvents at room temperature but that can absorb solvents and swell. In contrast, the soluble organic material is called bitumen.

Two types of oil shale are found in Estonia – Kukersite and Dictyonema. Kukersite – the main object of the present research – is the oil shale variety of industrial interest due to its higher organic matter content and oil yield. Kukersite oil shale deposits were formed in Middle-Late Ordovician age (Hints et al., 2007). The mineral component of Kukersite oil shale largely consists of carbonates – 58.2% calcite, 12.6% dolomite. It also contains sandy-clay minerals – 11.8% quartz, 10.0% illite, 4.0% feldspar, and 3.4% pyrite (Bondar and Koel, 1998). The organic component of Kukersite oil shale is believed to be formed primarily from extinct marine photosynthetic microorganisms of a single type (Lille, 2003^a).

Kukersite kerogen is a highly aliphatic macromolecule of high oxygen content. A two-dimensional model of Kukersite kerogen was proposed by Lille et al. (2003^b). The designed model of kerogen with an empirical formula of $C_{421}H_{638}O_{44}S_4NCl$ and a mass of 6581 amu is presented in Figure 1. Table 1 shows the typical elemental composition of Kukersite kerogen. Based on H/C and O/C atomic ratios, Kukersite kerogen is classified as Type I/II kerogen according to the van Krevelen diagram (Vandenbroucke and Largeau, 2007). The distribution of oxygen in Kukersite kerogen is presented in Table 2. It is evident that the oxygen component is largely composed of hydroxyl and ether functional groups (approximately 70%). Due to high concentrations of oxygen-containing functional groups that can form hydrogen bonds, a significant number of non-covalent cross-links (mainly hydrogen bonds) can be found in Kukersite kerogen in addition to covalent cross-links.

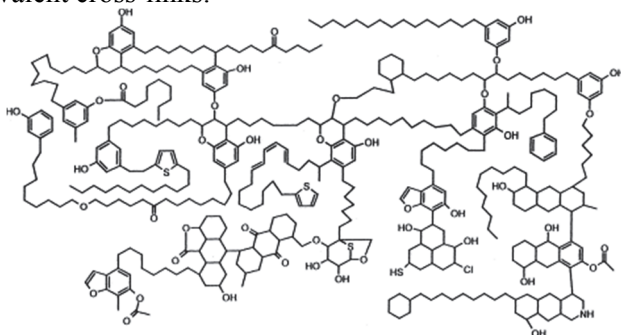


Figure 1. Two-dimensional model of Kukersite oil shale kerogen (Lille et al., 2003^b).

Table 1. Elemental composition of Kukersite kerogen (Urov and Sumberg, 1999).

Element	Average content, wt%	Atomic ratio	
C	77.3		
H	9.8	H/C	1.52
O	10.8	O/C	0.10
N	0.4	N/C	0.004
S	1.7	S/C	0.008

Table 2. Distribution of oxygen in Kukersite kerogen.

Functional group		Average content, % of oxygen	
		(Lille, 2003 ^a)	(Губергриц, 1966)
Hydroxyl	–OH	42	29.4
Ether	–O–	27	40.0
Ester	–OC(=O)–	17	16.0
Carbonyl	>C=O	14	13.3
Carboxyl	–C(=O)OH		1.3
Total		100	100.0

1.2. Solvent swelling studies on solid fossil fuels

The solvent swelling technique is commonly used for the characterization of solid fossil fuel macromolecular structures, i.e., oil shale kerogens and coals. The technique allows for the determination of kerogen and coal solubility parameters and number average molecular weights between cross-links and allows for changes in cross-link densities to be tracked.

At swelling equilibrium, the free energy change for solvent–macromolecule interactions (i.e., solvent dissolution in the macromolecule) is balanced by the elastic restoring force of the macromolecular network (Larsen and Li, 1994). The swelling extent in a system that follows regular solution theory is determined by a match between the material and solvent Hildebrand solubility parameters. The Hildebrand or total solubility parameter is defined as the square root of the cohesive energy density. The swelling maximum should occur in a solvent with a Hildebrand solubility parameter that is equal to the material solubility parameter. The latter is used for the determination of kerogen and coal solubility parameters. However, the swelling limits of cross-linked materials, such as kerogen and coal, are determined by the network cross-link density: a higher cross-link density corresponds with a more rigid network and, as a result, a lower capacity to swell.

Drawing from regular solution theory, which assumes an absence of strong specific interactions between solvents and macromolecules, the Flory-Rehner and Kovac swelling models were developed (Flory, 1953; Kovac, 1978). The Flory-Rehner equation can be applied for the estimation of number average molecular weight between cross-links:

$$M_c = - \frac{V_1 v_2^{1/3} \rho - \frac{1}{2} V_1 v_2 \rho}{\ln(1-v_2) + v_2 + \chi v_2^2} \quad (1)$$

where M_c is the number average molecular weight between cross-links, V_1 is the solvent molar volume, v_2 is the volume fraction of a polymer at equilibrium swelling, ρ is the polymer density, and χ is the Flory-Huggins interaction parameter.

The Flory-Rehner model was adapted by Kovac for studying solvent swelling in coals. The assumption of a Gaussian distribution in the chain lengths between cross-links was removed and a new parameter, N , was introduced. The resultant Kovac's equation is as follows:

$$M_c = - \frac{V_1 v_2^{1/3} \rho + N^{-1} V_1 v_2^{-1/3} \rho}{\ln(1-v_2) + v_2 + \chi v_2^2} \quad (2)$$

where N represents the number of repeating units between cross-link points.

The solvent swelling technique and Flory-Rehner and Kovac swelling models were first broadly applied for the study of coals and later utilized for a number of oil shale kerogens.

1.2.1. Review of solvent swelling studies on solid fossil fuels

Fields of application for solid fossil fuel solvent swelling and example references to the available literature are summarized in Table 3.

Table 3. Fields of application for solid fossil fuel solvent swelling. The author's publications are shown in italic.

Field	Oil shale	Coal
Estimation of number average molecular weight between cross-links	Ballice, 2003 Larsen and Li, 1994 Larsen and Li, 1997 ^c <i>Article II</i>	Ballice, 2004 Larsen and Green, 1985 Larsen and Shawver, 1990 Lucht and Peppas, 1987 ^a
• Model of solid fossil fuel devolatilization		• Solomon et al., 1988
Cross-link density change:		
during maturation	Kelemen et al., 2006 Larsen and Li, 1997 ^c Larsen et al., 2002	
during thermal treatment at prepyrolysis temperature regions	Kilk et al., 2010 <i>Article I</i>	Nomura and Thomas, 1998 Solomon et al., 1990

in pyrolysis residue	Ballice and Larsen, 2003	Nomura and Thomas, 1998 Solomon et al., 1990
during oxidative weathering		Liotta et al., 1983
Determination of solubility parameter	Larsen and Li, 1994 Larsen and Li, 1997 ^c Savest et al., 2007 <i>Article I; Article II</i>	Ballice, 2004 Kirov et al., 1967
Effects of preswelling on extractability and liquefaction		Amemiya et al., 1989 Hu et al., 2000 Kiraz et al., 2004 Larsen et al., 1997 ^a
Fundamental questions:		
Effects of kerogen type or coal rank	Ballice, 2003 Larsen and Li, 1997 ^b Shadle et al., 1989	Larsen and Li, 1997 ^b Shadle et al., 1989
Impacts of specific interactions	<i>Article IV</i>	Green and West, 1986 Suuberg et al., 1994 Szeliga and Marzec, 1983
Effects of solvent steric properties	<i>Article IV</i>	Green and West, 1985 Ndaji and Thomas, 1995
Swelling kinetics		Murata et al., 2008 Otake and Suuberg, 1989; 1997; 1998
Swelling in binary solvent mixtures	<i>Article I</i> <i>Article III</i> <i>Article V</i>	Green and Larsen, 1984 ^b Yun and Suuberg, 1998 Jones and Prawitasar, 1995
Estimation of the number of hydrogen-bond cross-links		Larsen et al., 1996

The major outcomes of published solvent-swelling studies on oil shales across different deposits are presented in Table 4. The kerogens types according to the van Krevelen diagram (Vandenbroucke and Largeau, 2007) and experimental methods applied are also noted. With one exception, all of the studies used the so-called test-tube method. This method is described in detail in section 1.2.2.

Kerogen swelling behaviors can be divided into two major types. Non-polar kerogens interact equally with H-bonding (i.e., hydrogen-bonding) and non-H-bonding solvents, and these systems follow regular solution theory fairly consistently. More polar kerogens with high O/C ratios swell considerably better in H-bonding solvents than in non-H-bonding solvents presumably due to specific interactions between H-bonding solvents and kerogen.

The solvent swelling technique is commonly applied for the determination of kerogen cross-link density and solubility parameters. Table 5 provides number average molecular weights between cross-links estimated through the Flory-

Rehner and Kovac models (see Equations 1 and 2). The literature data on determined Hildebrand solubility parameters of kerogens are listed in Table 6. It is evident that solubility parameter values remain within the range of 19.4–24.3 MPa^{1/2}.

Table 4. The major outcomes of published solvent swelling studies on oil shales.

Oil shale under examination	Solvent swelling method	Major outcomes	Reference
Green River (Type I), Colorado, USA	Volumetric “test-tube method”	Swelling behavior roughly follows regular solution theory and appears to be independent of hydrogen-bonding. High kerogen cross-link density.	Larsen and Li, 1994
Uinta Basin (Type I), USA	Volumetric “test-tube method”	The cross-link density increases at early maturation, remains roughly constant at approximately 20–80% maturation and increases sharply above 80% maturation. The kerogen solubility parameter remains constant during maturation.	Larsen and Li, 1997 ^c
Paris Basin Toarchian kerogen (Type II), France	Volumetric “test-tube method”	The cross-link density increases during maturation while the kerogen solubility parameter remains constant.	Larsen et al., 2002
Rundle (Type I), Australia	Volumetric “test-tube method”	Compared to non-polar Green River kerogen, polar Rundle kerogen swelling is affected to a higher degree by specific interactions between kerogen and H-bonding solvents.	Larsen and Li, 1997 ^b
Rundle (Type I), Australia	Volumetric “test-tube method”	Through examinations of swelling data, a solvent system that effectively moistens and isolates kerogen from aqueous solutions during oil shale enrichment procedures was identified.	Siskin et al., 1989
Göynük (Type I), Beypazari (Type II), Turkey	Volumetric “test-tube method”	Swelling behavior roughly follows regular solution theory. The number average molecular weights between cross-links calculated for Type I and Type II kerogens are found to be only slightly different.	Ballice, 2003
Char obtained through Göynük pyrolysis	Volumetric “test-tube method”	Cross-link density slightly decreases with an increase in the pyrolysis final temperature, and pyrolysis time has a small effect. Regular solution theory is not followed.	Ballice and Larsen, 2003

Fushun (Type II), China	Volumetric “test-tube method”	H-bonding solvents are identified as the most effective swelling agents. Swelling ratios decrease after pyrolysis.	Liu et al., 2011
Draupne (Type II), North Sea	Volumetric “test-tube method”	An extended Flory-Rehner and regular solution theory model framework allows for the prediction of kerogen swelling in solvent mixtures.	Ertas et al., 2006
Marine shales (Type II), hydrogen-rich coaly shales (Type IIIC)	Volumetric “test-tube method”	A successful application of a model framework developed in a previous paper (Ertas et al., 2006) for predicting kerogen-swelling behavior. Lower swelling ratios in Type IIIC kerogens than in Type II kerogens are associated with higher maturation levels. Weak temperature dependence is found for swelling in the range of 30–150°C.	Kelemen et al., 2006
Oil shales from different deposits across the USA	Gravimetric method	Type II kerogen swelling is lower than that of Type I due to higher aromaticity levels and thus more rigid structures. Type I kerogen swelling is more rapid than those of Type II and III.	Shadle and Khan, 1989

Table 5. Number average molecular weights between the cross-links, M_c , of different kerogens.

Oil Shale	Flory-Rehner	Kovac N = 1	Kovac N = 2	Kovac N = 3	Reference
Green River					Larsen and Li, 1994
42% mineral	242	866	620	537	
38% mineral	238	879	630	547	
17% mineral	207	817	590	514	
5.2% mineral	215	808	581	505	
Uinta Basin					Larsen and Li, 1997 ^c
<5% maturation	2000				
20% maturation	1300				
35% maturation	1400				
80% maturation	1400				
100% maturation	300				
Göynük	247	933	678	593	Ballice, 2003
Bey pazari	208	790	576	504	Ballice, 2003
Kukersite	229	861	621	541	Savest, 2010
Dictyonema	83	373	274	241	Article II
Paris Basin	M_c decreases with maturity				Larsen et al., 2002

Table 6. Hildebrand solubility parameters, δ , for oil shale kerogens.

Oil Shale	Total solubility parameter, δ		Method of determination	Reference
	MPa ^{1/2}	(cal/cm ³) ^{1/2}		
Green River (Type I), Colorado, USA	19.4–20.5 19.4	9.5–10 9.5	Solvent swelling. Calculated using Siskin's structure and van Krevelen's method.	Larsen and Li, 1994
Uinta Basin (Type I), USA <i><5% maturation</i> <i>20% maturation</i> <i>35% maturation</i> <i>80% maturation</i> <i>100% maturation</i>	19.4 19.4 20.5 20.5 19.4	9.5 9.5 10 10 9.5	Solvent swelling.	Larsen and Li, 1997 ^c
Rundle (Type I), Australia	20.5 20.3	10 9.9	Solvent swelling. Calculated using Siskin's structure and van Krevelen's method.	Larsen and Li, 1997 ^b
Göynük (Type I), Turkey	20.0–21.1	9.8–10.3	Solvent swelling.	Ballice, 2003
Bey pazari (Type II), Turkey	20.0–21.1	9.8–10.3	Solvent swelling.	Ballice, 2003
Draupne (Type II), North Sea	24.3	11.9	Optimum fit of experimental swelling data and Regular solution theory	Ertas et al., 2006
Marine shales (Type II)	22.5	11.0	Optimum fit of experimental swelling data and Regular solution theory	Kelemen et al., 2006
Hydrogen-rich coaly shales (Type IIIC)	23.3	11.4	Optimum fit of experimental swelling data and Regular solution theory	Kelemen et al., 2006
Kukersite (Type I/II)	22 19.3±1.82	10.8 9.43±0.89	Solvent swelling and Gee's method (Gee, 1943). Atomistic simulation	Savest et al., 2007; <i>Article I</i>
Dictyonema (Type II)	22	10.8	Solvent swelling and Gee's method (Gee, 1943).	<i>Article II</i>
Paris Basin Toarchian kerogen (Type II), France	δ remains constant throughout maturation		Solvent swelling.	Larsen et al., 2002

1.2.2. Solvent swelling techniques

Various experimental methods were developed for the investigation of macromolecular structure solvent swelling behavior in solid fossil fuels. Methods applied for coals can be generally divided into two groups: gravimetric and volumetric techniques. The masses of swollen and dry samples were measured to account for gravimetric methods while the solvent-induced volumetric expansion of the material volume was determined through volumetric methods. The latter approach was applied both for single coal particles and fine-grained bulk samples.

Gravimetric techniques, which followed the vapor sorption method, involved holding a preweighed coal sample in a container that was saturated with solvent vapors at a constant temperature until swelling equilibrium was achieved, after which the sample was removed and reweighed (Lucht and Peppas, 1987^a). Evacuations from absorption containers prior to the vapor sorption experiments were also reported (Shadle and Khan, 1989). Mass changes associated with solvent vapor sorption can be measured progressively by the McBain-Bakr Balance, as was conducted by Nelson et al., who also measured solvents filling the sample pores by comparing the results of gravimetric and pycnometric techniques (Nelson et al., 1980). Rather than vapor, a liquid solvent was used by Kirov et al. as a swelling agent; a coal sample was weighed before immersion into the solvent and then under the equilibrium swelling condition (Kirov et al., 1967). Mayo et al. weighed a centrifuged, swollen coal sample and then a dried coal sample (Mayo et al., 1988).

Volume changes in a single coal particle were traced using a pair of microscopic video cameras, and volume expansion was calculated from particle images recorded over a duration of 24 hours (Gao et al., 1998; Murata et al., 2008). A microscope and laser diffraction particle sizer were used to measure particle size distributions of dry and swollen coal samples and thereby determine average sample volumetric swelling ratios (Turpin et al., 1996). A microdilometer was also used to measure the linear expansion of coal particles immersed in solvent (Cody et al., 1991).

A simple approach for determining the volumetric extent of swelling was applied for fine-grained coal samples in bulk. The approach involved measuring the height of a coal sample bed in a constant diameter test tube, adding solvent to the test tube, shaking the mixture, and, finally, measuring the height of the swollen sample after equilibration (Hombach, 1980; Szeliga and Marzec, 1983; Jones et al., 1991). A special apparatus was constructed by Aida and Squires to measure dynamic solvent swelling in a fine-grained coal bed (Aida and Squires, 1985). Within the apparatus, a coal sample enclosed in a glass tube was separated from the solvent by a stainless steel filter (at the bottom of the tube). Solvent-induced coal swelling was measured by tracking the movement of a sliding piston placed on top of the sample. This design was later adopted by Hall et al. (1992).

The most popular technique is a volumetric solvent swelling approach that was first invented by Liotta et al. (1983). This so-called test-tube method was thoroughly studied, developed, described in detail and presented in comparison to

gravimetric measurements by Green et al. (1984^a). The method developed for coal solvent swelling studies was adapted to the study of oil shale, and the majority of studies focused on oil shale solvent swelling have used this method. Green's test-tube method has been used in over 50 articles on coal and oil shale solvent swelling. To describe the method in brief, a fine-grained, solid fuel sample is placed in a constant diameter test tube, centrifuged and measured with respect to the dry sample's initial height (h_i). A swelling agent is then added in excess, the content of the tube is thoroughly mixed and centrifuged again, and the final height of the swollen sample is measured (h_f). The results using this method are presented as the swelling ratio $Q = h_f/h_i$. This basic procedure was modified in subsequent articles by several authors. Centrifugation times varied from 3 min (Ballice, 2003) to 30 min (Siskin et al., 1989). Different centrifugation rates were also applied: 1000 rpm (Kelemen et al., 2006), 1725 rpm (Green et al., 1984^a), 2000 rpm (Siskin et al., 1989), 3000 rpm (Önal and Akol, 2003), 4400 rpm (Xie et al., 2000), and 7500 rpm (Otake and Suuberg, 1997; Suuberg et al., 1994). In the procedure reported by Larsen et al., the tube was tapped by hand on a hard surface and repeatedly centrifuged to reach a minimum sample height (Larsen and Shawver, 1990; Larsen et al., 2002). In addition, different sample sizes, solvent volumes and test tube dimensions were used. Equilibration durations and mixing intensities were also varied. With respect to the considerable extraction effect, supernatant over a sample bed could also be replaced with fresh solvent.

As will be discussed later, results obtained through the test-tube method can be sensitive to sample compaction levels within the test tube. To eliminate this effect, another method was developed and applied in the present research in addition to the classical test-tube method. The differential scanning calorimetry (DSC) technique is widely used in a variety of fields such as fossil fuels and polymer solvent swelling research. The DSC-based method for the determination of kerogen swelling extents was developed based on the literature data reviewed in sections 1.3 and 1.4.

1.2.3. Approaches to the presentation of solvent swelling experimental results

Solvent swelling studies on solid fossil fuels often use the equilibrium volumetric swelling ratio, Q , as a measure of swelling extent. The swelling ratio is defined as the ratio of the swollen sample volume to the dry sample volume. The swollen sample volume is the sum of the initial dry material volume and the solvent volume absorbed by the material (Green et al., 1984^a). Based on these definitions, the macromolecular material volume fraction (i.e., kerogen or coal) at equilibrium swelling is typically calculated as $1/Q$. The latter is required for the calculation of number average molecular weights between crosslinks in the polymer network using the Flory-Rehner (Flory, 1953) and Kovac (1978) equations.

In contrast to the volumetric swelling ratio, the equilibrium gravimetric swelling ratio is used in the gravimetric experimental method (Green et al., 1984^a;

Shadle and Khan, 1989). The gravimetric swelling ratio or weight ratio is defined as the ratio of the swollen sample weight to the dry sample weight.

Another approach to expressing the swelling power of different solvents involves calculating the solvent molar uptake from the volumetric swelling ratio Q . Suuberg et al. (1994) presented swelling data as the molar uptake of solvent per unit volume of coal, which was calculated as $(Q - 1)/V_s$, where V_s is the molar volume of the solvent. Green and West (1985; 1986) calculated solvent molar uptake per gram of coal according to the equation: $(\text{moles absorbed} / \text{g of coal}) = (Q - 1)/(\rho V_s)$, where ρ is the coal density and V_s is the solvent molar volume.

A common method used for the graphical presentation of swelling results involves plotting the volumetric swelling ratio against the Hildebrand solubility parameter for the solvents used. According to regular solution theory, a bell-shaped curve with the maximum at the solubility parameter that is equal to the kerogen (or coal) solubility parameter is expected for systems that follow regular solution theory.

To evaluate the influence of specific solvent properties on swelling extent, swelling results can be plotted against corresponding property values. The influence of solvent molar volumes has been examined using this method (Green and West, 1985; 1986). Additionally, to evaluate the role of solvent electron donor-acceptor properties, solvent Gutmann electron donor and acceptor numbers and their combinations were placed on an abscissa axis (Szeliga and Marzec, 1983; Suuberg et al., 1994). The Gutmann electron donor number, DN, is defined as the molar enthalpy value for the reaction between the donor-solvent and SbCl_5 as a reference acceptor in a 10^{-3} M solution of dichloroethane (Gutmann, 1978). The Gutmann electron acceptor number (AN) is defined as a dimensionless number that is related to the NMR chemical shift of ^{31}P in Et_3PO in the particular solvent, with hexane used as a reference solvent on one hand, and $\text{Et}_3\text{PO}-\text{SbCl}_5$ in 1,2-dichloroethane on the other, to which the acceptor numbers of 0 and 100 are assigned, respectively (Gutmann, 1978).

1.3. DSC in polymer solvent swelling studies

Polymer solvent swelling represents one of the polymer science fields in which DSC is applied. DSC experiments have shown that organic solvent in a swollen polymer-solvent system exists in two states: so-called freezable and non-freezable solvent (Honiball et al., 1988; Yang et al., 2000; Salmerón Sánchez et al., 2002; Lue and Yang, 2005; Wu and McKenna, 2008). It should be noted here that in the present study, physical gels and water-polymer systems are not considered.

Freezable solvent can be detected using DSC as it undergoes crystallization and melting processes. Non-freezable solvent forms a homogeneous phase with a polymer structure (Yang et al., 2000; Salmerón Sánchez et al., 2002), which does not contribute to the crystallization and subsequent melting of free solvent. This solvent type is also referred to as bound solvent, which denotes the existence of polymer-solvent interactions that prevent solvent molecules from forming solvent

crystals (Klein and Guenet, 1989). The solvation of polymer network chains and the presence of a “non-frozen benzene area” were also shown through nuclear magnetic resonance studies (Oikawa and Murakami, 1984).

Representative DSC studies focusing on swollen polymers are summarized in Table 7. The behavior of the freezable solvent (also referred to as free or bulk solvent) was in several cases identical to the behavior of the pure solvent – the melting point and fusion enthalpy of the freezable state solvent remained constant regardless the solvent content in the system and were in a reasonably good agreement with the pure solvent properties. However, in a number of cases, deviations relative to pure solvent melting peaks were detected using DSC thermograms. These deviations include, for example, the appearance of several endothermic peaks and peak shoulders, tailing in the melting peak, and the presence of major differences between pure solvent and swollen polymer solvent melting temperatures (ΔT). These deviations indicate that freezable solvent (or part of it) may be somehow involved in polymer–solvent interactions and that it may therefore differ from the bulk state of pure solvent. It has been suggested that the peak tail is attributed to the melting of small confined crystals within the gel (Wu and McKenna, 2008).

Table 7. Literature data from DSC experiments conducted on swollen polymer samples.

Polymer	Solvent	Max swelling	Non-freezable solvent		Freezable solvent thermogram	Reference
		$\frac{g_{solv}}{g_{polymer}}$	$\frac{g_{solv}}{g_{polymer}}$			
PDMS*	water		0	const	one melting peak, close to the melting temperature of the bulk solvent	Yoshikawa et al., 1991 and 1992
	methanol		0.1			
	2-propanol		0.47			
	1-butanol	1.36	1.02			
	1-pentanol	1	0.14			
	1-octanol	0.82	0			
PDMS	water	0.0045	0.0045	not const	solvent at equilibrium swelling is non-freezable	Yang et al., 2000
	ethanol	0.021	0.021			
	benzyl alcohol	0.013	0.013			
	ethyl acetate	0.917	0.301-0.348	two melting peaks		
	benzene	1.14	0.41-0.59	two melting peaks		

	cyclohexane	1.28	0.142-0.143		one melting peak, $\Delta T = 0.9 \pm 5.7^\circ\text{C}$	
	hexane	1.99	0.37-0.69		one melting peak, $\Delta T = 6 \pm 6.4^\circ\text{C}$	
PDMS	cyclohexane	1.08-3.81	0.32	const	peak tailing	Wu and McKenna, 2008
	cyclooctane	0.88-3.07		not const	two melting peaks	
PDMS	water	0.01	0.00021	const	$\Delta T = 0.02^\circ\text{C}$	Lue and Yang, 2005
	benzene	1.06	0.17		$\Delta T = 2.03^\circ\text{C}$	
	toluene	0.88	0.2		$\Delta T = 0.56^\circ\text{C}$	
	xylene	1	0.22		$\Delta T = 1.04^\circ\text{C}$	
	cyclohexane	1.3	0.54		$\Delta T = 2.05^\circ\text{C}$	
PEA**	benzene	1.17	<0.43	not const	two endothermic peaks separated by an exothermic peak	Salmerón Sánchez et al., 2002
PEA	p-xylene	5.67	0.1-0.16	const	shoulder on the high temperature side of the melting peak	Stathopoulos et al., 2011

* PDMS: poly(dimethyl siloxane)

** PEA: poly(ethyl acrylate)

The DSC method has been applied in very few cases for the investigation of solvent physical states in swollen coals (Hall and Larsen, 1993) and coal extracts (Suzuki et al., 2004), and these studies are described in section 1.4.

1.4. DSC application in solid fossil fuel studies

Differential Scanning Calorimetry (DSC) is a commonly used tool in the fields of coal and oil shale research. DSC has been applied in studies on coal pyrolysis and chemical reactivity under inert (Mahajan et al., 1976; Hefta et al., 1986; Janikowski and Stenberg, 1989), hydrogen (Mahajan et al., 1977; Hefta et al., 1986; Janikowski and Stenberg, 1989), and carbon monoxide (Hefta et al., 1986) atmospheric conditions. DSC has been used in investigations of second-order phase transitions in coals and coal-solvent systems (Lucht et al., 1987^b; Hall and Larsen, 1991; Antxustegi et al., 1993). Suuberg et al. applied a combination of DSC and solvent swelling techniques to classify changes in coal macromolecular structures that occur at elevated temperatures or as a result of solvent treatment (Yun and Suuberg, 1993; Takanohashi et al., 1999). The proposed method for characterizing irreversible heat effects on coal structures using DSC thermograms

was also applied in later studies (Shui and Wang, 2010). A method for estimating the strength distribution of non-covalent bonds in coal using DSC and TG (thermogravimetry) was presented by Miura et al. (1994). Another application of DSC was suggested by Rajeshwar et al. (1981), through which a linear correlation between decomposition enthalpies of organic matter and oil yields for Green River formation oil shale was found, and it was suggested that DSC may be used for rapid resource evaluations of oil shale deposits.

DSC has also been used to investigate the physical state of solvent in swollen coals and coal extracts. Hall and Larsen (1993) showed that NMP (N-methyl-2-pyrrolidone) that is bound in swollen coal behaves as part of a network structure while excess NMP behaves as a free solvent during DSC experiments. The results of thermogravimetric analysis (TGA) confirm that large quantities of NMP in coal exist in a bound state. The authors thus suggested a formation of metastable coal–NMP gel with an NMP content of approximately 65 wt% as an explanation for the absence of an NMP melting peak for swollen samples of respective composition. Identical DSC experiments using pyridine also showed the existence of non-freezable solvent in pyridine-swollen coal. DSC was later used to examine coal extract solutions (Suzuki et al., 2004). It was found that significant levels of non-freezable NMP exist in mixtures of NMP and coal extract, forming a coal extract–NMP gel.

2. EXPERIMENTAL SECTION

2.1. Oil shale samples

The particle size of the oil shale samples was under 100 μm . The samples were dried at 105–110°C for one hour in an air atmosphere and then cooled in a desiccator shortly before the swelling experiments were conducted.

- *Soluble fraction influence on swelling.* Studies examining partially cross-linked high-density polyethylene have shown that the presence of unattached polymer chains (sol macromolecules) within both the swollen polymer network (gel fraction) and solvent outside of the swollen network has a significant effect on swelling extent (Nandi and Winter, 2005). The effect of solubles on coal solvent swelling was also observed – the degree of coal swelling decreased with an increase in dissolved material concentration in the surrounding solution (Larsen et al., 1991). However, the effects of solubles may be neglected in the case of small sol macromolecule concentrations (Nandi and Winter, 2005). Thus, inasmuch as extraction yields of Kukersite and Dictyonema are known to represent no more than 2.5% of organic matter (Kogerman, 1931; Koel et al., 2001), we can neglect the influence of the sol fraction and assume that Kukersite and Dictyonema kerogen solvent swelling strictly involves cross-linked polymer network swelling.
- *Mineral matter effect.* Clay minerals are known to swell in organic solvents (Graber and Mingelgrin, 1994). Thus, clay-rich oil shales, such as Dictyonema, should be treated to remove clay minerals or to transform the minerals into nonswellable forms. Other minerals are considered to be inert during swelling experiments, and the volume occupied by inorganic materials can be taken into account to obtain the swelling ratio on a dry mineral matter free basis:

$$Q_{dmmf} = \frac{Q-y}{1-y} \quad (3)$$

where $y = \frac{x_{min} \cdot \rho_{org}}{x_{org} \cdot \rho_{min} + x_{min} \cdot \rho_{org}}$, x_{min} is the mass fraction of mineral matter, x_{org} is the mass fraction of kerogen, ρ_{org} is the kerogen density, and ρ_{min} is the mineral matter density.

2.1.1. Raw Kukersite oil shale sample

The organic content of the Kukersite oil shale sample was 38 wt% (ash – 46.5 wt%; carbonate CO_2 – 16.5 wt%; SO_4^{2-} in ash – 3.2 wt%). The sample was characterized by an elemental composition on a total sample basis (wt%): C – 36.3, H – 4.1, N – 1.1.

2.1.2. Concentrated Kukersite oil shale kerogen sample

The oil shale kerogen sample used in this work was obtained from Estonian Kukersite oil shale using a flotation technique (Koch et al., 1973). The sample possessed an organic matter content of 91%. The organic matter elemental composition of the concentrated kerogen sample was as follows (wt%): C – 73.3, H – 8.8, N – 1.6, O+S – 16.3 (by difference). These values were determined using an Exeter Analytical model CE440 elemental analyzer.

The apparent density of the kerogen sample, determined by measuring the mass and volume of water displaced by the known mass kerogen sample (ГОСТ 2160-92), was 1.23 g/cm³. This value of apparent density, which was determined using the so-called pycnometer method, was used as the kerogen sample true density for this study.

2.1.3. Dictyonema oil shale sample

The Dictyonema oil shale sample elemental analysis results were as follows (wt%): C – 6.7, H – 0.9, N – 0.3, residue – 92.1. The organic content was 13 wt%. Acid treatment with HF was used to convert original shale minerals to nonswellable forms because Dictyonema is known to contain significant proportions of clay minerals that can swell or shrink in organic solvents. The HF treatment procedure is described in the Materials and Methods section of Article II. No original clay minerals were observed after the acid treatment, and the only original mineral that remained was pyrite. The most prevalent mineral that formed was hieratite (K₂SiF₆). The organic content of the acid-treated sample was 25 wt%.

2.2. Solvents

Organic solvents used in the solvent swelling experiments are listed in Table 8. All solvents were of reagent grade and were thus used without further purification. Specific solvent properties of interest in this study are shown in Table 8, including Hildebrand or the total solubility parameter (Belmares et al., 2004; Karger and Snyder, 1978; Larsen and Li, 1994; Smallwood, 1996; Zeng et al., 2007) and Gutmann electron donor and acceptor numbers – DN and AN (Behbehani et al., 2001; Gutmann, 1978; Linert, 2001; Malavolta et al., 2002). The electron donor and acceptor properties of the solvents were quantitatively expressed as Gutmann electron donor and acceptor numbers due to the widespread use of the Gutmann's scale (Gutmann, 1978) in the field of solid fossil fuel solvent swelling. This scale was also chosen due to the availability of data on solvents used in the present work.

Table 8. Solvents used for the oil shale kerogen solvent swelling experiments (see text for references).

Solvent	Hildebrand solubility parameter	Electron donor number (DN)	Electron acceptor number (AN)
	MPa ^{1/2}	–	–
Acetone	20.3	17	12.5
Acetonitrile	24.3	14.1	19.3
Aniline	21.1	33.3	28.8
Benzene	18.8	0.1	8.2
Benzyl alcohol	24.8	23.0	36.8
Cyclohexanol	20.3		
Dichloromethane	20.3	1.0	20.4
Diethylamine	16.4	50.0	9.4
Diethyl ether	15.6	19.2	3.9
DMF ^a	24.5	26.6	16.0
Ethanol	26.0	20.0	37.1
Hexane	14.7	0.0	0.0
MEK ^b	19.0	14.3	12.9
Methanol	29.7	19.0	41.3
1-Methylnaphthalene	20.3		
Nitrobenzene	20.5	4.4	14.8
Nitroethane	22.7	5.0	15.8
Nitromethane	26.0	2.7	20.5
NMP ^c	23.1	27.3	13.3
n-Propanol	24.5	19.8	37.7
o-Xylene	18.0	4.8 ^d	2.4 ^d
Propylamine	18.2	55.5 ^e	4.8 ^e
Pyridine	21.9	33.1	14.2
Tetrahydrofuran	18.6	20.0	8.0
Tetralin	19.4		
Toluene	18.2	0.1	3.3

^a DMF – N,N-dimethylformamide

^b MEK – methyl ethyl ketone

^c NMP – N-methyl-2-pyrrolidone

^d calculated values for xylene isomer mixture

^e Ethylamine DN and AN values are used for propylamine

Additional data on the solvents used in the DSC experiments are presented in Table 9: molar mass (NIST Database), density measured at 22°C, calculated molar volume, and melting point (NIST Database). The densities of the solvents used were verified using an Anton Paar DMA 5000M density meter at 22°C (mean ambient laboratory temperature). The molar volumes of the solvents were calculated as $V_M = M/\rho$, where M is the molar mass and ρ is the solvent density.

Table 9. Solvents used in the swelling experiments according to the DSC-based measurement procedure (see text for references).

Solvent	Molar mass	Density (22°C)	Molar volume	Melting point
	g/mol	g/cm ³	cm ³ /mol	°C
Acetonitrile	41.05	0.780	52.6	-45
Aniline	93.13	1.020	91.3	-6
Benzene	78.11	0.877	89.1	5.5
Benzyl alcohol	108.14	1.044	103.6	-16
Diethylamine	73.14	0.702	104.2	-50
DMF ^a	73.09	0.949	77.0	-60
NMP ^b	99.13	1.031	96.2	-24
o-Xylene	106.17	0.878	120.9	-25
Propylamine	59.11	0.714	82.8	-83
Pyridine	79.10	0.981	80.6	-41
Tetralin	132.20	0.967	136.7	-35

^a DMF – N,N-dimethylformamide

^b NMP – N-methyl-2-pyrrolidone

The solvent set was compiled based on the following principles. First, the presence of both non-polar and specifically interacting hydrogen-bonding solvents as a fundamental difference in the swelling powers of these two solvent groups was expected. Second, a wide range of DN and AN should exist to precisely determine the influence of solvent electron donor-acceptor properties on swelling. The range of total solvent solubility parameters should then cover the predicted kerogen solubility parameter region. Finally, solvent selection was restricted by the experimental procedures. Namely, the density of a solvent should not be equal to or greater than the density of the oil shale sample, as this would prevent a uniformly tight packed bed of oil shale particles from forming in the centrifugation process. Additionally, if the phase following the volumetric swelling experiment involves conducting a DSC measurement, the solvent melting point should be high enough to ensure solvent crystallization during a DSC run. Thus, the lowest possible solvent melting point used in the DSC experiments was set through the DSC cooling system parameters.

2.3. Volumetric solvent swelling method

According to a so-called *test-tube method*, the volumetric swelling extent of the fine-grained sample is determined by measuring the height of a sample contained in a test tube both before and after it equilibrates in a solvent. Centrifugation in a standard laboratory centrifuge is conducted to compact the fine-grained particle bed prior to taking measurements. No strictly standardized experimental procedure has been developed for this method, and the initial procedure developed by Green (Green et al., 1984^a) has been modified by other researchers in numerous

ways (an overview is given in section 1.2.2). The procedure has also been modified in the present research to achieve higher degrees of measurement repeatability.

The swelling-describing parameter calculations based on the results obtained from the test-tube-type volumetric swelling experiments are valid only if the void volume fraction in the swollen sample is equal to that of the dry sample or, in other words, if the sample packing density has not changed. A detailed discussion on this topic is presented in Article IV (p. 840) based on equations summarized in Table 1, Article IV. Unfortunately, the test-tube volumetric swelling experiments do not provide any insight into possible changes in void volume fraction levels.

2.3.1. Basic volumetric solvent swelling procedure

A fine-grained kerogen sample (up to 0.25 g) was placed into a test tube with a constant diameter of 5 mm, centrifuged, mixed with the solvent and centrifuged again. Three rounds of centrifugation cycling were carried out, and the heights of the dry and swollen kerogen samples were measured using a caliper ruler after the third centrifugation. The height of the swollen kerogen sample was remeasured after 24 hours and referenced in calculations as the final sample height. All of the experiments were conducted at room temperature. This modified volumetric test-tube method is described in detail in Article III, section 2.2 and Article IV, section 2.3.

The swelling extent was determined by the swelling ratio, Q , which was defined as the ratio of the swollen sample volume to the dry sample volume and calculated as the ratio of the sample final height to the sample initial height: $Q = h_f/h_i$. An illustration of the test tubes containing the samples is presented in Figure 2.

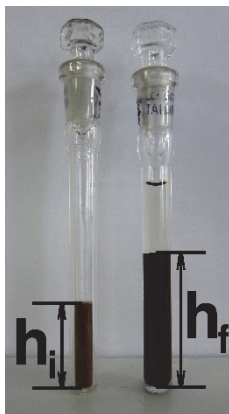


Figure 2. Dry kerogen sample in a test tube (left) and swollen kerogen sample in a test tube (right), both after centrifugation. The initial and final sample heights are marked as h_i and h_f , respectively.

2.3.2. Swelling in binary solvent mixtures

Swelling experiments with binary solvent mixtures were conducted using three different experimental procedures:

- According to the first procedure, solvent mixtures of desired composition were prepared and used as swelling agents following the basic volumetric test-tube method described in section 2.3.1. This procedure is used in Article III.
- The second procedure involved a two-stage swelling process. For the first phase, the kerogen sample was swollen to equilibrium in one solvent (the complete procedure for single solvent swelling was followed). For the second phase, the solvent above the swollen kerogen sample was removed from the tube using a syringe, and another solvent was added until the desired solvent mixture composition was obtained. The system was thoroughly mixed, centrifuged, and left to swell to a new equilibrium state. The final height of the sample was then measured. The second solvent was added in excess so that both solvents were in considerable excess relative to the kerogen single solvent uptake. The final solvent mixture composition was determined gravimetrically by measuring the mass of the first solvent remained in a test tube after the first stage and the mass of the second solvent placed in a test tube during the second stage. This procedure is used in Article V.
- For the third procedure, the second solvent was added in a dropwise fashion over several phases. After the first stage, a small dose of the second solvent was added to the test tube (using a micropipette). The system was then mixed and centrifuged, and the swelling equilibrium was measured after 48 hours. This sequence was repeated until a maximum second solvent concentration of approximately 5 mol% (on the basis of the total solvent amount present in the system) was reached. This procedure is used in Article V.

For all of the above procedures, the swelling ratio, Q , was calculated as the ratio of the final height to the initial height of the sample: $Q = h_f/h_i$.

2.4. Swelling extent determination using the DSC-based method

Kerogen solvent swelling was conducted in accordance with the volumetric solvent swelling procedure reported in section 2.3.1. The swelling extent was then determined not directly from volumetric measurements but using a method that is based on differential scanning calorimetry (DSC). The DSC-based method was developed during the present research to determine the validity of a constant void volume fraction silent assumption for a packed bed sample and to evaluate the reliability of the results obtained through the test-tube method. The DSC-based method is described in detail in Article IV.

2.4.1. *Sample preparation*

- Solvent swelling in a *single solvent* was performed as described in section 2.3.1.
- The swelling procedure for *solvent mixtures* was similar to the two-stage procedures described in section 2.3.2. A non-polar solvent (benzene, o-xylene or tetralin) was used as the first solvent (or base solvent), and a strong H-bonding solvent (NMP) was used as the second solvent. After equilibrium swelling was achieved in the base solvent, an exact amount of NMP was added (with a micropipette) into the test tube until the desired NMP to kerogen mass ratio was reached. The content of the test tube was then thoroughly mixed. To ensure full NMP molecules access to the kerogen structure, the content of the test tube was mixed several times over a minimum of 24 hours (up to 6 days were needed for tetralin mixture equilibration). The test tube was then centrifuged to precipitate kerogen particles and produce a swollen kerogen sample packed bed.

Supernatant over the swollen kerogen bed was removed from the test tube. The test tube was then weighed to determine the mass of the solvent that was present in the swollen kerogen bed. A total of 7–28 mg of sample material from the swollen packed bed was transferred from the test tube to a preweighed aluminum DSC pan, hermetically sealed, and weighed.

2.4.2. *Experimental procedure*

A differential scanning calorimeter NETZSCH DSC 204 HP Phoenix equipped with a CC200L liquid nitrogen cooling system was used. Experiments were performed under atmospheric pressure with an inert gas (nitrogen) flow rate of 40 mL/min and using 40- μ L hermetically sealable standard aluminum DSC pans. Prior to each measurement, the DSC cell was purged with inert gas (nitrogen) for at least 10 min.

Hermetically sealed samples were cooled to -120°C at a rate of $10^{\circ}\text{C}/\text{min}$, equilibrated at -120°C for 10 min, and then heated to 40°C at the same rate. After the DSC run had been completed, the pan lid was pierced, and the pan containing the swollen kerogen sample was placed in a vacuum oven to determine the kerogen mass and overall solvent mass in the DSC sample. The sample was dried at 110°C until a constant weight was obtained (until the weight loss reached less than 0.2% within 1 h). The overall mass of the solvent in the DSC sample was calculated as the difference between the initial mass of the DSC sample and the dry kerogen mass. The mass of the solvent bound to the kerogen structure was calculated as the difference between the solvent overall mass and the free solvent mass. The free solvent mass was obtained from the melting peak area of the swollen sample, assuming that enthalpy from free solvent fusion in the swollen kerogen sample is equal to that of pure solvent. The solvent mass uptake was then

calculated as the ratio of the bound solvent mass to the dry kerogen mass. For the experiments on binary solvent mixtures, calculations were carried out using the enthalpy of fusion for base solvents due to low NMP concentrations present in these mixtures.

The results are presented in terms of the solvent mass uptake, molar uptake and volumetric swelling ratio. Void volume fractions in a dry and swollen kerogen sample packed bed were calculated from a combination of volumetric swelling measurements and DSC data. All of the calculation details are presented in Article IV, section 2.5.

The solvent melting peak onset temperature on a DSC thermogram was reported as the bulk solvent melting temperature.

2.4.3. Methodological background and evaluation

DSC studies on swollen polymers and coals (reviewed in sections 1.3 and 1.4) have cited the existence of a non-freezable portion of the solvent that forms a homogeneous phase with a swollen macromolecular structure. In the present research, DSC experiments conducted on the samples consisted of swollen kerogen particles and solvent between the particles (as it occurs in a test tube during volumetric swelling experiments), i.e., within the equilibrated system of swollen kerogen and surrounding solvent (this type of system is therefore not completely identical to polymers systems). The results show that the volume of solvent undergoing crystallization and melting processes during a DSC run is less than the total solvent amount present in the sample (see Figure 1 and a related discussion in section 3.1, Article IV for more details). Analogous to what was found for polymers and coals, a portion of solvent is bound to the kerogen macromolecule and therefore does not contribute to crystallization and subsequent melting processes. This was found to be true for both non-polar and hydrogen-bonding solvents.

It is evident that surrounding solvent volumes (solvent between the particles) participate in freezing and melting processes. The assumption that this is the only type of freezable solvent present in the sample was evaluated through an analysis of DSC thermograms. Regardless of the polarity and hydrogen-bonding properties of the solvents, only one endotherm was found in the heating curve and one exotherm was identified in the cooling curve, and neither overlapping peaks nor significant peak tailing were observed. These observations support the view that the DSC-detected melting process strictly corresponds to the melting of the bulk solvent between swollen kerogen particles. In addition, the low swelling extents of kerogen indicate the existence of a tightly cross-linked kerogen structure, suggesting that absorbed solvent molecules should be more or less influenced by the kerogen macromolecular structure (for a comparison, see literature data on polymer solvent uptakes and bound solvents provided in Table 7, section 1.3). In this case, sufficiently large crystallizable domains of absorbed solvent molecules similar to those observed in polymers may not develop.

A series of experiments was performed to evaluate the DSC-determined constancy of the non-freezable bound solvent for each solvent–kerogen system. The evaluation was based on examinations and comparisons of original samples (obtained directly from volumetric test-tube-type experiments) and partially dried samples. Three solvents (DMF, propylamine, and benzene) were used. Figure 3 demonstrates that the calculated amount of non-freezable solvent is roughly constant for each solvent–kerogen system above the “bound solvent limit”, i.e., independent of the total solvent amount present (see solid points in Figure 3). This result shows that variations in solvent volumes between particles do not cause changes in calculated non-freezable solvent amounts.

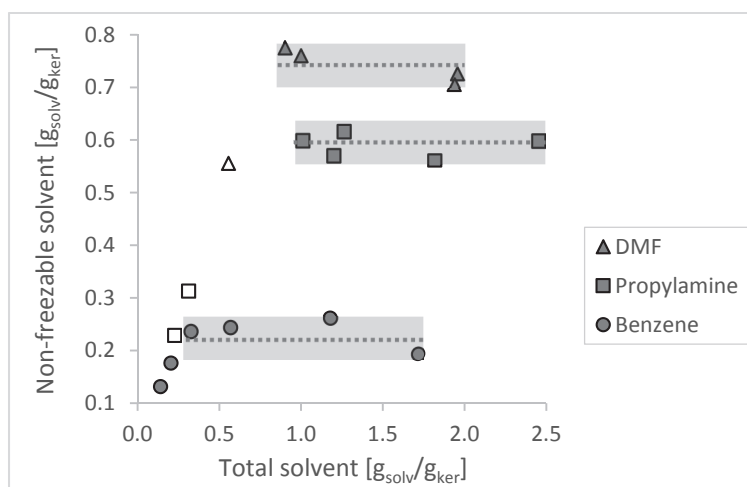


Figure 3. Calculated non-freezable solvent content in the swollen kerogen sample vs. the gravimetrically determined total solvent content in the sample. Unshaded points correspond to experiments with no solvent melting peak – the solvent present in the sample is non-freezable. Thick, shaded lines show the average standard deviations obtained from calculated non-freezable solvent results, and dashed lines denote average values.

For samples with total solvent contents below the “bound solvent limit,” no solvent melting peak was found to be present (see unshaded points for DMF and propylamine in Figure 3), i.e., the solvent present in the sample appears to be non-freezable, as was expected. However, this region is outside of the scope of the present research and is therefore not studied in detail.

This point is merely highlighted to show that in the case of low total benzene concentrations (below a calculated non-freezable solvent limit of 0.22 g_{soliv}/g_{ker}), a minor free solvent melting peak was still present (Figure 3). This corresponds to only ~0.1 mg of solvent (analogous to 0.01–0.03 grams of solvent per gram of kerogen), which is lower than the average standard deviation of our experimental results and thus could not significantly affect the conclusion above. This anomaly

may also be caused by experimental complications: 1) samples were obtained after partial solvent evaporation and thus could be not homogeneous due to non-uniform evaporation; and 2) in the sealed DSC crucible, a portion of solvent likely evaporated (estimated at up to 0.03 mg) and existed in a gaseous state before the experiments began and thus undergone phase transitions during the DSC run.

In Figure 3, the sample with a total DMF content of $0.9 \text{ g}_{\text{solv}}/\text{g}_{\text{ker}}$ and calculated non-freezable solvent limit of $0.75 \text{ g}_{\text{solv}}/\text{g}_{\text{ker}}$ was obtained by removing solvent between particles using a filter paper. According to observations made by eye, nearly all of the solvent between the particles was removed, and the majority of solvent left in the sample was absorbed by kerogen (of course, minor deposits of solvent remained between the particles because the drying procedure was fairly rough, causing some particles to remain fused together; particle-related cavities and capillaries may also have been present). Regardless of this fact, the experiment resulted in no more than 0.15 g/g of freezable solvent that could have been absorbed by kerogen (less than 17% of the total solvent in the system), indicating that the solvent absorbed by kerogen should be primarily non-freezable or bound.

In conclusion, the DSC-based method can be used to determine the amount of solvent that is present in a kerogen–solvent mixture that does not contribute to the swelling process (solvent between kerogen particles) or to the resulting quantity of non-freezable bound solvent (the solvent that causes swelling and is therefore also quantitatively measurable using the test-tube volumetric swelling technique).

Correlations between results obtained using the DSC-based and volumetric test-tube methods

To facilitate the discussion of research results (presented in section 3), a number of specific details on data obtained via DSC and volumetric measurements are presented here. The swelling extent of concentrated Kukersite kerogen obtained through the DSC-based technique was greater than the value produced via test-tube volumetric measurements in almost all of the cases with the exception of tetralin (roughly equal results were obtained for swelling in tetralin). Numerical results expressed as the swelling ratio and solvent mass uptake are reported in Table 3, Article IV.

It is important to note here that all test-tube method calculations are carried out under an assumption of constant void volume fraction. The possibility of void volume fraction reduction (i.e., compression of the sample bed) may have been detected in Dictyonema swelling studies (Article II) that showed an apparent shrinking of Dictyonema kerogen, which may be an experimental artifact from differences in the packing densities of dry and swollen sample beds. It was proposed and confirmed through DSC-based technique that Kukersite kerogen swelling results obtained via the test-tube method appear to be understated due to the elevated packing density (or in other words, decreased void volume fraction) of the swollen sample compared to the dry sample packing density. Relative data

and a discussion are presented in Article IV (see Table 3, Figure 2 and the discussion provided in section 3.2, Article IV).

A correlation exists between the void volume fraction change and the amount of solvent absorbed by kerogen (see Figure 2, Article IV), which may be attributable to the increased flexibility of kerogen particles under solvent impact. Similar to the process of void volume fraction change, the difference in swelling ratios obtained using the two different techniques also correlates empirically with the amount of solvent absorbed by kerogen (see Figure 3, Article IV). Both correlations follow approximately exponential trends. For the latter, a rough empirical equation can be proposed: $Q_{DSC} - Q_{t.tube} = 0.0011 \cdot e^{3.1021 \cdot Q_{DSC}}$.

It should be noted that while the outcomes and conclusions presented in this section may be valid for a specific combination of volumetric experimental procedure (described in section 2.3.1) and material under study (Kukersite oil shale kerogen), they may be not characteristic of the test-tube-type volumetric swelling technique in general.

Application of the DSC-based method for the study of kerogen swollen in non-specifically interacting solvent mixed with a small quantity of high DN solvent

Another swelling system studied through the DSC-based method was that of concentrated Kukersite kerogen swollen in non-polar solvent (benzene, o-xylene or tetralin) with small quantities of specifically interacting solvent (NMP). Solvent swelling studies of coal (Larsen et al., 1996) have shown that small volumes of specifically interacting solvent (with high DN) used in combination with non-specifically interacting solvent can be readily absorbed by coal to the extent that no high DN solvent remains at the solvent bulk phase. Assuming that kerogen would exhibit similar trends, the DSC-based method for single-solvent swelling can also be applied to systems of this type because a melting process detectable by DSC would refer to a bulk phase that is presumably consistent with only one solvent, i.e., a non-specifically interacting solvent. The presence of NMP in bulk phase and thus the validity of the assumption can be traced by DSC as described below.

The solvent melting temperature is responsive to the presence of dissolved substances. In the context of the present study, NMP is a solute, and the presence of NMP in bulk phase should result in a decline of the solvent melting peak onset temperature seen in the DSC thermogram. The plot of solvent melting peak onset temperatures against the quantity of NMP added to kerogen that is preswollen in benzene is shown in Figure 4. Analogous trends were found for samples that were preswollen in o-xylene and tetralin. The results show that the solvent melting peak onset temperature remains nearly constant until a limit of approximately 0.7–0.8 mmol of NMP added per 1 gram of kerogen. The latter suggests the presence of only a small amount of NMP (or even the absence of NMP) in bulk phase. At higher initial NMP concentrations, melting temperatures significantly differ from

the pure benzene, o-xylene and tetralin identifying presence of NMP in bulk phase.

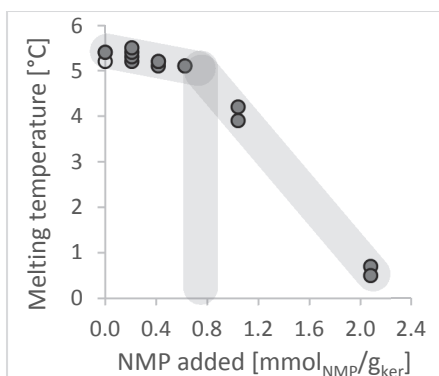


Figure 4. Solvent melting peak onset temperature vs. amount of NMP added to kerogen preswollen in benzene. The unshaded point denotes the pure benzene melting temperature.

To evaluate DSC performance from this perspective, the supernatants over the swollen kerogen sample bed of selected test tubes were analyzed via gas chromatograph (GC), and exact concentrations of NMP in the supernatant (in bulk phase) were determined (for experimental procedure see section 2.5). On the other hand, concentrations of NMP in bulk phase were determined from solvent melting temperatures measured via DSC. For the latter, a set of tetralin–NMP mixtures of different concentrations was prepared, respective melting temperatures were measured by DSC and a linear correlation between the NMP concentration and melting temperature was obtained. Because the difference between pure tetralin melting points and tetralin deposits between kerogen particles (in the case of swelling in a single solvent) was 0.3°C, this effect was accounted for, and the linear correlation line was shifted upwards by 0.3°C. The results of the two techniques were in reasonably good agreement until NMP concentrations reached approximately 1.4 mol%. At higher NMP concentrations, NMP concentrations in supernatant that were determined from bulk solvent melting temperatures measured by DSC appeared to be slightly underestimated. Analogous control examinations were performed using selected xylene- and benzene-preswollen samples with low NMP concentrations. It should be noted here that although the results from both techniques were interpreted as concentrations in bulk phase, the analyzed samples differed; GC analysis was performed using supernatant while DSC thermograms referred to the free solvent present between swollen kerogen particles from the kerogen packed bed.

It can be concluded that until a certain amount of NMP is added (0.7–0.8 mmol_{NMP}/g_{ker}), most NMP traces are absorbed by kerogen, resulting in the presence of primarily base solvent in bulk phase. The present study also shows

that the DSC-based method can be used to determine the swelling extent of kerogen in non-polar solvent–NMP mixtures with low NMP concentrations. Moreover, the presence of NMP in bulk phase can be detected directly from the bulk solvent melting peak onset temperature drop shown by the DSC thermogram.

2.5. GC analysis of supernatant over a swollen kerogen sample

After volumetric swelling experiments with binary solvent mixtures were completed, supernatants from some selected samples were analyzed via GC-MSD: Agilent Technologies 7890A Gas Chromatograph equipped with an Agilent 5975C Mass Spectrometer Detector. Supernatant volumes of 0.1–0.4 ml were diluted in dichloromethane and strained through a membrane filter with a pore size of 0.20 μm to remove floating kerogen particles that may have been present in the supernatant. The solution was analyzed via GC-MSD, and the amount of NMP present in the supernatant was calculated. The amount of NMP absorbed by kerogen was calculated as the difference between the total NMP added to a test tube and the NMP present in the supernatant, i.e., remaining in bulk phase. The amount of base solvent absorbed by kerogen was calculated as the difference between the amount of total absorbed solvent determined via DSC and the amount of absorbed NMP determined via GC.

3. RESULTS AND DISCUSSION

Oil shale kerogen solvent swelling was conducted according to volumetric solvent swelling procedures (see section 2.3). The swelling extent was determined either through volumetric measurements or through the use of DSC-based method (see section 2.4). The swelling systems studied in the present research are listed in Table 10. The table includes information on the systems examined, measurements applied, oil shale samples analyzed, number of solvents used, and articles in which results are reported.

Table 10. Swelling systems studied through the present research.

Swelling system under investigation	Types of measurements used to determine the swelling extent	
	Volumetric	DSC-based
Swelling in a single solvent	<ul style="list-style-type: none"> • Kukersite kerogen, 91% org. matter. 11 solvents. Article IV. • Kukersite raw oil shale, 38% org. matter. 22 solvents. Article I. • Dictyonema, concentrated through HF treatment, 25% org. matter. 22 solvents. Article II. • Dictyonema raw oil shale, 15% org. matter. 20 solvents. 	<ul style="list-style-type: none"> • Kukersite kerogen, 91% org. matter. 11 solvents. Article IV.
Swelling in binary solvent mixtures with broad concentration ranges	<ul style="list-style-type: none"> • Kukersite kerogen, 91% org. matter. 11 pre-prepared mixtures. Article III. • Kukersite kerogen, 91% org. matter. 3 mixtures, 2-step procedure. Article V. • Kukersite raw oil shale, 38% org. matter. 2 pre-prepared mixtures. Article I. 	
A small amount of specifically interacting solvent added to kerogen that is preswollen in non-specifically interacting (base) solvent	<ul style="list-style-type: none"> • Kukersite kerogen, 91% org. matter. 1 base solvent, 2 specifically interacting solvents. Article V. 	<ul style="list-style-type: none"> • Kukersite kerogen, 91% org. matter. 3 base solvents, 1 specifically interacting solvent.

3.1. Oil shale kerogen swelling in pure single solvent

Solvent swelling processes in Kukersite and Dictyonema oil shales that are submerged in single solvents have been studied (see Table 10). The test-tube method was applied for all of the samples, and the DSC-based method was applied for the concentrated Kukersite kerogen sample.

The main object of the research was Kukersite oil shale kerogen. Swelling ratios obtained for raw Kukersite oil shale are presented in Article I and replotted in Figure 5 for more convenient handling. Concentrated Kukersite kerogen swelling ratios determined using both methods are presented in Figure 4, Article IV as a function of the solubility parameter.

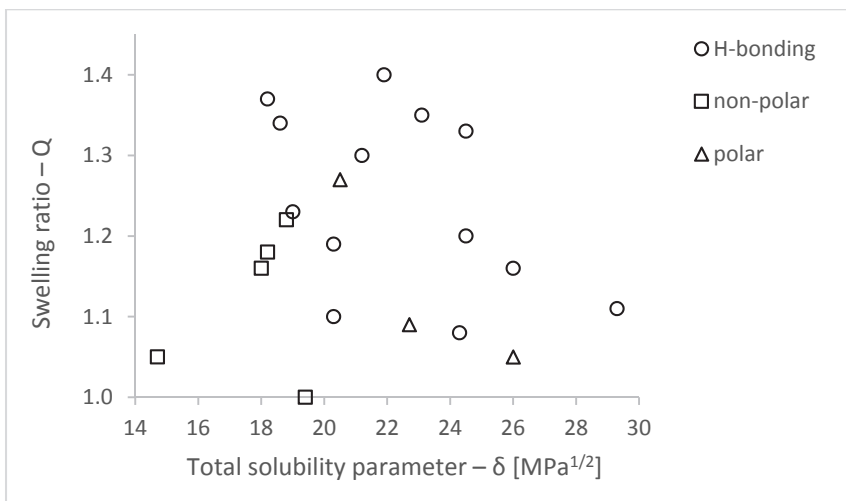


Figure 5. Swelling ratio of raw Kukersite oil shale vs. solvent total solubility parameter (data from Article I). Solvent types are specified in the legend.

Swelling ratio plotting against solvent solubility parameters is the most common method used to present kerogen solvent swelling results. According to regular solution theory, a bell-shaped curve with the maximum at a solubility parameter being equal to the kerogen solubility parameter is expected. This type of behavior is roughly followed in Green River (Larsen and Li, 1994) and Paris Basin Toarcian (Larsen et al., 2002) oil shale kerogens. For this type of system, the solubility parameter for kerogen can be determined from the position of the curve maximum, and the number average molecular weight between cross-links can be predicted through the application of the Flory-Rehner and Kovac equations (see Equations 1 and 2).

However, no bell-shaped curve can be identified in the Kukersite swelling plot (see Figure 5). To eliminate the potential effect of mineral matter, a concentrated kerogen sample was selected for further research. As has already been noted,

results obtained from the test-tube method can be affected by centrifugation process. To avoid the effect of potential compressibility in the sample, the DSC-based method was applied to determine the swelling ratios of concentrated Kukersite kerogen. As is shown in Figure 4, Article IV, no bell-shaped curve is obtained for concentrated Kukersite kerogen regardless of the method used to obtain measurements. It is evident that the swelling extent of Kukersite kerogen is not determined by the match of kerogen and solvent solubility parameters. Thus, the following discussion aims to move away from a focus on “ideal” behavior determined by regular solution theory. The following analysis of results and outline of subsequent research reveal factors that affect Kukersite swelling and explore the swelling potential of this kerogen type.

It was found that the primary factor that determines kerogen swellability is the presence of kerogen–solvent specific interactions. Figure 5 shows that non-H-bonding (polar and non-polar) solvents are not efficient swelling agents for Kukersite kerogen, and only H-bonding (or specifically interacting) solvents are able to cause extended swelling. Specifically interacting solvents have the capacity to form solvent–kerogen hydrogen bonds and thus can disrupt kerogen–kerogen hydrogen bonds that serve as non-covalent cross-links. This reduced level of effective cross-link density results in the development of higher swelling ratios with specifically interacting (H-bonding) solvents. The same conclusion can be drawn for the results of concentrated Kukersite kerogen swelling irrespective of experimental methods used (the volumetric test-tube method or the DSC-based method).

However, a more detailed comparison of the results obtained from the two different methods shows one specific difference. For test-tube measurements, swelling ratios of specifically interacting solvents with high DN remain at the same level, while for DSC-based measurements, the scatter is significant (see Figure 4, Article IV). It was proposed that swelling in high DN solvents may be additionally affected by the size of solvents molecules (or solvent molar volume). Molar solvent uptake decrease with an increase of solvent molar volume can be observed in Figure 6, Article IV. The data are replotted in Figure 6 to show the effect of solvent molar volume on the swelling ratio. Thus, it can be concluded that a relatively large solvent molecule size can act as a limiting factor in swelling processes due to steric restrictions characteristic of the tightly cross-linked Kukersite kerogen structure. In the case of test-tube measurements, this effect is likely hidden as a result of sample bed compression during centrifugation.

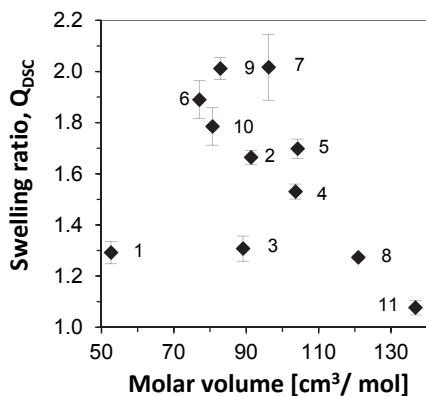


Figure 6. Kukersite kerogen swelling ratio obtained using the DSC method as a function of solvent molar volume. Data from Article IV are replotted. See Table 2 in Article IV to identify solvents by reference numbers.

The swelling ratios of strictly non-specifically interacting solvents also failed to generate a bell-shaped curve. An unexpected swelling result was obtained for tetralin – no observable swelling of Kukersite oil shale occurred when the sample was submerged in this solvent ($Q=1$, see Figure 5). Extremely low levels of swelling in concentrated Kukersite kerogen submerged in tetralin was detected through both volumetric and DSC-based methods – swelling levels were less than 10% of maximum swelling value for Kukersite kerogen. A comparison between the swelling results of non-polar solvents with similar solubility parameters shows that solvents with relatively large molar volumes, such as tetralin, are considerably less effective at inducing Kukersite kerogen swelling than solvents with smaller molar volumes such as benzene and o-xylene, which caused kerogen to swell to approximately 30% of its maximum swelling value. To provide a comparison, oil shales from other deposits – Green River and Rundle oil shales – show another form of swelling behavior. Namely, no fundamental differences are found between swelling behaviors that occur in solvents of large molecule sizes (tetralin and 1-methylnaphthalene) and those that occur in small molecule sizes (benzene, o-xylene and toluene). For Green River, swelling in non-polar solvents resulted in swelling to 52–80% of maximum extent with variations depending on the oil shale demineralization procedure applied (Larsen and Li, 1994). The rundle kerogen swelling extent in non-polar solvents of large molar volumes is slightly higher than value for solvents of small molar volumes – 76–82% vs. 59–68% of maximum swelling, respectively (Larsen and Li, 1997^b). It can be proposed that relatively large tetralin molecules may not be able penetrate into the tightly cross-linked Kukersite kerogen structure, resulting in low Kukersite swelling in tetralin. An additional study was performed to examine this phenomenon in greater detail, which is discussed at length in section 3.3. The experiment involved adding a small amount of specifically interacting solvent (which is able to reduce kerogen cross-link density) to kerogen samples that were preswollen in non-polar solvents

of differing molar volumes. The promotion of cross-link density reduction and network relaxation through the addition of small volumes of H-bonding solvent was previously shown by Larsen et al. in reference to coal (Larsen et al., 1996).

Referring again to the kerogen solubility parameter, the solubility parameters of Kukersite (Article I) and Dictyonema (Article II) kerogens were proposed largely for illustrative purposes using the Gee method (Gee, 1943; Yagi et al., 1992), which is based on regular solution theory. The obtained value was 22.0 MPa^{1/2} for both kerogens. Uncertainty in the obtained results was comparable to the entire solubility parameter range for the solvents studied due to the absence of a clear relationship between the swelling ratio and solvent solubility parameter. The results obtained through the DSC-based method did not suggest a different value or provide a more accurate measure of the Kukersite kerogen solubility parameter.

The number average molecular weight between crosslinks for Kukersite kerogen was estimated through the classical Flory-Rehner and Kovac models (see Equations 1 and 2) using swelling ratios obtained through the volumetric test-tube method and the DSC-based method. The results of the calculations are reported in Table 11. It is observable that with all other parameters in the equation held constant, higher swelling ratios obtained from the DSC-based method resulted in a higher average M_c value. The different results obtained from the volumetric measurements for the two different oil shale samples are attributable to the presumably lower compressibility of the swollen raw oil shale sample during centrifugation as a result of its higher mineral matter content.

Table 11. Kukersite kerogen number average molecular weight between cross-links estimated by the Flory-Rehner and Kovac models based on swelling data obtained through the volumetric test-tube method and the DSC-based method with all other parameters in the equations held constant. The solvent sets used were identical.

Sample	Experimental method	Flory-Rehner	Kovac N = 1	Kovac N = 2	Kovac N = 3
Raw oil shale, 38% org.matter	Volumetric	184	688	493	428
Kerogen, 91% org.matter	Volumetric	123	463	335	292
Kerogen, 91% org.matter	DSC-based	312	1178	825	708

It should be noted that the M_c calculation for Kukersite kerogen may also be affected by the fact that swelling in different solvents corresponds with swelling that occurs in a network of different effective cross-link densities depending on the capacity for the solvent to disrupt non-covalent cross-links. Additionally, the swelling extent may be affected by solvent molecule size, resulting in unreasonably low swelling ratios for solvents with large molecule sizes and thus low apparent M_c values.

The M_c values calculated using the Flory-Rehner equation are clearly underestimated given that the number average molecular weight of Kukersite kerogen pyrolysis products obtained through direct pyrolysis with a Field Ionization Mass Spectrometer (FIMS) was significantly higher – approximately 400 amu (Oja, 2013). Assuming that the latter value denotes the mass of the “average repeating structural unit” and applying Kovac’s equation with 1, 2 and 3 average repeating structural units between cross-links ($N = 1, 2, 3$), it is evident that the most reliable value (~ 800 amu) was obtained through Kovac’s equation with $N = 2$ and when DSC-based swelling data were used.

3.2. Swelling in binary solvent mixtures over the entire concentration range

It was established in section 3.1 that specific interactions between solvents and kerogen play an important role in Kukersite kerogen solvent swelling. To better understand the influence of specific interactions and to evaluate possibilities for increasing the swelling extent of Kukersite, binary solvent mixtures were used in concentrated Kukersite kerogen swelling experiments. Volumetric test-tube-type solvent swelling experiments were performed using 11 pre-prepared binary solvent mixtures composed from 9 different organic solvents. The results are presented and discussed in detail in Article III.

The mixtures can be divided into four specific groups based on the combination electron donor-acceptor properties of the two solvents. The characteristic swelling behaviors for Kukersite kerogen were observed for each group. The first behavior type refers to mixtures consisting of solvents with high DN (NMP, propylamine, pyridine) and solvents with low (benzene, nitromethane) or medium (diethyl ether) electron donor numbers. Low fractions (10–20 mol%) of high DN solvent are sufficient to increase swelling to approximately the same levels observed for the pure high DN solvents. However, further a high DN solvent concentration increase does not increase swelling, i.e., the swelling ratio remains roughly constant. Exactly the same trend was obtained for raw Kukersite oil shale swelling in a benzene–NMP mixture (Article I). This type of behavior was previously reported for Illinois No. 6 coal submerged in chlorobenzene–pyridine mixtures (Green and Larsen, 1984^b) and is attributed to the ability of a specifically interacting solvent to disrupt cross-links in kerogen, permitting the non-specifically interacting solvent to more effectively induce swelling in the structure. This phenomenon was examined and discussed in greater detail in section 3.3.

The second behavior type is characteristic of mixtures of non-polar solvents (benzene) and solvents with weaker electron donor values than the high DN solvents mentioned above (n-propanol). The swelling ratios of benzene–propanol mixtures are higher than those obtained from these two single solvents, and the swelling maximum occurs in a roughly equimolar mixture composition. However, the obtained level is lower than the swelling exhibited in high DN solvents. This

behavior appears to be a result of two effects: solubility parameter matching between kerogen and swelling agents (i.e., solvent mixtures) and the ability of n-propanol to disrupt kerogen–kerogen non-covalent cross-links. A roughly analogous trend was observed in the case of raw Kukersite oil shale swelling, however, the swelling maximum shifted towards higher benzene concentrations (Article I).

The third behavior type was observed in mixtures with a strong electron donor (NMP, propylamine) and a strong electron acceptor (n-propanol). Swelling ratios decrease proportionally with an increase in n-propanol concentrations. It can be proposed that the electron-donating properties of NMP and propylamine are limited by n-propanol, which acts as an electron acceptor for high DN solvents.

Finally, solvent mixtures that include two non-polar solvents (benzene–toluene) or two strong electron-donating solvents (NMP–pyridine) did not induce significantly higher levels of swelling than single solvents.

A two-stage experimental procedure was carried out for Kukersite kerogen solvent swelling to provide a point of comparison (Article V). Three solvent mixtures from the first three characteristic groups described above were examined. Following this procedure, swelling was first carried out using one solvent, and then a limited amount of another solvent was added to obtain the required solvent mixture composition. Although some deviations between the results of the two techniques (pre-prepared mixtures or subsequent adding of two solvents) were observed, similar characteristic swelling trends were obtained through both procedures. A more detailed discussion on this study is presented in Article V, section 3.1.

The results of the study confirm the primary role of specific interactions in Kukersite kerogen solvent swelling. Though solvent–kerogen solubility parameter match may have some influence on the swelling extent, it is of secondary importance. The highest swelling ratios were obtained for mixtures with broad solubility parameter ranges: 17–25 MPa^{1/2}.

The results show that the highest swelling ratios obtained from the binary mixtures are not significantly greater than swelling ratios obtained from the pure high DN solvents (such as pyridine, NMP and propylamine). Thus, the limited swelling extent for high DN solvents cannot be increased significantly through the use of binary solvent mixtures.

To determine the possible influence of sample compression during centrifugation, the correlation equation for the test-tube and DSC-based results (presented in section 2.4.3) was used to correct the obtained volumetric swelling ratios. Given the roughness of the correlation, the corrected values are presented mainly for illustrative purposes (see Figures 2–4, Article V). The results suggest that the corrected swelling ratios do not indicate significant differences in qualitative swelling trends.

3.3. The impact of specifically interacting solvent on preswollen kerogen sample

Studies on Kukersite kerogen swelling in binary solvent mixtures have shown that the presence of a relatively small amount of specifically interacting (strong electron-donating) solvent such as NMP in combination with non-specifically interacting solvent results in a drastic swelling ratio increase (see section 3.2). To more precisely study the impact of specifically interacting solvent, very small amounts of high DN solvent (0.2–2.1 mmol of solvent per gram of dry kerogen) were added to kerogen that was preswollen in non-specifically interacting non-polar solvent (referred to as base solvent in the context of the present research topic). The swelling extents for the benzene–NMP, o-xylene–NMP and tetralin–NMP mixtures were determined using the DSC-based method; volumetric measurements in a test tube were performed with toluene–NMP and toluene–propylamine mixtures.

The results show that swelling ratios increase with an increasing amount of NMP added to kerogen that is preswollen in base solvent (see Figure 5 in Article V and Figure 7). For all solvent pairs, the initial increase in the swelling ratio with the addition of NMP is too high to be attributed solely to NMP absorption observable through the slope of the NMP-induced swelling line (see figures: a slanting line denotes the swelling ratio increase that is associated with a total absorption of NMP under conditions in which base solvent absorption levels remain constant.). It is evident that base solvent uptake increases with the addition of NMP. This confirms the existence of kerogen–kerogen non-covalent cross-links that can be disrupted by strong electron-donating solvents through the formation of solvent–kerogen hydrogen-bonds. The reduced cross-link density that results allows kerogen to contain a higher level of non-specifically interacting solvent. The increase in base solvent uptake was also confirmed via the GC analysis of supernatant over swollen kerogen beds (for experimental details, see section 2.5).

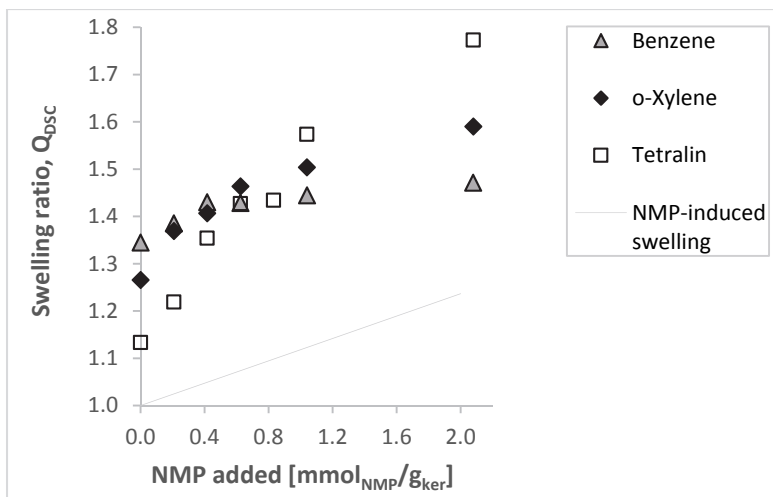


Figure 7. Swelling ratio calculated from DSC data vs. amount of NMP added to a preswollen system. Base solvents are specified in the legend.

As was already highlighted in section 2.4.3, the solvent melting peak onset temperature demonstrates that before the limiting amount of NMP was added to the preswollen system (0.7–0.8 mmol_{NMP}/g_{ker}), the majority of the NMP volume had been absorbed by kerogen. To be more precise, NMP absorption in tetralin-based mixtures of this range accounted for 75–90% of the initial NMP content, as determined by GC. As a point of comparison, the total (or 100%) absorption of high DN solvent (pyridine) by coal was reported by Larsen (Larsen et al., 1996).

It is also critical to note that no fundamental differences between the results obtained for NMP–toluene and propylamine–toluene mixtures were identified (see Figure 5, Article V). It can be concluded that the swelling process is determined by the ability of a solvent to specifically interact with kerogen (both NMP and propylamine are strong electron donors) and not by the specific selection of high DN solvent.

Another objective of the present study was to examine the hypothesis proposed in section 3.1, which predicted that the low swelling ratio for tetralin compared to benzene and o-xylene may be attributed to the relatively large molecule size of tetralin, which may prevent molecules from penetrating the tightly cross-linked Kukersite kerogen structure. The swelling results obtained for the kerogen–tetralin–NMP system confirmed this hypothesis. Figure 7 demonstrates that when steric restrictions (abundant non-covalent cross-links) are removed by NMP, the swelling ratio in tetralin rapidly increases reaching a level determined by its solubility parameter.

4. CONCLUSIONS

A widely used volumetric solvent swelling method applying fine-grained sample centrifugation was critically revised. Taking into account an observed apparent shrinking of Dictyonema kerogen, the need to confirm the validity of a silent assumption of constant void volume fraction in a tightly packed sample bed was specified. For this reason, a DSC-based method for determining the extent of kerogen solvent swelling was developed. An analysis based on the experimental data obtained through the developed method showed that the void volume fraction in a sample packed bed did not remain constant throughout so-called test-tube experiments. Namely, the swollen Kukersite kerogen sample in the test tube was typically packed more tightly than the dry sample. A determined decrease of void volume fraction was presented as a cause of the understated results of the test-tube method. A dependence of sample bed packing efficiency on the amount of absorbed solvent was observed, and this correlation is supposed to be specific for the system under investigation.

However, despite generating certain quantitative inaccuracies, the volumetric test-tube method remains a useful technique for qualitative analysis given the method's wide scope of applicability for swelling in single solvents and solvent mixtures. The DSC-based method provides more accurate quantitative results for the kerogen swelling extent in single solvents due to the elimination of the void fraction effect. The collection of solvents analyzed in swelling experiments through the DSC-based method was restricted by the limiting value of solvent melting temperature. The DSC-based method was also adapted for a specific combination of solvents used as swelling agents: non-specifically interacting solvent in combination with a small volume of specifically interacting solvent.

The results of swelling experiments for single solvents obtained through both measurement techniques led to a conclusion that only solvents that are able to form hydrogen bonds and that act as electron donors can show an extended swelling extent. It was suggested that the increased swellability of kerogen was caused by the material's reduced effective cross-link density. Namely, kerogen non-covalent cross-links were disrupted by strong electron-donating solvents. At the same time, low swellability in non-specifically interacting solvents resulted from high effective cross-link densities that were combined through covalent and non-covalent cross-links.

Results based on single solvent experiments were further confirmed through swelling experiments with solvent mixtures of strong electron-donating solvent and non-specifically interacting solvent. Even small amounts of specifically interacting solvent were able to relax the kerogen structure, causing the uptake of non-polar solvent to significantly increase. At high DN solvent concentrations of approximately 10–20%, the swelling ratio was approximately equal to the swelling ratio obtained for this specifically interacting solvent when used as a single solvent. It was impossible to exceed this maximum limit of swellability regardless of the solvent concentration and combinations used. Swelling

experiments with binary solvent mixtures also confirmed that the solvent solubility parameter plays a secondary role in Kukersite kerogen solvent swelling. Similar characteristic swelling trends were obtained through the application of two swelling procedures for solvent mixtures: 1) using pre-prepared binary solvent mixtures, 2) adding solvents in two steps.

It was found that molar volume of the solvent (the size of solvent molecules) can limit swelling in tightly cross-linked Kukersite kerogen. This effect is more evident when applying DSC-based methods because the effect may be hidden by sample bed compression during centrifugation when applying volumetric measurements. This conclusion drawn from experiments using single solvents was confirmed by analyzing the effect of adding specifically interacting solvents to kerogen samples pre-swollen in non-polar solvents of different molar volumes. When steric restrictions (abundant non-covalent cross-links) were removed by the specifically interacting solvent, the initially low swelling ratio in the solvent with large molecules size rapidly increased, reaching a level determined by the solvent solubility parameter.

The estimated Kukersite kerogen number average molecular weight between cross-links, M_c , calculated from swelling data obtained through the DSC-based method, was higher than the value derived from the results of volumetric measurements. Under conditions in which all other parameters in the equation remained unchanged, higher swelling ratios resulted in higher M_c values, which appeared to be more reliable indicators for Kukersite kerogen.

REFERENCES

- Aida, T.; Squires, T. G. (1985). Solvent swelling of coal. 1: Development of an improved method for measuring swelling phenomena. – *Prepr. - Am. Chem. Soc., Div. Fuel Chem.*, 30 (1), 95–101.
- Alpern, B.; Lemos de Sousa, M. J. (2002). Documented international enquiry on solid sedimentary fossil fuels; coal: Definitions, classifications, reserves-resources, and energy potential. – *Int. J. Coal Geol.*, 50 (1–4), 3–41.
- Amemiya, K.; Kodama, M.; Esumi, K.; Meguro, K.; Honda, H. (1989). Coal swelling using binary mixtures containing THQ. – *Energy Fuels*, 3 (1), 55–59.
- Antxustegi, M. M.; Mackinnon, A. J.; Hall, P. J. (1993). Effects of glass formation by solvents in differential scanning calorimetry investigations of solvent swollen coals. – *Energy Fuels*, 7 (6), 1026–1029.
- Ballice, L. (2003). Solvent swelling studies of Göynük (Kerogen Type-I) and Beypazari oil shales (Kerogen Type-II). – *Fuel*, 82 (11), 1317–1321.
- Ballice, L.; Larsen, J. W. (2003). Changes in the cross-link density of Goynuik oil shale (Turkey) on pyrolysis. – *Fuel*, 82 (11), 1305–1310.
- Ballice, L. (2004). Solvent swelling studies of Soma lignite (Turkey). – *Oil Shale*, 21 (2), 115–123.
- Behbehani, G. R.; Hamed, M.; Rajabi, F. H. (2001). The solvation of urea, tetramethylurea, TMU, in some organic solvents. – *The Internet Journal of Vibrational Spectroscopy*, 5 (6) [www.ijvs.com/volume5/edition6/section3.html]
- Belmares, M.; Blanco, M.; Goddard, W. A.; Ross, R. B.; Caldwell, G.; Chou, S. H.; Pham, J.; Olofson, P. M.; Thomas, C. (2004). Hildebrand and Hansen solubility parameters from molecular dynamics with applications to electronic nose polymer sensors. – *J. Comput. Chem.*, 25 (15), 1814–1826.
- Bondar, E.; Koel, M. (1998). Application of supercritical fluid extraction to organic geochemical studies of oil shales. – *Fuel*, 77 (3), 211–213.
- Cody, G. D.; Davis, A.; Eser, S.; Hatcher, P. G. (1991). The application of microdilatometry to solvent swelling of coals. – *Prepr. - Am. Chem. Soc., Div. Fuel Chem.*, 36 (3), 1307–1313.
- Ertas, D.; Kelemen, S. R.; Halsey, T. C. (2006). Petroleum expulsion part 1. Theory of kerogen swelling in multicomponent solvents. – *Energy Fuels*, 20 (1), 295–300.
- Flory, P. J. (1953). Principles of polymer chemistry. New York: Cornell University Press.
- Gao, H.; Artok, L.; Kidena, K.; Murata, S.; Miura, M.; Nomura, M. (1998). A novel orthogonal microscope image analysis method for evaluating solvent-swelling behavior of single coal particles. – *Energy Fuels*, 12 (5), 881–890.
- Gee, G. (1943). Interaction between rubber and liquids. IV. Factors governing the absorption of oil by rubber. – *Transactions, Inst. Rubber Ind.*, 18, 266–281.
- Graber, E. R.; Mingelgrin, U. (1994). Clay swelling and regular solution theory. – *Environ. Sci. Technol.*, 28 (13), 2360–2365.

Green, T. K.; Kovac, J.; Larsen, J. W. (1984^a). A rapid and convenient method for measuring the swelling of coals by solvents. – *Fuel*, 63 (7), 935–938.

Green, T. K.; Larsen, J. W. (1984^b). Coal swelling in binary solvent mixtures: pyridine–chlorobenzene and N,N-dimethylaniline–alcohol. – *Fuel*, 63 (11), 1538–1543.

Green, T. K.; West, T. A. (1985). Coal swelling in n-amines and n-alcohols. – *Prepr. - Am. Chem. Soc., Div. Fuel Chem.*, 30 (4), 488–492.

Green, T. K.; West, T. A. (1986). Coal swelling in straight-chain amines: evidence for specific site binding. – *Fuel*, 65 (2), 298–299.

Gutmann V. (1978). The donor-acceptor approach to molecular interactions. New York: Plenum Press.

Hall, P. J.; Larsen, J. W. (1991). Evidence for low-temperature second-order phase transitions in coal/solvent systems using differential scanning calorimetry. – *Energy Fuels*, 5 (1), 228–229.

Hall, P. J.; Thomas, K. M.; Marsh, H. (1992). The relation between coal macromolecular structure and solvent diffusion mechanisms. – *Fuel*, 71 (11), 1271–1275.

Hall, P. J.; Larsen, J. W. (1993). Evidence for the formation of stable coal-N-methylpyrrolidinone and coal-pyridine gels. – *Energy Fuels*, 7 (1), 47–51.

Hefta, R. S.; Schobert, H. H.; Kube, t. I. W. R. (1986). Calorimetric pyrolysis of a North Dakota lignite. – *Fuel*, 65 (9), 1196–1202.

Hints, O.; Nõlvak, J.; Viira V. (2007). Age of Estonian Kukersite oil shale – Middle or late Ordovician? – *Oil Shale*, 24 (4), 527–533.

Hombach, H. P. (1980). General aspects of coal solubility. – *Fuel*, 59 (7), 465–470.

Honiball, D.; Huson, M. G.; McGill, W. J. (1988). A nucleation theory for the anomalous freezing point depression of solvents in swollen rubber gels. – *J. Polym. Sci., Part B: Polym. Phys.*, 26 (12), 2413–2431.

Hu, H.; Sha, G.; Chen, G. (2000). Effect of solvent swelling on liquefaction of xinglong coal at less severe conditions. – *Fuel Process. Technol.*, 68 (1), 33–43.

Janikowski, S. K.; Stenberg, V. I. (1989). Thermal analysis of coals using differential scanning calorimetry and thermogravimetry. – *Fuel*, 68 (1), 95–99.

Jones, J. C.; Boother, M.; Brown, M. (1991). On the solvent-induced swelling of low-rank coals. – *J. Chem. Technol. Biotechnol.*, 52 (2), 257–264.

Jones, J. C.; Prawitasari, B. (1995). The swelling of a low-rank coal in benzene–pyridine and toluene–pyridine mixtures. – *J. Chem. Technol. Biotechnol.*, 64 (2), 207–209.

Karger, B. L.; Snyder, L. R.; Eon, C. (1978). Expanded solubility parameter treatment for classification and use of chromatographic solvents and adsorbents. – *Anal. Chem.*, 50 (14), 2126–2136.

Kelemen, S. R.; Walters, C. C.; Ertas, D.; Kwiatek, L. M. (2006). Petroleum expulsion part 2. Organic matter type and maturity effects on kerogen swelling by solvents and thermodynamic parameters for kerogen from regular solution theory. – *Energy Fuels*, 20 (1), 301–308.

Kilk, K.; Savest, N.; Yanchilin, A.; Kellogg, D. S.; Oja, V. (2010). Solvent swelling of Dictyonema oil shale: Low temperature heat-treatment caused changes in swelling extent. – *J. Anal. Appl. Pyrolysis*, 89 (2), 261–264.

Kiraz, A.; Sinağ, A.; Tekes, A. T.; Misirlioğlu, Z.; Canel, M. (2004). Effect of pre-swelling on extractability and solvent swelling of Ermenek lignite (Turkey). – *Energy Sources*, 26 (5), 431–439.

Kirov, N. Y.; O'Shea, J. M.; Sergeant, G. D. (1967). The determination of solubility parameters for coal. – *Fuel*, 46, 415–424.

Klein, M.; Guenet, J.-M. (1989). Effect of polymer chain microstructure on solvent crystallization: implications on polymer solvation and on physical gelation. – *Macromolecules*, 22 (9), 3716–3725.

Koch, P. R.; Kirret, O. G.; Oamer, P. E.; Ahelik, V. P.; Kõrts, A. V. (1973). Studies on the flotation process of Estonian Kukersite. Thesis of all-union conference on the beneficiation of oil shales; Academy of Sciences USSR: Moscow. p 115–122. [in Russian] Исследование процесса флотации горючего сланца – кукерсита.

Koel, M.; Ljovin, S.; Hollis, K.; Rubin, J. (2001). Using neoteric solvents in oil shale studies. – *Pure Appl. Chem.*, 73 (1), 153–159.

Kogerman, P. N. (1931). On chemistry of Estonian oil shale „Kukersite”. Monograph. Oil shale research laboratory, University of Tartu, Estonia. Mattiesen: Tartu, Bulletin No 3.

Kovac, J. (1978). Modified Gaussian Model for Rubber Elasticity. – *Macromolecules*, 11 (2), 362–365.

Larsen, J. W.; Green, T. K.; Kovac, J. (1985). The nature of the macromolecular network structure of bituminous coals. – *J. Org. Chem.*, 50 (24), 4729–4735.

Larsen, J. W.; Shawver, S. (1990). Solvent swelling studies of two low-rank coals. – *Energy Fuels*, 4 (1), 74–77.

Larsen, J. W.; Cheng, J. C.; Pan, C.-S. (1991). Solvent extractions of coals during analytical solvent swelling. A potential source of error. – *Energy Fuels*, 5 (1), 57–59.

Larsen, J. W.; Li, S. (1994). Solvent swelling studies of Green River kerogen. – *Energy Fuels*, 8 (4), 932–936.

Larsen, J. W.; Gurevich, I.; Glass, A. S.; Stevenson, D. S. (1996). A method for counting the hydrogen-bond cross-links in coal. – *Energy Fuels*, 10 (6), 1269–1272.

Larsen, J. W.; Flowers, R. A.; Hall, P. J.; Carlson, G. (1997^a). Structural rearrangement of strained coals. – *Energy Fuels*, 11 (5), 998–1002.

Larsen, J. W.; Li, S. (1997^b). An initial comparison of the interactions of Type I and III kerogens with organic liquids. – *Org. Geochem.*, 26 (5-6), 305–309.

Larsen, J. W.; Li, S. (1997^c). Changes in the macromolecular structure of a type I kerogen during maturation. – *Energy Fuels*, 11 (4), 897–901.

Larsen, J. W.; Parikh, H.; Michels, R. (2002). Changes in the cross-link density of Paris Basin Toarcian kerogen during maturation. – *Org. Geochem.*, 33 (10), 1143–1152.

Lille, Ü. (2003^a). Current knowledge on the origin and structure of Estonian Kukersite kerogen. – *Oil Shale*, 20 (3), 253–263.

Lille, Ü.; Heinmaa, I.; Pehk, T. (2003^b). Molecular model of kukersite kerogen evaluated by ¹³C MAS NMR spectra. – *Fuel*, 82 (7), 799–804.

Linert, W. (2001). Chromotropism of coordination compounds and its application in solution. – *Coord. Chem. Rev.*, 218, 113–152.

Liotta, R.; Brons, G.; Isaacs, J. (1983). Oxidative weathering of Illinois No.6 coal. – *Fuel*, 62 (7), 781–791.

Liu, Y.; Xue, X.; He, Y. (2011). Solvent swelling behavior of fushun pyrolysis and demineralized oil shale. – *Advanced Science Letters*, 4 (4–5), 1838–1841.

Lucht, L. M.; Peppas, N. A. (1987^a). Macromolecular structure of coals. 2. Molecular weight between crosslinks from pyridine swelling experiments. – *Fuel*, 66 (6), 803–809.

Lucht, L. M.; Larson, J.M.; Peppas, N.A. (1987^b). Macromolecular structure of coals. 9. Molecular structure and glass transition temperature. – *Energy Fuels*, 1 (1), 56–58.

Lue, S. J.; Yang, S. W. (2005). Sorption of organic solvents in poly(dimethyl siloxane) membrane. I. Permeant states quantification using differential scanning calorimetry. – *J. Macromol. Sci., Part B: Phys.*, 44 (5), 711–725.

Mahajan, O.P.; Tomita, A.; Walker, Jr. P. L. (1976). Differential scanning calorimetry studies on coal. 1. pyrolysis in an inert atmosphere. – *Fuel*, 55 (1), 63–69.

Mahajan, O.P.; Tomita, A.; Nelson, J.R.; Walker, Jr. P. L. (1977). Differential scanning calorimetry studies on coal. 2. hydrogenation of coals. – *Fuel*, 56 (1), 33–39.

Malavolta, L.; Oliveira, E.; Cilli, E. M.; Nakaie, C. R. (2002). Solvation of polymers as model for solvent effect investigation: proposition of a novel polarity scale. – *Tetrahedron*, 58 (22), 4383–4394.

Mayo, F. R.; Zevely, J. S.; Pavelka, L. A. (1988). Extractions and reactions of coals below 100°C. 1. Solubilities of coals in pyridine and amines. – *Fuel*, 67 (5), 595–599.

Miura, K.; Mae, K.; Takebe, S.; Wakiyasu, H.; Hashimoto, K. (1994). A new method for estimating strength distribution of noncovalent bondings in coal by differential scanning calorimetry. – *Energy Fuels*, 8 (4), 874–880.

Murata, S.; Sako, T.; Yokoyama, T.; Gao, H.; Kidena, K.; Nomura, M. (2008). Kinetic study on solvent swelling of coal particles. – *Fuel Process. Technol.*, 89 (4), 434–439.

Nandi, S.; Winter, H. H. (2005). Swelling behavior of partially cross-linked polymers: a ternary system. – *Macromolecules*, 38 (10), 4447–4455.

Ndaji, F. E.; Thomas, K. M. (1995). Effects of solvent steric properties on the equilibrium swelling and kinetics of solvent swelling of coal. – *Fuel*, 74 (6), 842–845.

Nelson, J. R.; Mahajan, O. P.; Walker, P. L. Jr. (1980). Measurement of swelling of coals in organic liquids: a new approach. – *Fuel*, 59 (12), 831–837.

NIST Standard Reference Database Number 69. [www] <http://webbook.nist.gov/chemistry/> (2013-05-06)

Nomura, S.; Thomas, K. M. (1998). Fundamental aspects of coal structural changes in the thermoplastic phase. – *Fuel*, 77 (8), 829–836.

Oikawa, H.; Murakami, K. (1984). Studies of the network structure of rubber vulcanizates by a cryoscopic method: 1. – *Polymer*, 25 (2), 225–229.

Oja, V. (2013). Molecular weight parameters of oil shale pyrolysis products. – *Abstracts of Papers of the Amer. Chem. Soc.*, 246, 107-ENFL.

Otake, Y.; Suuberg, E. M. (1989). Determination of the kinetics of diffusion in coals by solvent swelling techniques. – *Fuel*, 68 (12), 1609–1612.

Otake, Y.; Suuberg, E. M. (1997). Temperature dependence of solvent swelling and diffusion processes in coals. – *Energy Fuels*, 11 (6), 1155–1164.

Otake, Y.; Suuberg, E. M. (1998). Solvent swelling rates of low rank coals and implications regarding their structure. – *Fuel*, 77 (8), 901–904.

Rajeshwar, K.; Jones, D. B.; DuBow, J. B. (1981). Characterization of oil shales by differential scanning calorimetry. – *Anal. Chem.*, 53 (1), 121–122.

Salmerón Sánchez, M.; Monleón Pradas, M.; Gómez Ribelles, J. L. (2002). Thermal transitions of benzene in a poly(ethyl acrylate) network. – *J. Non-Cryst. Solids*, 307–310, 750–757.

Savest, N.; Oja, V.; Kaevand, T.; Lille, Ü. (2007). Interaction of Estonian kukersite with organic solvents: A volumetric swelling and molecular simulation study. – *Fuel*, 86 (1-2), 17–21.

Savest N. (2010). Solvent swelling of Estonian oil shales: low temperature thermochemical conversion caused changes in swelling: PhD Thesis. Tallinn, Tallinn University of Technology.

Shadle, L. J.; Khan, M. R. (1989). Investigation of oil shale and coal structure by swelling in various solvents. – *Prepr. - Am. Chem. Soc., Div. Petroleum Chem.*, 34 (1), 55–61.

Shui, H.; Wang, Z. (2010). Effect of solvent pretreatments on the aggregation behavior of Upper Freeport coal. – *Energy Fuels*, 24 (2), 1063–1068.

Siskin, M.; Brons, G.; Payack, J. F. Jr. (1989). Disruption of kerogen-mineral interactions in Rundle Ramsay Crossing oil shale. – *Energy Fuels*, 3 (1), 108–109.

Smallwood, I. M. (1996). Handbook of organic solvent properties. London: Arnold.

Solomon, P. R.; Hamblen, D. G.; Carangelo, R. M.; Serio, M. A.; Deshpande, G. V. (1988). General Model of Coal Devolatilization. – *Energy Fuels*, 2 (4), 405–422.

Solomon, P. R.; Serio, M. A.; Deshpande, G. V.; Kroo, E. (1990). Cross-linking reactions during coal conversion. – *Energy Fuels*, 4 (1), 42–54.

Stathopoulos, A. T.; Kyritsis, A.; Colomer, F. J. R.; Ribelles, J. L. G.; Shinyashiki, N.; Christodoulides, C.; Pissis, P. (2011). Polymer segmental dynamics and solvent thermal transitions in poly(ethyl acrylate)/p-xylene mixtures. – *J. Polym. Sci., Part B: Polymer Physics*, 49 (6), 455–466.

Suuberg, E. M.; Otake, Y.; Langer, M. J.; Leung, K. T.; Milosavljevic, I. (1994). Coal makromolecular network structure analysis: solvent swelling thermodynamics and its implications. – *Energy Fuels*, 8 (6), 1247–1262.

Suzuki, M.; Norinaga, K.; Iino, M. (2004). Macroscopic observation of thermal behavior of concentrated solution of coal extracts. – *Fuel*, 83 (16), 2177–2182.

Szeliga, J.; Marzec, A. (1983). Swelling of coal in relation to solvent electron-donor numbers. – *Fuel*, 62 (10), 1229–1231.

Takanohashi, T.; Terao, Y.; Iino, M.; Yun, Y.; Suuberg, E. M. (1999). Irreversible structural changes in coals during heating. – *Energy Fuels*, 13 (2), 506–512.

Turpin, M.; Rand, B.; Ellis, B. (1996). A novel method for the measurement of coal swelling in solvents. – *Fuel*, 75 (2), 107–113.

Urov, K.; Sumberg, A. (1999). Characteristic of oil shales and shale-like rocks of known deposits and outcrops. – *Oil Shale*, 16 (3 special: monograph), 1–64.

Vandenbroucke, M.; Largeau, C. (2007). Kerogen origin, evolution and structure. – *Org. Geochem.*, 38 (5), 719–833.

Wu, J.; McKenna, G. B. (2008). Anomalous melting behavior of cyclohexane and cyclooctane in poly(dimethyl siloxane) precursors and model networks. – *J. Polym. Sci., Part B: Polym. Phys.*, 46 (24), 2779–2791.

Xie, K.-C.; Li, F.; Feng, J.; Liu, J. (2000). Study on the structure and reactivity of swollen coal. – *Fuel Process. Technol.*, 64 (1), 241–251.

Yagi, Y.; Inomata, H.; Saito, S. (1992). Solubility parameter of an N-isopropylacrylamide gel. – *Macromolecules*, 25, 2997–2998.

Yang, H.; Nguyen, Q. T.; Ding, Y.; Long, Y.; Ping, Z. (2000). Investigation of poly(dimethyl siloxane) (PDMS)–solvent interactions by DSC. – *J. Membr. Sci.*, 164 (1-2), 37–43.

Yoshikawa, M.; Matsuura, T.; Cooney, D. (1991). Studies on the state of permeant in the membrane and its effect on pervaporation phenomena. – *J. Appl. Polym. Sci.*, 42 (5), 1417–1421.

Yoshikawa, M.; Matsuura, T. (1992). A calorimetric study of various alcohols in a poly(dimethylsiloxane) membrane. – *Polymer*, 33 (21), 4656–4658.

Yun, Y.; Suuberg, E. M. (1993). New applications of differential scanning calorimetry and solvent swelling for studies of coal structure: prepyrolysis structural relaxation. – *Fuel*, 72 (8), 1245–1254.

Yun, Y.; Suuberg, E. M. (1998). Cooperative effects in solvent swelling of a bituminous coal. – *Energy Fuels*, 12 (4), 798–800.

Zeng W, Du Y, Xue Y, Frisch HL. (2007). Solubility parameters. – *Physical properties of polymers handbook*, Chapter 16, 289–303. Editor J. E. Mark. New York: Springer.

Önal, Y.; Akol, S. (2003). Influence of pretreatment on solvent-swelling and extraction of some Turkish lignites. – *Fuel*, 82 (11), 1297–1304.

ГОСТ 2160-92. Solid mineral fuel. Methods for determination of density. (2002). Межгосударственный стандарт. Топливо твёрдое минеральное. Методы определения плотности. Москва: ИПК Издательство стандартов. [in Russian]

Губергриц, М. Я. (1966). Термическая переработка сланца-кукерсита. Таллин: Валгус.

ACKNOWLEDGEMENTS

I would like to express my deep gratitude to my supervisor, Professor Vahur Oja, for his guidance, support and sharing of academic knowledge throughout our collaboration over the last eight years.

I am very grateful to the coauthors of the articles included in my dissertation for their fruitful contributions, and I especially thank Dr. Natalja Savest, Dr. Oliver Järvik and Dr. Alexey Yanchilin. I would like to thank all of my colleagues at the Department of Chemical Engineering for sharing their advice and theoretical and practical knowledge and for helping me throughout this project. Special appreciation goes to Ilme Rohtla, Dr. Inna Kamenev, Sven Kamenev and Marika Viisimaa for their support, encouragement and help. I would also like to thank Alfred Elenurm and Zachariah Steven Baird for their assistance.

I send my warmest gratitude to my family and friends for their invaluable support over my years of study.

This work was partially supported by the Graduate School of Functional Materials and Technologies, which received funding from the European Social Fund under project 1.2.0401.09-0079 in Estonia. Financial support provided by the Estonian Science Foundation under Grants G7222 and G9297 and by the Estonian Minister of Education and Research under financing target SF0140022s10 is also gratefully acknowledged.

ABSTRACT

In the present research, solvent swelling of Estonian Kukersite oil shale kerogen submerged in single organic solvents and binary solvent mixtures was studied.

Kukersite is a strategic resource in Estonia that is primarily used to provide fuel for power stations and as a raw material for shale oil production. Kerogen is a cross-linked macromolecular form of organic matter that represents a major organic component of oil shale. In addition to covalent cross-links, there are numerous non-covalent cross-links (mainly hydrogen bonds) in Kukersite kerogen due to its high level of oxygen-containing functional groups. The solvent swelling technique is widely used to characterize the macromolecular structures of kerogens and coals (i.e., solid fossil fuels). The technique allows for the determination of the kerogen solubility parameter and number average molecular weight between cross-links while also allowing for changes in cross-link densities to be tracked.

Though previous Kukersite solvent swelling studies have suggested that specific kerogen–solvent interactions (mainly hydrogen bonds) play an important role in the swelling process, these interactions have not been studied in detail. Although valuable qualitative information on Kukersite kerogen cross-link density change during low temperature treatments has been obtained, the value of the estimated kerogen number average molecular weight between cross-links remained questionable.

The primary aim of this research was to evaluate the swelling potential of Kukersite kerogen by studying the role of specifically interacting (hydrogen-bonding) solvents, as they appear to have a great influence on Kukersite kerogen swelling and, consequently, on the estimated kerogen number average molecular weight between cross-links.

Kerogen solvent swelling was conducted in accordance with the general procedure of the widely applied Green's volumetric method, involving the equilibration of a fine-grained kerogen sample submerged in solvent that is contained in a test tube, which is followed by centrifugation to obtain a tightly packed sample bed. Two approaches were used for the determination of the kerogen swelling extent. The first approach involved measuring the heights of dry and swollen samples contained in test tubes according to the volumetric method. The second approach applied differential scanning calorimetry (DSC) to measure the amount of non-freezable solvent present in swollen kerogen samples, which should be equal to the amount of solvent absorbed by kerogen, i.e., swelling-causing solvent. According to the literature review, this study was the first to utilize DSC to determine the swelling extent of fossil fuels.

While the DSC-based method provided more accurate quantitative results for the extent of kerogen swelling in single solvents than the volumetric test-tube method, the method's applicability was restricted by solvent melting temperatures. Based on the results of the DSC-based method, it was found that the swollen Kukersite kerogen sample in the test tube was generally packed more

tightly than the dry sample. The latter phenomenon was presented as a reason for the understated results of the test-tube method. However, it was concluded that despite introducing degrees of quantitative inaccuracy, the volumetric test-tube method remains a useful technique for qualitative analysis.

The results obtained through both measurement techniques led to a conclusion that the match between kerogen and solvent Hildebrand solubility parameters is of secondary importance in Kukersite kerogen swelling and only solvents that form hydrogen bonds acting as electron donors can show an extended swelling due to an ability to reduce the effective cross-link density of kerogen by disrupting kerogen–kerogen hydrogen bonds that serve as non-covalent cross-links. The latter outcome was confirmed through swelling experiments with solvent mixtures that combined a strong electron-donating solvent and a non-specifically interacting solvent. The results showed that the maximum limit of swellability, determined by strong electron-donating solvents, could not be exceeded through the use of different solvent combinations or mixture concentrations. Swelling experiments with binary solvent mixtures also confirmed that the solvent solubility parameter plays a secondary role in the solvent swelling of Kukersite kerogen. Similar swelling trends were obtained using two separate solvent swelling procedures: 1) using pre-prepared binary solvent mixtures, 2) adding solvents in two steps.

It was found that the solvent molecule size can limit the swelling of tightly cross-linked Kukersite kerogen. A small amount of specifically interacting solvent added to non-polar solvent can act as a swelling promoter, disrupting kerogen non-covalent cross-links (i.e., hydrogen bonds) and thus allowing for the penetration of larger non-polar solvent molecules into the kerogen structure. Thus, differences in the swelling behaviors of Kukersite oil shale and oil shales originating from some other deposits, in the case of solvents with large molecule sizes, can be explained by the high cross-link density of Kukersite kerogen that is caused by an abundance of non-covalent cross-links.

The estimated Kukersite kerogen number average molecular weight between cross-links, M_c , calculated based on swelling data obtained through the DSC-based method was higher than the value derived from volumetric measurements. When all other parameters in the equation were held constant, higher swelling ratios resulted in the higher M_c average value, and this value appeared to be more reliable for Kukersite kerogen.

KOKKUVÕTE

Käesolevas töös uuriti kukersiitse põlevkivi kerogeeni pundumist puhastes orgaanilistes lahustites ning lahustite binaarsetes segudes.

Kukersiit on Eesti strateegiline maavara, mida kasutatakse peamiselt elektrienergia ning põlevkiviõli tootmiseks. Põlevkivi on settekivim, mis koosneb mineraalsest ja orgaanilisest osast, mille peamiseks komponendiks on kerogeen – võrkstruktuurne makromolekulaarne orgaaniline aine. Tänu kõrgele hapnikkusisaldavate funktsionaalrühmade sisaldusele lisaks kovalentsetele ristsidemetele esineb kukersiidi kerogeenis ka palju vesiniksidemeid, mis täidavad mittekovalentsete ristsidemete rolli. Pundumine orgaanilistes lahustites on laialt levinud meetod kerogeeni ja kivisöe makromolekulaarse struktuuri iseloomustamiseks. Seda kasutatakse kerogeeni lahustuvusparameetri ja ristsidemetevahelise arvkeskmise molekulmassi määramiseks ning ristsidemete tiheduse muutuse jälgimiseks.

Varajasemad kukersiidi pundumise uuringud töid esile kukersiidi kerogeeni ja lahusti vaheliste spetsiifiliste vastasmõjude tähtsa rolli pundumisprotsessis, ent need vastasmõjud vajasis täiendavaid uuringuid. Saadi väärtuslikku kvalitatiivset infot termilise töötlemisega kaasneva ristsidemete tiheduse muutuse kohta, kuid ristsidemetevahelise arvkeskmise molekulmassi hinnanguline väärtus jäi küsitavaks.

Käesoleva töö põhieesmärgiks oli hinnata kukersiidi kerogeeni pundumispotentsiaali uurides spetsiifiliste vastasmõjudega lahustite rolli, kuna need avaldavad olulist mõju kukersiidi pundumisele ja selle tulemusena ka ristsidemete vahelise arvkeskmise molekulmassi väärtuse hindamisele.

Kerogeeni pundumine viidi läbi vastavalt tahkete fossiilkütuste (põlevkivi ja kivisöe) valdkonnas laialt kasutatavale volumeetrilisele meetodile nn katseklaasi meetodile. Meetod seisneb pulbrilise kerogeeni proovi ja lahusti segu tasakaalustamises katseklaasis ning sellele järgnevas tsentrifuugimises tiheda proovikihi saamiseks. Pundumise määra mõõtmiseks kasutati kahesugust lähenemist. Esimesel juhul mõõdeti kerogeeni kuiva ja pundunud proovi kihi kõrgus, nagu seda eeldabki katseklaasi meetod. Teisel juhul kasutati diferentsiaalset skaneerivat kalorimeetrit (differential scanning calorimeter – DSC), millega määrati mittekristalliseeruva lahusti s.o kerogeeni poolt absorbeeritud ehk pundumist põhjustanud lahusti hulk pundunud kerogeeni proovis. Kirjanduse andmetel on see esimene uurimistöö, milles DSC-d kasutati selleks, et määrata fossiilkütuse pundumise määra.

DSC-põhine meetod andis kvantitatiivselt täpsemaid tulemusi kerogeeni pundumise määra kohta puhaste lahustite kasutamisel, kui seda oli võimalik saada proovi mahu muutuse mõõtmise kaudu. DSC-põhise meetodi tulemused näitasid, et pundunud kerogeeni proovi kiht oli üldjuhul surutud tihedamini kokku (st vaba mahu osa kihis oli väiksem) kui kuiva proovi kiht. See asjaolu võib olla katseklaasi meetodil määratud pundumist iseloomustavate parameetrite madalamate väärtuste põhjuseks. Kuid vaatamata tulemuste teatud

kvantitatiivsele ebatäpsusele jääb katseklaasi meetod siiski kasulikuks meetodiks kvalitatiivsete andmete saamiseks.

Mõlema meetodiga saadud mõõtmistulemustest järeldati, et kerogeeni ja lahusti Hildebrandi lahustuvusparameetrite vaheline sobivus ei olnud määrav tegur kukersiidi kerogeeni pundumisel ning ainult need lahustid, mis on võimelised moodustama vesiniksidemeid olles elektronidoonorid, põhjustasid kõrgendatud pundumist tänu nende võimele vähendada efektiivset ristsidemete tihedust lõhkudes kerogeen–kerogeen vesiniksidemeid s.o mittekovalentseid ristsidemeid. Viimane leidis kinnitust ka katsetes, kus pundumisagensina kasutati lahustite binaarseid segusid, mis koosnesid lahustist, mis käitub kui tugev elektronidoonor, ja mittepolaarsest lahustist. Lisaks sellele tulemused näitasid, et tugevate elektronidoonoritega saavutatud ülemist pundumise piiri ei ületatud erinevate lahustite kombinatsioonidega. Katsed lahustite binaarsete segudega kinnitasid solvendi Hildebrandi lahustuvusparameetri sekundaarset tähtsust kukersiidi kerogeeni pundumisel. Sarnased pundumistendentsid saadi kasutades ettevalmistatud binaarseid lahustite segusid ning lisades kahte lahustit üksteise järel.

Leiti, et lahusti molekulide suurus võib olla piiravaks teguriks tiheda võrkstruktuuriga kukersiidi kerogeeni pundumisel. Spetsiifiliste vastasmõjudega lahusti (lisatuna väikeses koguses mittepolaarsele lahustile) võib olla pundumise soodustajaks, kuna lõhub kerogeeni mittekovalentseid ristsidemeid (vesiniksidemeid) ning sellega võimaldab mittepolaarse lahusti suurte molekulide paremat juurdepääsu kerogeeni struktuuri. Järelikult pundumisel suuremolekulistes lahustites võib kukersiidi käitumise omapära (võrreldes teiste leiukohtade põlevkividega) põhjuseks olla mittekovalentsete ristsidemete olemasolu tõttu kõrgendatud ristsidemete tihedus.

Kukersiidi kerogeeni ristsidemete vahelise arvkeskmise molekulmassi hinnanguline väärtus, mille arvutamisel kasutati DSC-põhise meetodiga saadud andmeid, oli kõrgem sellest väärtusest, mis oli saadud katseklaasi meetodi andmete põhjal (teiste arvutusel kasutatavate parameetrite võrdsuse tingimusel). Kõrgemat kukersiidi kerogeeni ristsidemete vahelist arvkeskmist molekulmassi väärtust võib hinnata kui usaldusväärsemat.

APPENDIX A
PUBLICATIONS

ARTICLE I

Savest, N.; **Hruljova, J.**; Oja, V. (2009). Characterization of thermally pretreated Kukersite oil shale using the solvent-swelling technique. – *Energy & Fuels*, 23 (12), 5972–5977.

Characterization of Thermally Pretreated Kukersite Oil Shale Using the Solvent-Swelling Technique

Natalja Savest, Jelena Hruļjova, and Vahur Oja*

Department of Chemical Engineering, Tallinn University of Technology, Ehitajate Road 5, 19086 Tallinn, Estonia

Received June 30, 2009. Revised Manuscript Received September 24, 2009

Equilibrium swelling of thermally pretreated kukersite oil shale has been investigated in 22 solvents and in 2 different binary mixtures to evaluate changes in the swelling behavior and solubility parameter. Swelling experiments were performed at room temperature on previously preheated samples. Variations in extent of solvent swelling as a function of the pretreatment temperature and time are shown. On the basis of swelling in high donor number solvents, kukersite oil shale shows structural relaxation before the onset of active pyrolysis. This is consistent with the behavior seen in coal pyrolysis studies on high tar yield, softening coals. The solubility parameters (Hildebrand and Hansen three-dimensional) of kerogen were tentatively determined from swelling data and found to be practically independent of the thermal pretreatment process conditions in the temperature range up to 350 °C.

1. Introduction

Use of oil shales has gained considerable interest in recent years because of increasing global energy demand and also the strategic domestic energy visions of countries with considerable oil shale resources. Oil shale resources are widespread all over the world, with usable reserves corresponding to more than 2.9 trillion barrels of shale oil.¹ There are different technologies in use or under development for oil shale being upgraded to valuable products, including surface retorting, energy production in power plants, and *in situ* retorting. Therefore, changes in oil shale organic matter structure at temperatures of oil shale thermobitumen formation (up to 350–400 °C) or in the active pyrolysis region (375–600 °C) are of interest in oil shale conversion to liquid fuels or chemicals, because the macromolecular structure of kerogen needs to be broken down to obtain oil.

Oil shales are complex heterogeneous materials, with an organic fraction consisting primarily of kerogen, a highly cross-linked macromolecular structure. In coal research, a number of studies have been performed on swelling of thermally pretreated coals, indicating loosening and/or tightening of coal structures in the temperature region prior to tar evolution or active pyrolysis (referred later in this paper as the low-temperature region).^{2–4} This phenomenon was found to depend upon coal rank: changes in lower rank coals indicate low-temperature cross-linking, whereas trends in higher rank coals vary from no observable changes to structural relaxation. It was observed that the extent of low-temperature cross-linking was associated with decomposition

of carboxyl groups and possibly hydroxyl groups because the formation of new cross-links before devolatilization happened together with CO₂ and water release.³ It has been concluded that low-temperature cross-linking results in low tar yield and can be a reason for the non-softening pyrolytic behavior seen in low-rank coals.² In coal studies, cross-linking and also changes in cross-linking have been estimated from swelling data in pyridine as a qualitative indicator of cross-link density^{2,3,5} or also studied in *N,N*-dimethylformamide (DMF),⁴ both high donor number solvents. Note that solvent swelling, a simple low-cost technique, has been widely used to characterize cross-linked structures, to determine solubility parameters (square root of the cohesive energy density), molecular weights between cross-links, or cross-link densities.

In this study, solvent swelling is applied to kukersite oil shale from Estonia. Kukersite oil shale is a high tar (or from industrial viewpoint, oil) yield oil shale, which shows softening behavior during pyrolysis.⁶ Although it has high oxygen content (above 10%) on an organic matter basis, the content of carboxyl functional groups is relatively low, for example, shown to be 1.3% on a total oxygen basis.⁷ Therefore, on the basis of what is seen in coal studies, one could expect structural relaxation rather than tightening of the structure during the low-temperature (prepyrolytic) thermal treatment.

This paper is an extension of the earlier works from this laboratory and is aimed at giving further insights on the mechanism of solvent swelling of kukersite oil shale.^{8,9} The experimental study has been extended to examine the influence of thermal pretreatment on solvent swelling behavior of Estonian oil shale kukersite: on the extent of swelling, on the importance of specific interactions in the swollen network, and on the solubility parameter of kerogen. The extent of

*To whom correspondence should be addressed. Telephone: +372-620-2852. Fax: +372-620-2856. E-mail: vahur.oja@ttu.ee.

(1) World Energy Council. *Survey of Energy Resources 2007*; World Energy Council: U.K., 2007.

(2) Suuberg, E. M.; Unger, P. E.; Larsen, J. W. *Energy Fuels* **1987**, *1*, 305–308.

(3) Solomon, P. R.; Serio, M. A.; Deshpande, G. V.; Kroo, E. *Energy Fuels* **1990**, *4*, 42–54.

(4) Watanabe, I.; Sakanishi, K.; Moschida, I. *Energy Fuels* **2002**, *16*, 18–22.

(5) Solomon, P. R.; Serio, M. A.; Suuberg, E. M. *Prog. Energy Combust. Sci.* **1992**, *18*, 133–220.

(6) Oja, V. J. *Anal. Appl. Pyrolysis* **2005**, *74*, 55–60.

(7) Gubergrits, M. *Thermochemical Conversion of Kukersite Oil Shale*; Valgus: Tallinn, Estonia, 1966 (in Russian).

(8) Savest, N.; Oja, V.; Kaevand, T.; Lille, U. *Fuel* **2007**, *86*, 17–21.

(9) Hruļjova, J.; Savest, N.; Oja, V.; Suuberg, E. M. *Fuel* **2009**, manuscript submitted.

Table 1. Solvent Parameters^a

solvent	Hildebrand solubility parameter (MPa ^{1/2})	Hansen dispersion solubility parameter (MPa ^{1/2})	Hansen polar solubility parameter (MPa ^{1/2})	Hansen hydrogen-bonding solubility parameter (MPa ^{1/2})	electron donor number	electron acceptor number
acetone	20.3	15.5	10.4	7.0	17.0	12.5
acetonitrile	24.3	15.3	18.0	6.1	14.1	18.9
aniline	21.2	19.4	5.1	10.2		
cyclohexanol	20.3	17.4	4.1	13.5		
DMF	24.5	17.4	13.7	11.3	26.6	16.0
ethanol	26.0	15.8	8.8	19.4	19.2	37.1
MEK	19.0	16.0	9.0	5.1		
methanol	29.3	15.1	12.3	22.3	19.1	41.3
NMP	23.1	18.0	12.3	7.2	27.3	13.3
<i>n</i> -propanol	24.5	16.0	6.8	17.4	19.8	37.7
propylamine	18.2	16.9	4.9	8.6		
pyridine	21.9	19.0	8.8	5.9	33.1	14.2
tetrahydrofuran	18.6	16.8	5.7	8.0	20.0	8.0
1-methylnaphthalene	20.3	20.6	0.8	4.7		
benzene	18.8	18.4	0.0	2.0	0.1	8.2
hexane	14.7	14.9	0.0	0.0	0.0	0.0
<i>o</i> -xylene	18.0	17.8	1.0	3.1		
tetralin	19.4	19.6	2.0	2.9		
toluene	18.2	18.0	1.4	2.0	0.1	3.3
nitrobenzene	20.5	20.0	8.6	4.1	4.4	14.8
nitroethane	22.7	16.0	15.5	4.5		
nitromethane	26.0	15.8	18.8	5.1	2.7	20.5

^a DMF, dimethylformamide; NMP, *n*-methyl-2-pyrrolidinone; MEK, methyl ethyl ketone.

swelling (macromolecule volume fraction in the swollen network) and solubility parameter are input parameters in swelling models that can be used to estimate cross-link density. It can at least be used to qualitatively track changes in cross-link density, because the extent of swelling varies inversely with the extent of cross-linking. Of course, dependent upon the swelling models chosen, other parameters, for example, changes in the interaction parameter or solubility parameter, influence evaluation of the cross-link density from swelling data.¹⁰

2. Experimental Section

Kokersite Oil Shale. Kokersite oil shale of 38 wt % of organic content (ash, 46.5 wt %; carbonate CO₂, 16.5 wt %; SO₄²⁻ in ash, 3.2 wt %) was used for experiments. Because the content of solvent extractables in kokersite oil shales is low, below 1.5% on an organic matter basis, then the oil shale was not treated for removal of solvent solubles. The sample was ground to a particle size below 100 μm. The oil shale was characterized by an elemental composition of C, 36.3 wt %; H, 4.1 wt %; and N, 1.1 wt %.

Solvents. The 22 solvents used in this study are listed in Table 1 together with their key characteristics: solubility parameters (Hildebrand or total),^{11–14} Hansen three-dimensional solubility parameters¹⁵ (dispersion, polar, and hydrogen bonding), and Guttmann's donor and acceptor numbers.^{16–18} All solvents were analytical-grade and used without further purification.

Solvent Swelling. Swelling experiments were performed at room temperature on raw and previously preheated oil shales. Details of the experimental technique are available elsewhere.⁹ Briefly, a few grams of oil shale sample were placed into a glass tube fitted with a cap (the glass tube inside diameter was 5.5 cm, and its length was 8 cm, excluding the cap region) and centrifuged 3 times at 6000 rpm for 5 min. The height of the sample was measured, and then the solvent was added in excess to the tube. The content was mixed to achieve complete wetting/mixing, and the tube was centrifuged 3 times at 6000 rpm for 5 min. The height of the swollen sample was measured after centrifugation and then remeasured in 48 h. The swelling behavior of shale was described by the volumetric swelling ratio calculated as $Q = h_2/h_1$, where h_1 is the initial height of the unswollen sample and h_2 is the equilibrium height of the swollen oil shale. To more conveniently present the results as a function of the donor number in some cases, molar solvent uptakes calculated as $(Q - 1)/V_m$ were used, where V_m stands for the solvent molar volume.

Volumetric swelling of kokersite in prepared binary mixtures was performed as shown in our previous paper.⁹ The binary mixtures of solvents were prepared with the desired concentration and were applied in excess, so that each solvent in the applied mixture volume was present in an amount larger than the previously determined solvent uptake volume in the pure solvent swelling.

Thermal Pretreatment. The experimental setup consisted of a sealable cylindrical stainless-steel tube with an inner diameter of 1 cm and a length of 10 cm. This sealed sample holder, containing the oil shale sample in a nitrogen atmosphere, was heated in a circulating air bath from room temperature at a fixed heating rate of 10 °C/min. When the sample reached a selected temperature, it was maintained there for the desired time and then cooled to room temperature. The thermal pretreatment temperatures were varied between 150 and 375 °C. The preheat temperature range did not exceed 375 °C, to avoid significant decomposition of kerogen.

3. Results and Discussion

Thermal-Pretreatment-Induced Changes in Swelling. Six solvents with different polarity, namely, NMP, THF, benzene,

- (10) Lucht, L. M.; Peppas, N. A. *AIP Conf. Proc.* **1981**, *70*, 28–48.
 (11) Karger, B. L.; Snyder, L. R.; Eon, C. J. *Chromatogr.* **1976**, *125*, 71–88.
 (12) Larsen, J. W.; Li, S. *Energy Fuels* **1994**, *8*, 932–936.
 (13) Belmares, M.; Blanco, M.; Goddard, W. A.; Ross, R. B.; Caldwell, G.; Chou, S. H. *J. Comput. Chem.* **2004**, *25*, 1814–26.
 (14) Larsen, W. J.; Parikh, H.; Michels, R. *Org. Geochem.* **2002**, *33*, 1143–1152.
 (15) Hansen, C. M. *Hansen Solubility Parameters: A User's Handbook*; CRC Press: Boca Raton, FL, 2000; pp 1–208.
 (16) Behbehani, G. R.; Hamed, M.; Rajabi, F. H. *Int. J. Vib. Spectrosc.* **2001**, *5* (www.ijvs.com).
 (17) Malavolta, L.; Oliveira, E.; Cilli, E. M.; Nakaie, C. R. *Tetrahedron* **2002**, *58*, 4383–4394.
 (18) Marcus, Y. *J. Solution Chem.* **1984**, *1*, 599–624.

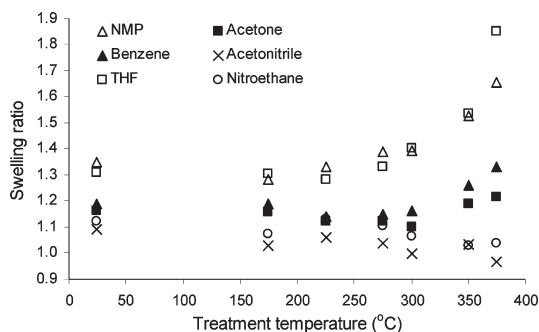


Figure 1. Comparison of the solvent swelling ratios in six solvents resulting from different pretreatment temperatures. The heat treatment time of 1 h was used.

acetone, acetonitrile, and nitroethane, were initially used to track changes in swelling, induced by the thermal pretreatment. Two of the solvents, NMP and THF, were selected to be, in large measure, similar in donor strength to pyridine and DMF, the solvents previously used in coal studies.^{2–4} Figures 1 and 2 present results of measurements of swelling ratios. The samples were pretreated from 175 to about 375 °C with residence times of 1 and 3 h, respectively. The kukersite swelling behavior, seen in these figures, shows that the six solvents appear to group into three pairs: NMP and THF, acetone and benzene, and acetonitrile and nitroethane.

Figure 1 corresponds to a treatment of 1 h. The pair of highest donor number solvents, NMP and THF, shows the highest swelling ratios over the entire pretreatment conditions studied. These are solvents with strong hydrogen-bond capabilities, and both are able to break kerogen–kerogen noncovalent interactions and form new solvent–kerogen noncovalent interactions. Swelling ratios in these solvents behaved similarly when the pretreatment temperatures were in the range from 175 to 350 °C; however, at 375 °C, THF gave greater swelling than NMP. The latter temperature was already in the range of considerable thermobitumen formation, as shown by a change in the solvent color to dark brown, because of an increased amount of soluble formation. It should be noted that solvent extractables from oil shale could influence swelling equilibrium through their effect on solvent activity; however, this effect favors a decrease in the swelling ratio rather than an increase.¹⁴ Therefore, the formation of thermobitumen would be expected to affect swellability opposite the trend seen of increasing swellability in Figure 1.

In the context of this study, the swelling in NMP and THF are expected to be similar to that in pyridine, which has been used as the qualitative indicator of the cross-link density in coal-swelling studies.^{2,3} On the basis of this, if swelling in these solvents is an indicator of the extent of cross-linking, then kukersite is showing a tendency to relax before major pyrolysis (devolatilization) onset. It is similar to the trend seen in high tar yield, softening coals and different from another oil shale from Estonia, *Dictyonema Agrillite*. This latter material is a low oil yield, non-softening oil shale,¹⁹ which was characterized by a decreasing swelling capacity with a pretreatment temperature increase.

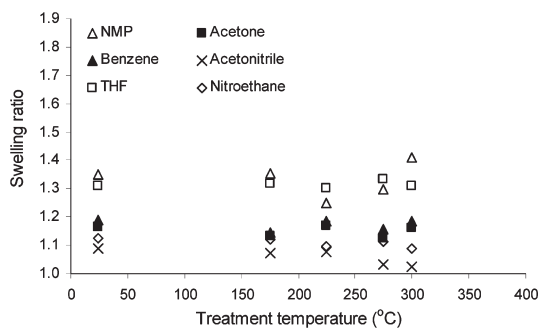


Figure 2. Comparative solvent swelling ratios in six solvents resulting from different pretreatment temperatures after 3 h of treatment time.

The second pair of solvents, benzene and acetone, shows, to a lesser extent, a similar trend to NMP and THF. The swelling in these solvents is characterized by lower swelling and a delayed onset of relaxation; the noticeable increase in the swelling ratio appears at higher temperatures, above 300 °C, compared to 225 °C in NMP and THF. Note that benzene has a solubility parameter of 18.8 MPa^{1/2}, donor number of 0.1, and acceptor number of 8.2, and for acetone, these values are 20.3 MPa^{1/2}, 17.0, and 12.5, respectively. Therefore, the strength of benzene, as the swelling agent, could be its solubility parameter match to the kerogen, and the strength of acetone, in addition to the solubility parameter (similarity in square root of the cohesive energy density), could be its moderate ability to disrupt kerogen–kerogen noncovalent interactions. Which effect if either is more important to describe the difference in the swelling behavior cannot be told from these results. Swelling in last pair of solvents, nitroethane and acetonitrile, shows a much different behavior than the other pairs; swelling capacity decreases with the heat treatment temperature and time. Note that these are poor swelling agents for kukersite; both are characterized by stronger electron acceptor than electron donor properties.

The results of 3 h thermal pretreatment are shown in Figure 2. The trends are in principle similar to those seen in Figure 1. No considerable changes were observed in the temperature range up to 300 °C. These experiments were not carried out to higher temperatures, in an effort to avoid considerable thermobitumen formation. Figure 3 presents fast heat treatment results. The sample was kept at the final heat treatment for 5 min and then cooled rapidly. The swelling in NMP and benzene shows no significant changes with the temperature up to the pretreatment temperature of 350 °C. An increase of the swelling ratio first appears at about 400 °C, around the onset of kukersite devolatilization.⁶ This is not unexpected, because the extent of structural changes occurring during thermal treatment is expected to be time-dependent, so that the changes observed at 350 °C in 1 h are not yet observable at these short times.

To summarize, the results of this investigation presented thus far in Figures 1–3 indicate that kukersite kerogen shows a tendency toward structural relaxation in the low-temperature region. This observation is qualitatively compatible to those seen in high tar yield, softening coals.³

On the basis of the data shown in Figures 1–3, three pretreatment conditions were selected for more detailed

(19) Oja, V.; Elenurm, A.; Rohtla, I.; Tali, E.; Tearo, E.; Yanchilin, A. *Oil Shale* 2007, 24, 101–108.

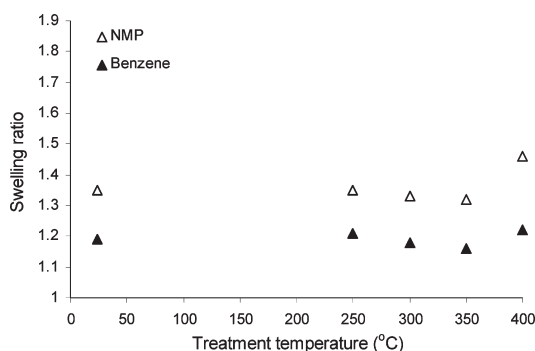


Figure 3. Comparison of solvent swelling ratios in NMP and benzene resulting from different pretreatment temperatures. Fast heat treatment with sample residence time of 5 min.

study using 22 solvents. The conditions were as follows: 1 h at 275 °C, 3 h at 300 °C, and 1 h at 350 °C. The highest temperature of 375 °C in Figure 1 was considered too close to the onset of active pyrolytic reactions based on the visual observation of solvent extraction. The data of Figure 4 illustrate the variation of swelling ratios with the Hildebrand solubility parameters of the solvents. This is a typical method of presentation of swelling results for solubility parameter estimation purposes. The solubility parameter concept would lead to the expectation of a bell-shape distribution of the swelling ratio, with the maximum value matching the macromolecular solubility parameter; often the solubility parameter is estimated from this type plot upon visual observation. In fossil fuel solvent swelling studies, the existence of such clearly defined bell-shape curves is only sometimes seen (with particular choices of solvents) and scattered behaviors, as seen in Figure 4, are usually observed. This indicates that the use of a single parameter, such as the Hildebrand solubility parameter, is clearly not sufficient to describe swelling in these systems. In Figure 4, the nontreated samples (open points) are compared to 350 °C for 1 h heat-treated samples (solid points). The two sets of results are also tabulated in Table 2. Data from the other thermal pretreatment conditions (275 °C for 1 h and 300 °C for 3 h) differed only slightly from the nontreated sample results and are not shown here. It can be seen that the open and solid points in Figure 4 show similar patterns; only the swelling extent magnitudes vary depending upon the solvent character. High swelling values in strongly polar solvents (THF, NMP, pyridine, propylamine, and DMF, for example) can be seen in both treated and untreated cases. These solvents can break kerogen–kerogen noncovalent interactions. In a previous paper from this laboratory,⁹ it was shown that kukersite swelling in pure solvents was solvent-donor-number-dependent, the highest swelling ratios were seen in higher donor number solvents, and the swelling ratio reaches an upper limit above certain donor number values.

Figure 5 replots the data presenting molar uptake as a function of the solvent donor number. The data show that the above observations hold also for the thermally pretreated sample. This suggests that in kukersite exist specific interactions (between moderately to strongly polar solvents and macromolecule structural units) in both nontreated and heat-treated samples and that randomly distributed weak

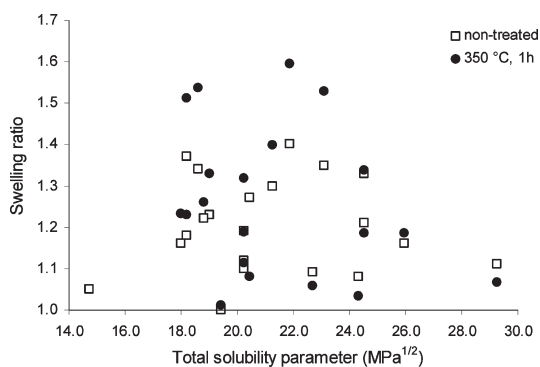


Figure 4. Solvent swelling of kukersite oil shale at room temperature. Results are compared for the nontreated sample and the sample that has undergone the thermal treatment at 350 °C for 1 h. See Table 1 to identify solvents by solubility parameter values.

Table 2. Solvent Swelling of Kukersite Oil Shale at Room Temperature^a

	nontreated sample		heat-treated sample	
	Q	$(Q - 1)/V_m$	Q	$(Q - 1)/V_m$
acetone	1.19	0.0025	1.19	0.0026
aniline	1.30	0.0033	1.40	0.0041
cyclohexanol	1.10	0.0010	1.32	0.0031
DMF	1.33	0.0043	1.34	0.0044
ethanol	1.16	0.0027	1.18	0.0032
MEK	1.23	0.0026	1.33	0.0037
methanol	1.11	0.0026	1.07	0.0016
NMP	1.35	0.0036	1.53	0.0055
<i>n</i> -propanol	1.20	0.0027	1.19	0.0025
propylamine	1.37	0.0045	1.51	0.0062
pyridine	1.40	0.0050	1.59	0.0074
tetrahydrofuran	1.34	0.0042	1.54	0.0066
1-methylnaphthalene	1.12	0.0009	1.11	0.0008
benzene	1.22	0.0025	1.26	0.0029
hexane	1.05	0.0004	1.00 ^b	0.0000
<i>o</i> -xylene	1.16	0.0013	1.23	0.0019
tetraline	1.00	0.0000	1.01	0.0001
toluene	1.18	0.0017	1.23	0.0022
acetonitrile	1.08	0.0016	1.03	0.0006
nitrobenzene	1.27	0.0026	1.08	0.0008
nitroethane	1.09	0.0013	1.06	0.0008
nitromethane	1.05	0.0009	1.06 ^c	0.0011

^a Swelling ratios, Q , and solvent molar uptakes, $(Q - 1)/V_m$, are shown for the nontreated sample and the sample that has undergone the thermal treatment at 350 °C for 1 h. DMF, dimethylformamide; NMP, *n*-methyl-2-pyrrolidinone; MEK, methyl ethyl ketone. ^b Approximated to 1; a slight shrinking was detected. ^c An approximate value because there were a thin layer of particles formed above the solvent layer.

interactions, which are the basis for regular solution theory, are of secondary importance.

Despite this, for illustrative purposes, the following straightforward determination of the kerogen solubility parameter is used by applying Gee's equation.²⁰ This is a Gaussian error function based approach of the principle that maximum swelling occurs in the solvent, with the solubility parameter equal to that of the cross-linked macromolecule. The formula of Gee

$$\frac{Q}{Q_{\max}} = \exp[-aQ(\delta_{\text{solvent}} - \delta)^2] \quad (1)$$

(20) Gee, G. *Trans., Inst. Rubber Ind.* **1943**, *18*, 266–281.

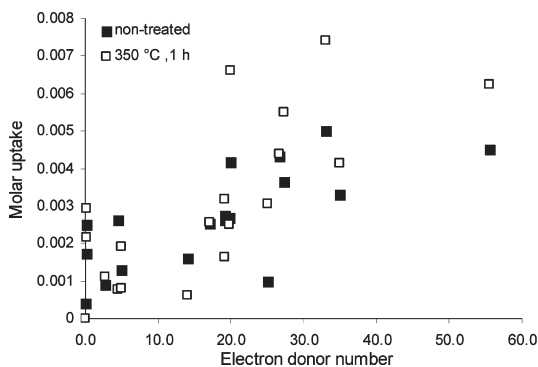


Figure 5. Variation of solvent molar uptake, $(Q - 1)/V_m$, with Guttman's electron donor numbers of solvents. Results are compared for the nontreated sample and the sample that has gone through thermal pretreatment at 350 °C for 1 h. See Table 1 to identify solvents by electron donor number values.

where Q and Q_{\max} are the swelling ratio and the maximum swelling ratio, respectively, δ_{solvent} and δ are the solubility parameters of the solvent and macromolecule, respectively, and a is a constant. The macromolecule solubility parameter can be determined from a rearranged eq 1 by plotting $[Q^{-1} \ln(Q_{\max}/Q)]^{1/2}$ versus δ_{solvent} .^{20–22} The three-dimensional Hansen solubility parameters were similarly estimated. The tentative solubility parameters thus obtained are given in Table 3. The results illustrate that the thermal pretreatment does not have a significant effect on solubility parameter values or, in other words, the thermal pretreatment conditions applied do not change the basic chemical nature of kukersite considerably.

Swelling of Heat-Treated Samples in Solvent Mixtures.

Another way of gaining insights into the process occurring in the kerogen network is through use of swelling in binary mixtures. Again, the solubility parameter concept suggests that, at maximum swelling, the solubility parameter of the macromolecule and in this case of the solvent mixture should match; in the other words, the solvent mixture and the macromolecule should have energetic similarity. Thus, the combination of solvents with lower and higher solubility parameters than that of the macromolecule can result in a maximum at higher swelling than in either solvent alone.²³ On the basis of the previous study from this laboratory,⁹ two types of binary mixtures were selected for these experiments: benzene–propanol and benzene–NMP. The basis for selecting these particular binary mixture components was that there should be non-associative behavior between each other (they are assumed not to be attracted to each other, which of course, is not entirely true).²⁴ Figures 6 and 7 are the results of swelling the kukersite samples in binary mixtures. The nature of the curves has been discussed in more details in earlier work from this laboratory.⁹ Binary mixture solubility parameters shown on the horizontal axes were based on

Table 3. Total and Hansen Solubility Parameters Obtained for Nontreated and Thermally Pretreated Kukersite Kerogens Using Gee's Equation^a

solubility parameter	275 °C for 1 h	350 °C for 1 h	300 °C for 3 h	nontreated
Hildebrand or total, δ	22.3	22.0	21.8	22.0
Hansen dispersion, δ_d	18.5	18.2	18.5	18.4
Hansen polar, δ_p	8.9	7.8	8.0	9.2
Hansen hydrogen-bonding, δ_h	10.3	9.7	8.2	10.5
$\delta_{\text{calc}} = \sqrt{\delta_d^2 + \delta_p^2 + \delta_h^2}$	23.0	22.1	21.8	23.1

^a The total solubility parameters δ_{calc} (in principle, the same as the Hildebrand solubility parameter) were calculated from three determined Hansen solubility parameters. Units are in $\text{MPa}^{1/2}$.

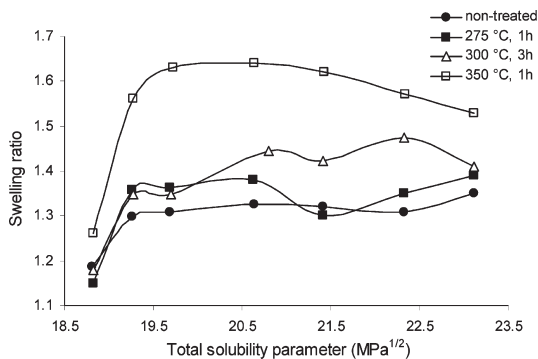


Figure 6. Swelling of raw and thermally pretreated samples in benzene–NMP mixtures as a function of the binary mixture solubility parameter. Solubility parameters of pure solvents are 18.8 and 23.1 $\text{MPa}^{1/2}$ for benzene and NMP, respectively, and molar volumes are 89.4 and 96.5 cm^3/mol correspondingly.

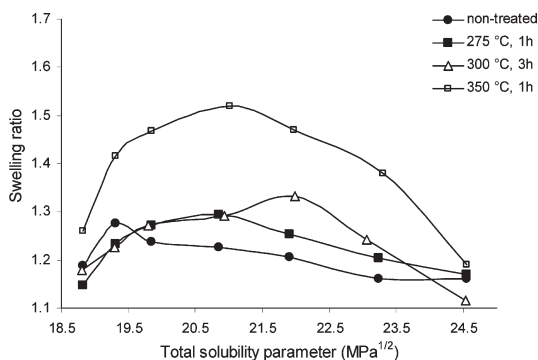


Figure 7. Swelling of raw and thermally pretreated samples in benzene–propanol mixtures as a function of the binary mixture solubility parameter. Solubility parameters of pure solvents are 18.8 and 24.5 $\text{MPa}^{1/2}$ for benzene and *n*-propanol, respectively, and molar volumes are 89.4 and 75.2 cm^3/mol correspondingly.

(21) Yagi, Y.; Inomata, H.; Saito, S. *Macromolecules* **1992**, *25*, 2997–2998.

(22) Alli, A.; Hazer, B.; Baysal, B. M. *Eur. Polym. J.* **2006**, *42*, 3024–3031.

(23) Tereshatov, V. V.; Senichev, V. Y.; Denisjuk, E. Y. In *Handbook of Solvents*; Wypych, G., Ed.; ChemTec Publishing: Toronto, Ontario, Canada, 2001; pp 318–327.

(24) Westbrook, P. A.; French, R. N. *Polym. Eng. Sci.* **2007**, *47*, 1554–1568.

mixture composition and calculated as follows: $\delta_{\text{mix}} = \sum(\theta_i \delta_i)$, where δ_{mix} is the solubility parameter of the binary solvent mixture and δ_i and θ_i are the solubility parameters and the volume fraction of the solvents in the binary mixture. This assumes that kukersite kerogen does not undergo selective uptake of solvents into the swollen network. For the benzene–NMP mixture, this may be only a crude

approximation, and it is probably not even the case for the swelling in the benzene–propanol mixture.⁹

The results from swelling experiments with the benzene–NMP mixture are shown in Figure 6. The behavior is typical of that seen in the previous study for kukersite kerogen swelling in a binary mixture of a nonpolar solvent and a strong electron donor.⁹ A total of 10–20% of NMP in the mixture (points corresponding to the total solubility parameter values below 20 MPa^{1/2} in Figure 6) is sufficient to raise the swelling ratio to a level comparable to that in pure NMP, the high donor number solvent. In the case of the nontreated sample, additional NMP does not change the swelling extent significantly.

A somewhat different pattern emerges for NMP swelling of the pretreated samples, especially of the 350 °C sample. In the case of the 350 °C sample, after a sharp increase at low NMP concentrations, for concentrations from 20 to 100%, the swelling ratios change smoothly with the mixture solubility parameter: first there is a slight increase, and then after passing through a maximum (at about 21 MPa^{1/2}), a decrease to a lower value corresponding to swelling in pure NMP. The swelling ratio at the maximum is considerably higher than that in pure NMP, about 1.64 relative to 1.53 in pure NMP. This might indicate that, although the specific interactions in the system of NMP with the kukersite are essential for breaking the noncovalent cross-links, the binary mixture solubility parameter match with kerogen segments contribute to finalize the extent of swelling.

Figure 7 shows the curves obtained from swelling experiments with benzene–propanol mixtures, a nonpolar solvent in the mixture with a moderate electron donor. Several observations can be made. The swelling behavior indicates something that is close to “ideal” thermodynamic swelling theories: a swelling ratio curve that smoothly changes through a maximum and that is considerably higher than the swelling capacity of pure solvents alone. An especially nicely shaped parabolic curve emerges in the case of the 350 °C sample. It is also seen that there is a variation in the maximum with pretreatment conditions and that the deviation between the swelling ratios at the curve maximum and those in pure solvents increases with a pretreatment temperature increase. For example, the thermal

pretreatment at 350 °C results in maximum swelling ($Q = 1.52$) close to the swelling in pure NMP ($Q = 1.53$) or pure THF ($Q = 1.54$).

Finally, it is of interest to note that an examination of the data in Figures 6 and 7 reveals at least two common features. First, the maxima (in some cases, local maxima, for the samples treated at 275 and 300 °C) seem to appear roughly at the same binary mixture solubility parameter values. Second, there seems to be similar trends with the pretreatment temperature in both figures: 275 °C pretreatment shows behavior close to the nontreated sample; 300 °C pretreatment indicates a swelling ratio increase at concentrations richer in the solvent with better donor properties; and in the case of 350 °C pretreatment, the network structure is clearly most relaxed and beginning to approach the “ideal” swelling behavior (at least to something that resembles it). These results show the combined importance of specific and non-specific interactions in swelling and suggest that the specific interaction influence decreases with an increasing severity of pretreatment.

4. Conclusions

The results of this investigation indicate that the kukersite kerogen shows tendency toward structural relaxation in the low-temperature prepyrolysis region. This observation is qualitatively compatible to those seen in high tar yield, softening coals.

It is also seen that the thermal pretreatment causes no drastic changes in a general pattern of swelling behavior: kukersite still swells to the greatest extent in high donor number solvents (with strong hydrogen-bond-forming capabilities); the swelling ratio reaches the upper limit, although with a somewhat different value, depending upon pretreatment, above certain donor number values; and the solubility parameter approach is of secondary importance in describing swellability, although its influence seems to grow with the extent of pretreatment.

Acknowledgment. The authors are very grateful to Professor Eric Suuberg from Brown University for helpful advice and editorial comments. The Estonian Science Foundation under grand G7222 supported the work presented here.

ARTICLE II

Kilk, K.; Savest, N.; **Hruljova, J.**; Tearo, E.; Kamenev, S.; Oja, V. (2010). Solvent swelling of Dictyonema oil shale. – *Oil Shale*, 27 (1), 26–36.

SOLVENT SWELLING OF DICTYONEMA OIL SHALE

K. KILK, N. SAVEST, J. HRULJOVA, E. TEARO,
S. KAMENEV, V. OJA *

Department of Chemical Engineering
Tallinn University of Technology
Ehitajate Rd. 5, 19086 Tallinn, Estonia

The present work investigates volumetric swelling of Estonian Dictyonema oil shale, as a representative of black shales of the Baltoscandian basin, in 22 solvents. This study shows that kerogen of Dictyonema oil shale is characterized by a low degree of swelling indicating a highly cross-linked structure. The relatively high swellability in high Guttmann's electron donor number solvents indicates the importance of non-covalent cross-links, such as hydrogen bonding, in swelling process and raises concern regarding the use of regular solution-based approaches. Despite this, the solubility parameter, a fundamental thermodynamic property, was tentatively determined from swelling data.

Introduction

Solvent swelling is a frequently applied low-cost technique to obtain experimental information on cross-linked macromolecular substances, including solid fuels such as coal [1, 2] and oil shales [3-6]. Solvent uptake data can determine solubility parameters and, by using suitable swelling models, the macromolecular structure can be characterized by estimating crosslink densities (or number average molecular weights between cross-links) [1, 6, 7]. The crosslink density (degree of cross-linking) has been a useful input parameter in coal devolatilization/pyrolysis modeling [8].

The present study uses the equilibrium solvent swelling data to characterize Dictyonema oil shale (Termadocian black shale) from Estonia – as a representative of the black shales of the Baltoscandian basin. Organic matter content of Dictyonema oil shales is typically 10–20% with an average elemental composition of (wt%) C: 58.3–76.0; H: 5.3–7.4; N: 1.88–4.24; S: 1.61–4.56; O: 12.22–34.3 [9]. The organic component of Dictyonema oil shales is known to contain relatively low amounts of solvent-soluble compounds – below 2.5%, organic matter basis [10]. Most importantly, as

* Corresponding author: e-mail vahur.oja@ttu.ee

being a low oil yield oil shale [11] (exemplary Fischer assay, ISO-647-74, yields (wt%, daf): oil – 19.6, semicoking gas – 16.5, semicoke – 45.4 and water – 18.5 [12]), its processing by *ex situ* retorting technologies is not considered economical. However, despite this, Dictyonema oil shale may be a prospective resource of energy and chemicals.

The specific objectives of this paper were to evaluate the role of specific interactions (non-covalent crosslinks) in swelling and to get some indication whether or not approaches based on classical regular solution theory could be used for determining, at least for indicative purposes, crosslink density in the case of Dictyonema oil shale.

Materials and methods

The Dictyonema oil shale sample of North-Estonia was taken from a layer about 10 m underground. Its organic content is 13 wt%. The sample was characterized as follows: ash 86%, carbonates 2%, and elemental analysis results (wt%) C – 6.7, H – 0.9, N – 0.3, residue – 92.1 (giving H/C ratio of 1.56). The elemental composition of the organic matter was determined by an elemental analyzer Exeter Analytical model CE440.

Dictyonema oil shales are known to contain significant amounts of clay minerals (mostly illite and smectite [13]) that can swell/shrink in organic solvents. For example, mixed-layer clays with 70% clay content, mostly illite and smectite, [14] have been shown to swell/shrink in solvents with solubility parameter values between 15 to 25 (MPa)^{1/2} (for example, the swelling ratios measured were 0.99 in hexane, 1.11 in acetone, 1.13 in acetonitrile or 1.19 in N,N-dimethylformamide). Therefore, acid treatment with HF was used to transform original shale minerals into nonswellable form, despite the fact that acid treatment may result in some changes in the kerogen [15]. For HF treatment, 0.5 litres of 1:1 HF (with water) was added slowly to 100 grams of previously crushed/ground (size < 1 mm) shale in an 1-liter flask at 0 °C. After mixing for 24 hours, the suspension was filtered and distilled-water washing was used to neutralize the acid-treated sample. The sample was dried in air at 100 °C for 1 hour. No original clay minerals were observed after acid treatment, the only original mineral left was pyrite. The major mineral formed was hieratite (K₂SiF₆). Finally, the sample was ground and sieved to get a size fraction of 0.32–100 µm. The organic content of the acid treated shale was roughly estimated to be about 25 wt%.

Solvent swelling experiments were performed with 22 solvents. All solvents were of analytical grade and used without further purification. They were selected to cover a wide range of solubility parameter values. The solvents are listed in Table 1 together with their key characteristics: molar volumes [16], solubility parameters (Hildebrand or total [6, 17, 18]; three dimensional Hansen solubility parameters [16]), Guttmann's electron donor numbers (EDN) and electron acceptor numbers (EAN) [19, 20].

Table 1. Key characteristics of solvents used in swelling studies: molar volumes (V_m), solubility parameters (Hildebrand δ ; dispersion δ_D ; polar δ_P ; hydrogen-bonding δ_H) and Guttmann's electron donor numbers (EDN), and electron acceptor numbers (EAN)

	Solvents	V_m , cm ³ /mol	δ , (MPa) ^{1/2}	δ_D , (MPa) ^{1/2}	δ_P , (MPa) ^{1/2}	δ_H , (MPa) ^{1/2}	EAN	EAN
1	Acetone	74.0	20.3	15.5	10.4	7.0	17.0	12.5
2	Acetonitrile	52.6	24.3	15.3	18.0	6.1	14.1	18.9
3	Aniline	91.5	21.3	19.4	5.1	10.2	35	
4	DMF	77.0	24.5	17.4	13.7	11.3	26.6	16.0
5	Ethanol	58.5	26.0	15.8	8.8	19.4	19.2	37.1
6	MEK	90.1	19.0	16.0	9.0	5.1		
7	Methanol	40.7	29.3	15.1	12.3	22.3	19.1	41.3
8	NMP	96.5	23.1	18.0	12.3	7.2	27.3	13.3
9	<i>n</i> -Propanol	75.2	24.5	16.0	6.8	17.4	19.8	37.7
10	Propylamine*	83.0	18.2	16.9	4.9	8.6	55.5	
11	Pyridine	80.9	21.9	19.0	8.8	5.9	33.1	14.2
12	Tetrahydrofuran	81.7	18.6	16.8	5.7	8.0	20.0	8.0
13	Benzylalcohol	103.6	24.8	18.4	6.3	13.7	23.0	36.8
14	Methylnaphthalene	138.8	20.3	20.6	0.8	4.7		
15	Benzene	89.4	18.8	18.4	0.0	2.0	0.1	8.2
16	Hexane	131.6	14.7	14.9	0.0	0.0	0.0	0.0
17	<i>o</i> -Xylene	106.8	18.0	17.8	1.0	3.1	5	
18	Toluene	102.7	18.2	18.0	1.4	2.0	0.1	
19	Nitrobenzene	71.5	20.5	20.0	8.6	4.1	4.4	3.3
20	Nitroethane	54.3	22.7	16.0	15.5	4.5	5	14.8
21	Nitromethane	63.9	26.0	15.8	18.8	5.1	2.7	
22	Dichloromethane**	106.8	20.3	18.2	6.3	6.1	0.0	20.5

DMF stands for dimethylformamide; NMP stands for *n*-methyl-2-pyrrolidinone; MEK stands for methyl ethyl ketone;

* ethylamine EDN and EAN values were used for propylamine;

** 1,2-dichloroethane EDN and EAN values were used for dichloromethane.

The volumetric solvent swelling procedure used was described in our previous paper [3]. In short, a few grams of oil shale sample was placed into a glass-tube with a cap (glass tube inside diameter 5.5 cm and length 8 cm without a cap region) and centrifuged three times at 6000 rpm for 5 minutes. The height of the sample was measured using a caliper ruler. Solvent in excess was added to the tube, mixed to achieve complete wetting/mixing and centrifuged three times at 6000 rpm for 5 minutes. The height of the sample was recorded after centrifugation and re-measured in 48 hours. The swelling behavior of Dictyonema oil shale is described by the volumetric swelling ratio calculated as $Q = h_2/h_1$, where h_1 – initial height of the un-swollen sample and h_2 – equilibrium height of swollen oil shale. In order to more conveniently compare/analyze results, also swelling ratio on a dry mineral matter-free basis, Q_{dmmf} , and molar solvent uptake as $(Q_{dmmf} - 1)/V_m$ were used. The Q_{dmmf} were determined from the equation (1):

$$Q_{dmnf} = \frac{Q - \frac{x_{min} \cdot \rho_{org}}{x_{org} \cdot \rho_{min} + x_{min} \cdot \rho_{org}}}{1 - \frac{x_{min} \cdot \rho_{org}}{x_{org} \cdot \rho_{min} + x_{min} \cdot \rho_{org}}}, \quad (1)$$

where x_{org} is the kerogen mass fraction, x_{min} is the mass fraction of mineral matter, ρ_{org} is the kerogen density (taken 1.15 g/cm³, estimated from densities of Type II kerogens [21–23]) and ρ_{min} is the density of mineral matter (taken 2.65 g/cm³, the density of oil shale mineral illite [24]).

Results and discussions

Table 2 presents swelling data of dried acid-treated Dictyonema oil shale samples in 22 solvents. The data is re-plotted in Fig. 1 to illustrate graphically variation of swelling ratios (dry mineral free matter basis) with Hildebrand solubility parameters of solvents. This is a traditional way to present swelling results for estimation of solubility parameter. Formation of a bell-shape curve

Table 2. Swelling characterized by means of swelling ratio Q and swelling ratio on dry mineral ash free basis Q_{dmnf} . The Q_{dmnf} was calculated using equation (1)

No	Solvent	Q	Q_{dmnf}
1	Acetone	0.95	0.89
2	Acetonitrile	0.95	0.89
3	Aniline	1.09	1.20
4	DMF	1.06	1.15
5	Ethanol	1.00	0.99
6	MEK	0.97	0.92
7	Methanol	0.98	0.96
8	NMP	1.03	1.07
9	<i>n</i> -Propanol	0.97	0.93
10	Propylamine	1.05	1.12
11	Pyridine	1.07	1.16
12	Tetrahydrofuran	1.06	1.13
13	Benzylalcohol	1.01	1.01
14	1-methylnaphthalene	0.99	0.97
15	Benzene	0.99	0.97
16	Hexane	0.96	0.91
17	<i>o</i> -Xylene	0.97	0.93
18	Toluene	1.02	1.04
19	Nitrobenzene	1.00	1.00
20	Nitroethane	0.98	0.96
21	Nitromethane	0.97	0.93
22	Dichloromethane	1.02	1.05

DMF stands for dimethylformamide;
 NMP stands for *n*-methyl-2-pyrrolidinone;
 MEK stands for methyl ethyl ketone;

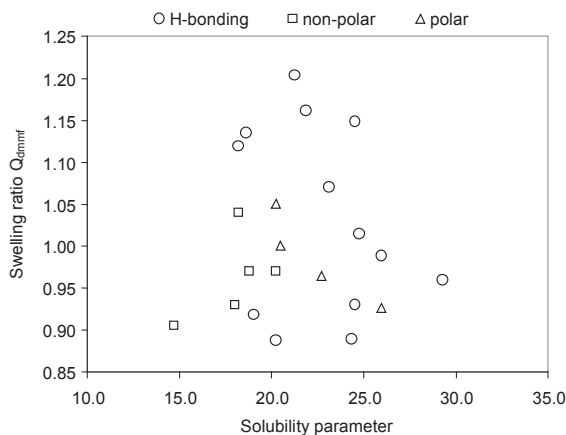


Fig. 1. Equilibrium swelling ratios, dry mineral matter free kerogen basis, as a function of solvent solubility parameters (Hildebrand solubility parameter). Circles correspond to swelling in hydrogen-bonding solvents, triangles in polar solvents and squares in non-polar solvents. See Table 1 to identify solvents by solubility parameter values and Table 2 by swelling ratio values.

should be expected when randomly distributed weak non-specific interactions dominate in swollen network. The swelling ratios and corresponding solvent solubility parameters in Fig. 1 show no clearly determinable pattern suggesting that chemical character causes specific interactions between solvents and kerogen plays important role in the swelling process. There are several observations that can be made regarding the swelling behavior of Dictyonema oil shale from this figure. It is useful to mention that our other unpublished data on several non-acid treated Dictyonema oil shales, both dried and non-dried, support the trends to be shown below.

First, comparison with literature data available on oil shales and coals reveals that Dictyonema oil shale is characterized by a considerably lower swelling capacity indicating the existence of tightly cross-linked structure. The maximum swelling ratio observed in mineral matter free bases was as low as 1.2 (see Fig. 1 and Table 2). For comparative purposes the following are some swelling extent maxima on dry ash free basis of some other oil shales: 1.4–1.7 for Kukersite oil shale, up to 1.8 for Rundle oil shale, 1.6–1.9 for Green River oil shale, 1.3–1.7 for Paris Basin Toarcian oil shale or about 1.6 for Göynyk oil shale. Note that these values are approximate, as these were estimated using equation (1) from available literature data [3–6]. Second, Dictyonema oil shale practically does not swell in non-polar solvents, and considerable swelling can be seen mostly in hydrogen-bonding solvents with high Gutmann's electron donor numbers (EDN). Generally, oil shale kerogens, the complex crosslinked macromolecules, are known to have

two types of cross-links: covalent and non-covalent ones. While the covalent crosslink density is constant, then the non-covalent crosslinks or specific shale-shale interactions can be disrupted by specifically interacting solvents causing higher swelling in these solvents. As Dictyonema oil shale shows significantly higher swellability in hydrogen bonding solvents with high EDN values (indicating importance of non-covalent or specific interactions such as hydrogen bonds), the data is re-plotted in Fig. 2 by means of molar solvent uptake as a function of EDN. The molar solvent uptake is used instead of the swelling ratio in order to eliminate the effect of solvent molar volume on solvent absorption extent. Figure 2 reveals that there could be a better correlation with swelling capacity. It can be seen how the molar solvent uptake increases with EDN increase up to a limiting value as expected [25] – the limiting molar solvent uptake is reached at about solvent EDN value of 25. It would follow that the greatest swelling extents are to be expected in hydrogen bonding solvents with highest EDN values, while some exceptions, toluene and dichloromethane (with practically zero EDN values and relatively high EAN values), could still result in comparatively greater swelling extents. Finally, noticeable shrinking, instead of swelling, was observed with several non-polar and polar solvents. It is worth noting that the shrinking appeared also in swelling of non-acid treated Dictyonema oil shale, in the case of both non-dried and dried samples. Although the shrinking is not a common experimentally seen behavior, still it is not

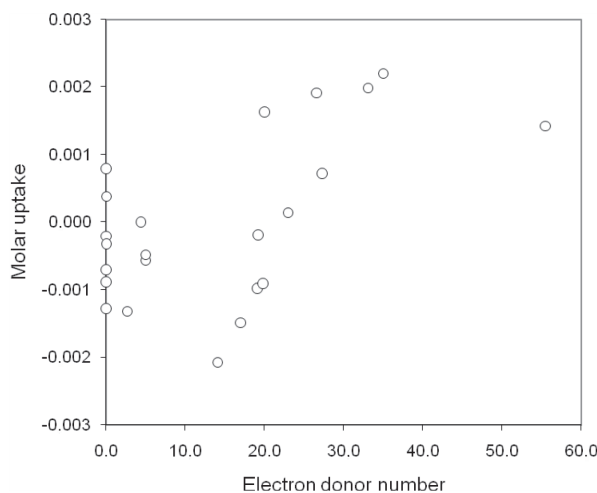


Fig. 2. Degree of swelling represented as a molar solvent uptake, $(Q_{dmf} - 1)/V_m$, versus solvent Guttmann's electron donor number. The shrinking behavior is the reason for the negative values of the molar solvent uptake in the case of several solvents.

unusual phenomenon in solvent swelling studies, and a slight shrinking has been observed also in other occasions: for example in the cases of petroleum asphaltenes [26], explained based on non-uniformity of the sample particle size, or in swelling of clay minerals [14]. One plausible reason for the shrinking behavior of Dictyonema oil shale could be rearrangement of kerogen structure in the presence of swelling agent assuming that the dry-state structure may not be the thermodynamically most stable one [27].

The major implication of the results shown in Table 2, also represented in Fig. 1 and 2, is that for Dictyonema oil shale, the highest swelling extents can be seen in specifically interacting solvents (in hydrogen bonding solvents with high EDN values, such as pyridine, NMP, tetrahydrofuran, propylamine), and this emphasizes the concern regarding the use of regular-solution based approaches. However, at present, there is no consensus as to what degree of non-ideality one should use regular solution based approaches. Therefore, simple models have been extended to quite complex systems, including coals [7] and oil shales [6], to estimate at least semi-quantitatively useful properties. Thus, the following is pursued only for comparative purposes as information on some other shales is available from literature: for Green River [6], Beypazari [4] and Göynük [4] oil shales using the Flory-Rehner model and its extension, the Kovak model [1, 28]. The main advantage of these models is that structure properties can be estimated from swelling data using a few key parameters: the macromolecule volume fraction in swollen network (from swelling ratio) and the Flory-Huggins interaction parameter (calculable from solubility parameter values of the macromolecule and the solvent).

In order to get a reasonable estimate on volume fraction of kerogen in swollen network (equal to reciprocal value of the swelling ratio) from swelling data, the lowest swelling ratio ($Q_{dmnf} = 0.89$ for acetone) was taken to be 1, and others were corrected accordingly by adding 0.11 to corresponding swelling ratios Q_{dmnf} . It could be assumed that the shrinking was caused by re-arrangement of molecular structures, and thus the lowest swelling ratio was taken to be a so-called „reference state”. Of course, this assumption is debatable.

Another largest source of uncertainty comes from the interaction parameter (χ) as the choice of proper value of χ is not presently clear. There has been a very limited amount of work found on the coal-solvent [29], and not at all for oil shale kerogen-solvent, interaction parameters. Therefore the solvent-kerogen interaction parameters were calculated in accordance with the suggestive equation [30]:

$$\chi = \chi_s + \frac{V_s}{RT}(\delta_s - \delta)^2, \quad (2)$$

where χ is interaction parameter, χ_s is taken constant with a value of 0.35, R is ideal gas constant, T is temperature, V_s is molar volume of the solvent, δ_s is solubility parameter of solvent and δ is solubility parameter of macromolecule, here of kerogen.

Table 3 presents tentative estimates of solubility parameters of Dictyonema oil shale kerogen (Hildebrand solubility parameter and three Hansen partial solubility parameters) from swelling data using Gee's approach [31, 32] – a graphical determination of solubility parameter, based on the assumption that the solubility parameter of a macromolecule matches the solubility parameter of solvents of maximum swelling (in principle the bell-shape curve seen Fig. 1). The formula of Gee is given as:

$$\frac{Q}{Q_{max}} = \exp[-aQ(\delta_s - \delta)^2], \quad (3)$$

where Q and Q_{max} are the swelling ratio and the maximum swelling ratio respectively, δ_s and δ are the solubility parameters of solvent and macromolecule respectively, and a is a constant. The macromolecule solubility parameter can be determined from a rearranged equation (3) by plotting $[Q^{-1} \ln(Q_{max}/Q)]^{1/2}$ versus δ_s of solvents used [31, 32]. Figure 3 shows an exemplary evaluation of the solubility parameters based on the Gee's approach for Hildebrand solubility parameter. The Hildebrand solubility parameter value of 22 (MPa)^{1/2} corresponds to the linear regression line interception of the horizontal axis or the ratio of intercept and slope. Again, the data scattering seen on the plot indicates that the randomly distributed weak interactions, which are the basis for regular solution theory, are of secondary importance. The three-dimensional Hansen solubility parameters were similarly estimated. It is noteworthy that close values of solubility parameter were obtained in the case of all solvents and in the case of reduced number of solvents (for the solvents with EDN < AEN), indicating rudeness of the method used.

Tentative calculations for the number average molecular weights between cross-links are presented in Table 4 for two equations (swelling models): Flory-Rehner and Kovac equations [1, 28]. The results seem to underestimate the number average molecular weights between the cross-links for Dictyonema oil shale. Generally, oil shale thermo-chemical conversion tarry products, both thermobitumen and pyrolysis tar, show much higher number average molecular weight values [33, 34].

Table 3. Solubility parameters [(MPa)^{1/2}] determined tentatively by Gee's method. The total solubility parameter (in principle the Hildebrand solubility parameter) calculated from three determined Hansen solubility parameters are shown for comparison

	$\delta_{Hildebrand}$	δ_D	δ_P	δ_H	$\delta_t = \sqrt{\delta_D^2 + \delta_P^2 + \delta_H^2}$
All solvents	22	19	6	12	23
Selected solvents*	22	18	6	11	22

* the selected solvents are solvents with EDN < EAN

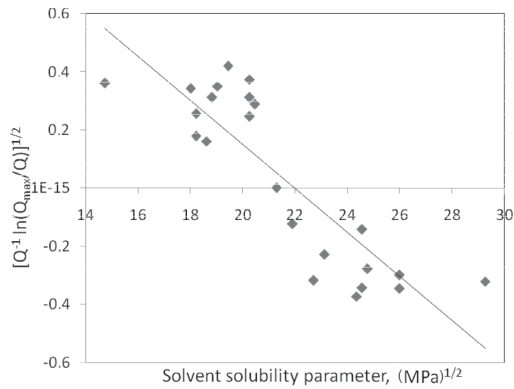


Fig. 3. Determination of the Hildebrand solubility parameter by plotting $[Q^{-1} \ln(Q_{max}/Q)]^{1/2}$ as a function of solubility parameters (δ_s) of solvents. The scatter on the plot indicates the role of non-covalent interactions (especially hydrogen bonds) and that of the randomly distributed weak interactions, which are the basis for regular solution theory, are of secondary importance.

Table 4. Average values of calculated number average molecular weights per cross-links for Dictyonema oil shale. Literature values for other oil shales (Green River [6], Göynük [4], Beypazari [4]) are shown for comparison

Oil shale	Flory-Rehner	Kovac $N = 1$	Kovac $N = 2$	Kovac $N = 3$
Dictyonema	83	373	274	241
Göynük	247	933	678	593
Beypazari	208	790	576	504
Green River (5.2% mineral)	215	808	581	505

N is the number of rotatable segments between branch points in the Kovac equation.

Conclusions

The low swelling capacity of Dictyonema oil shale in organic solvents suggests a highly cross-linked structure of the kerogen. Sensitivity of swellability to solvent donor numbers indicates the importance of non-covalent crosslinks (kerogen-solvent specific interactions such as hydrogen bonds) and suggests that models, that expect randomly distributed weak interactions, may not be suitable for describing Dictyonema oil shale. The simplest models used show underestimation of the number average molecular weights between crosslinks.

Acknowledgements

The authors wish to thank the Institute of Geology of TTU for providing Dictyonema Agrillite samples. This work received financial support from the Estonian Science Foundation, under Grant 7222.

REFERENCES

1. *Lutch, L. M., Peppas, N. A.* Crosslinked macromolecular structures in bituminous coals: Theoretical and experimental considerations // AIP Conf. Proc. 1981. Vol. 70, No. 1. P. 28–48.
2. *Otake, Y., Suuberg, E. M.* Temperature dependence of solvent swelling and diffusion processes in coals // Energ. Fuel. 1997. Vol. 11, No. 6. P. 1155–1164.
3. *Savest, N., Oja, V., Kaevand, T., Lille, U.* // Fuel. 2007. Vol. 86, No. 1–2. P. 17–21.
4. *Ballice, L.* Solvent swelling studies of Göynük (Kerogen Type-I) and Beypazari oil shales (Kerogen Type-II) // Fuel. 2003. Vol. 82, No. 11. P. 1317–1321.
5. *Larsen, J. W., Li, S.* An initial comparison of the interactions of Type I and III kerogens with organic liquids // Org. Geochem. 1997. Vol. 26, No. 5/6. P. 305–309.
6. *Larsen, J. W., Li, S.* Solvent swelling studies of Green River kerogen // Energ. Fuel. 1994. Vol. 8, No. 4. P. 932–936.
7. *Solomon, P. R., Serio, M. A., Suuberg, E. M.* Coal pyrolysis: experiments, kinetic rates and mechanisms // Prog. Energ. Combust. 1992. Vol. 18. No. 2. P. 133–220.
8. *Solomon, P. R., Hamblen, D. G., Carangelo, R. M., Serio, M. A., Deshpande, G. V.* General model of coal devolatilization // Energ. Fuel. 1988. Vol. 2, No. 4. P. 405–422.
9. *Fomina, A. S.* Chemical Composition of Baltic Oil Shale Kerogen // United Nations Symposium on the Development and Utilization of Oil Shale Resources. – Tallinn: Academy of Science of Estonian SSR, 1968.
10. *Koel, M., Ljovin, S., Hollis, K., Rubin, J.* Using neoteric solvents in oil shale studies // Pure Appl. Chem. 2001. Vol. 73, No. 1. P. 153–159.
11. *Oja, V.* Is it time to improve the status of oil shale science? // Oil Shale. 2007. Vol. 24, No. 2. P. 97–99.
12. *Elenurm, A., Oja, V., Tali, E., Tearo, E., Yanchilin, A.* Thermal processing of dictyonema argillite and kukersite oil shale: transformation and distribution of sulfur compounds in pilot-scale Galoter process // Oil Shale. 2008. Vol. 25, No. 3. P. 328–334.
13. *Loog, A., Kurvits, T., Aruväli, J., Petersell, V.* Grain size analysis and mineralogy of the Tremadocian Dictyonema shale in Estonia // Oil Shale. 2001. Vol. 18, No. 4. P. 281–297.
14. *Graber, E. R., Mingelgrin, U.* Clay swelling and regular solution theory // Environ. Sci. Technol. 1994. Vol. 28, No. 13. P. 2360–2365.
15. *Mesci, N., Senelet, A., Togrul, T., Olcay, A.* Effect of acid treatment on volumetric swelling ratios of coals // Turk. J. Chem. 2001. Vol. 25, No. 4. P. 397–403.
16. *Hansen, C. M.* Hansen Solubility Parameters: A User's Handbook. – Boca Raton, Florida: CRC Press, 2000.
17. *Karger, B. L., Snyder, L. R., Eon, C.* An expanded solubility parameter treatment for classification and use of chromatographic solvents and adsorbents. Parameters for dispersion, dipole and hydrogen bonding interactions // J. Chromatogr. 1976. Vol. 125, No. 1. P. 71–88.
18. *Terada, M., Marchessault, R. H.* Determination of solubility parameters for poly(3-hydroxyalkanoates) // Int. J. Biol. Macromol. 1999. Vol. 25, No. 1–3. P. 207–215.

19. *Behbehani, G. R., Hamed, M., Rajabi, F. H.* The solvation of urea, tetramethylurea, TMU, in some organic solvents // *Int. J. Vib. Spec.* 2001. Vol. 5, No. 6. [<http://www.ijvs.com/volume5/edition6/section3.html>].
20. *Malavolta, L., Oliveira, E., Cilli, E. M., Nakaie, C. R.* Solvation of polymers as model for solvent effect investigation: proposition of a novel polarity scale // *Tetrahedron.* 2002. Vol. 58, No. 22. P. 4383–4394.
21. *Okiongbo, K. S., Aplin, A. C., Larter, S. R.* Changes in Type II kerogen density as a function of maturity: evidence from the Kimmeridge clay formation // *Energ. Fuel.* 2005. Vol. 19, No. 6. P. 2495–2499.
22. *Senfile, J. T., Yordy, K. L., Barron, L. S., Crelling, J. C.* Whole rock and isolated kerogen characterization studies: observations of sample type preparations upon petrographic and chemical characterization of New Albany Shale // *Org. Geochem.* 1991. Vol. 17, No. 2. P. 275.
23. *Stankiewicz, B. A., Kruge, M. A., Crelling, J. C., Salmon, G. L.* Density gradient centrifugation: application to the separation of macerals of type I, II, and III sedimentary organic matter // *Energ. Fuel.* 1994. Vol. 8, No. 6. P. 1513–1521.
24. *Smith, J. W.* Relationship of Oil Yield to Oil Shale Industry // *United Nations Symposium on the Development and Utilization of Oil Shale Resources.* - Tallinn: Academy of Science of Estonian SSR, 1968.
25. *Suuberg, E. M., Otake, Y., Langner, M. J., Leung, K. T., Milosavljevic, I.* Coal macromolecular network structure analysis: solvent swelling thermodynamics and its implications // *Energ. Fuel.* 1994. Vol. 8, No. 6. P. 1247–1262.
26. *Carbognani, L., Rogel, E.* Solvent swelling of petroleum asphaltenes // *Energ. Fuel.* 2002. Vol. 16, No. 6. P. 1348–1358.
27. *Larsen, J. W., Flores, C. I.* Kerogen chemistry 5. Anhydride formation in, solvent swelling of, and loss of organics on demineralization of Kimmeridge shales // *Fuel Process. Technol.* 2008. Vol. 89, No. 4. P. 314–321.
28. *Barr-Howell, B. D., Peppas, N. A.* Importance of junction functionality in highly cross-linked polymers // *Polym. Bull.* 1985. Vol. 13, No. 2. P. 91–96.
29. *Peppas, N. A., Lucht, L. M.* Macromolecular structure of coals. X. Thermodynamic interaction parameter for solvents and coal networks // *Polym. Bull.* 1986. Vol. 16, No. 4. P. 375–379.
30. *Farve, E.* Swelling of crosslinked polydimethylsiloxane networks by pure solvents: influence of temperature // *Eur. Polym. J.* 1996. Vol. 32, No. 10. P. 1183–1188.
31. *Gee, G.* Interaction between rubber and liquid. IV. Factors governing the absorption of oil by rubber // *Trans. Inst. Rubber Ind.* 1943. Vol. 18. P. 266–281.
32. *Yagi, Y., Inomata, H., Saito, S.* Solubility parameters of an N-isopropylacrylamide gel // *Macromolecules.* 1992. Vol. 25, No. 11. P. 2997–2998.
33. *Oja, V.* Characterization of tars from Estonian Kukersite oil shale based on their volatility // *J. Anal. Appl. Pyrolysis.* 2005. Vol. 74, No. 1–2. P. 55–60.
34. *Suuberg, E. M., Sherman, J., Lilly, W. D.* Product evolution during rapid pyrolysis of Green River Formation oil shale // *Fuel.* 1987. Vol. 66, No. 9. P. 1176–1184.

ARTICLE III

Hruljova, J.; Savest, N.; Oja, V.; Suuberg, E. M. (2013). Kukersite oil shale kerogen solvent swelling in binary mixtures. – *Fuel*, 105, 77–82.



Kukersite oil shale kerogen solvent swelling in binary mixtures

Jelena Hruljova^a, Natalja Savest^a, Vahur Oja^{a,*}, Eric M. Suuberg^b

^a Department of Chemical Engineering, Tallinn University of Technology, Ehitajate Road 5, 19086 Tallinn, Estonia

^b Division of Engineering, Brown University, Providence, RI 02912, USA

HIGHLIGHTS

- ▶ Examined kukersite kerogen structure using solvent swelling in binary mixtures.
- ▶ Established that specific kerogen-solvent interactions play a role in swelling.
- ▶ High swellability with mixed solvents over a broad range of solubility parameters.
- ▶ Electron donor strength plays a key role in determining extent of swelling.

ARTICLE INFO

Article history:

Received 20 January 2012

Received in revised form 12 April 2012

Accepted 20 June 2012

Available online 10 July 2012

Keywords:

Oil shale

Kerogen

Kukersite

Solvent swelling

Binary solvent mixture

ABSTRACT

This work presents experimental data on volumetric swelling of Estonian kukersite oil shale kerogen in 11 different binary mixtures, prepared using nine different solvents. Variations in equilibrium swelling ratios have been studied as a function of mixture composition. The results confirm the important role of specific interactions in determining the swelling behavior of this kerogen. Swelling of kukersite kerogen in mixtures with high electron donor number solvents (such as pyridine, propylamine, and NMP) show the highest values of equilibrium swelling ratios over the very broad solubility parameter range. In terms of maximizing swelling of this kerogen, binary solvent mixtures do not offer particular advantage relative to pure, strong electron donor solvents.

© 2012 Elsevier Ltd. All rights reserved.

1. Introduction

Volumetric expansion in solvents (solvent swelling) is a widely used, low-cost technique for determining the solubility parameters of fossil fuels with cross-linked macromolecular structures. The swelling data may be used to determine Hansen's three-dimensional solubility parameters [1], to characterize solvent-macromolecule interactions, and utilizing suitable theoretical models [2–4], for calculating cross-link densities, molecular weights between cross-links, and the number of repeat units per cross-link of a macromolecular structure.

Swelling is a complex phenomenon, especially in heterogeneous macromolecular networks such as oil shale kerogens or coals. Many coal related studies have shown that although volumetric swelling is a valuable tool for understanding macromolecular structure, swelling theories, especially those based on regular solution theory, are not reliably applicable to systems containing specifically interacting heteroatoms, especially those

with hydrogen bond-forming capabilities [5,6]. However, oil shale swelling studies indicate that most oil shales investigated follow regular solution theory reasonably closely [3,4,7–9]. Hence, there is not always a complexity of swelling behavior in oil shale kerogens like that usually seen with coals.

The cross-link density of a macromolecular network directly determines its swellability and existence of cross-links, covalent and non-covalent, prevents infinite swelling (i.e., dissolution). In principle, all oil shale kerogens can have two types of cross-links, just as have been discussed for coals. Non-covalent cross-links, or strong specific kerogen–kerogen intramolecular interactions, can be broken by specifically interacting solvents that interact with the kerogen similarly or more strongly than do other parts of the kerogen structure. Such solvents render the structure more swellable and penetrable by other solvents. It has also been observed in both coal and polymer swelling studies that mixed solvents of certain types can significantly increase both the rate and extent of equilibrium swelling [10,11], through a combined effect of increasing the penetrability of the macromolecular structure and increasing the thermodynamic/chemical compatibility of the mixture with the macromolecular structure.

* Corresponding author. Tel.: +372 620 2852; fax: +372 620 2856.

E-mail address: vahur.oja@ttu.ee (V. Oja).

Our previous studies [12,13] on kukersite oil shale kerogen swelling has shown that the maximum swelling occurs in high electron donor number (EDN) solvents such as pyridine, methyl ethyl ketone or 1-methyl-2-pyrrolidone (NMP), indicating the role of specific interactions such as hydrogen bonds. In this regard the kukersite oil shale kerogen differs somewhat from oil shale kerogens that have been shown to follow regular solution theory reasonably closely [3,4,7–9].

The objective of this study is to investigate further the role of specific interactions in kukersite kerogen, through use of solvent pairs. This paper presents experimental data on the equilibrium swelling of kukersite oil shale kerogen in 11 different binary mixtures using the usual volumetric swelling technique (so called “test tube” technique) at room temperature. It presents simple global behavioral results – changes in solvent mixture composition relative to initial mixture composition as compositional distributions inside the swollen network were not studied here. While a large number of studies are available on oil shale kerogen swelling in a single solvent, much less attention has been directed at swelling in multicomponent solvent mixtures, despite the potential that such information offers for understanding the macromolecular structure.

2. Experimental

2.1. Oil shale sample and solvents

The oil shale kerogen sample used here was obtained from kukersite oil shale (from a commercial grade oil shale with organic matter content of about 35%) and it had a 91% organic matter content. The kerogen was isolated from the parent oil shale by a flotation technique [14]. The flotation technique was selected as chemical isolation methods may change the organic structure of oil shales. In the context of this paper, it is important to note, that oil shale kerogens have macromolecular structures that are practically insoluble in organic solvents at room temperature. The yields of solubles, or extractables, from kukersite oil shale (the object of this study) in typical organic solvents do not exceed 1.5% of the organic matter [29].

The elemental composition of the organic matter was 73.3 wt.% C, 8.8 wt.% H, 1.6 wt.% N, 16.3 wt.% O + S (by difference), determined using an Exeter Analytical model CE440 elemental analyzer. This indicates that the kerogen has high oxygen content (above 10%). Generally, for kukersite oil shale kerogens hydroxyl and carbonyl groups have been shown to contribute about half of the total organic oxygen, for example 42% and 13% respectively, on a total organic oxygen basis [15].

The samples were ground to <100 µm particle size. All samples were pre-dried 1 h at 105–110 °C in air (a standard oil shale drying procedure) before swelling measurements.

The nine solvents used in preparing the binary solvent mixtures were all of reagent grade. Some solvent characteristics of interest in this study are shown in Table 1, including total (or Hildebrand) solubility parameter [3,16,17], Gutmann's electron donor number (EDN) and acceptor number (EAN) [18–20], and molar volume [21].

2.2. Swelling procedure

Solvent mixtures of desired composition were prepared and used for swelling the kerogen. The solvent mixtures were used in large excess so that each solvent in the mixture was present in an amount much larger than the previously established solvent uptake volume (in pure solvent swelling experiments). This was done in an attempt to minimize any change in solvent mixture

Table 1
Properties of the solvents used.

Solvent	Solubility parameter, δ (MPa) ^{1/2}	EDN	EAN	Molar volume (cm ³ mol ⁻¹)
Benzene	18.8	0.1	8.2	89.4
Diethyl ether	15.6	19.2	3.9	104.8
Nitrobenzene	20.5	4.4	14.8	102.7
Nitromethane	26.0	2.7	20.5	54.3
NMP ^a	23.1	27.3	13.3	96.5
n-Propanol	24.5	19.8	37.7	75.2
Propylamine ^b	18.2	55.5	4.8	83.0
Pyridine	21.9	33.1	14.2	80.9
Toluene	18.2	0.1	3.3	106.8

^a NMP stands for 1-methyl-2-pyrrolidone.

^b Ethylamine EDN and EAN values were used for propylamine.

composition associated with possible selective absorption of solvent components by the kerogen.

In order to get sufficiently reliable data we have re-examined the swelling procedure presented in our previous paper [12]. It was found that the swelling results, especially for the isolated kerogen as used here, were somewhat affected by the centrifugation procedure. Therefore, solvent swelling in this study was determined following a modified experimental procedure.

An oil shale kerogen sample, up to 0.25 g, was placed into a constant diameter glass tube, fitted with a cap to minimize solvent loss during the experiment. The glass tube had an inside diameter of 5.5 mm and length 8 cm, excluding the cap. The tube was centrifuged three times at 6000 rpm for 5 min each. The reason for this was that it was found that shifting the position of the tube relative to the rotor in between spinning periods gave an easier to read initial height. The height of the dry kerogen sample was thus measured after the third centrifugation. Solvent was then added to the tube, in excess, and mixed to achieve complete wetting/mixing with the kerogen and then the tube was again centrifuged three times at 6000 rpm for 5 min each.

A preliminary swelling measurement could already be taken then, because the swelling was fast enough to be essentially complete by this point in time. The actual reported final height of the sample was then measured after allowing 24 and/or 48 h of swelling in solvent. It was found that the extra time rarely resulted in additional swelling beyond what was observed in the first few minutes, but only the longer time results are reported here, to ensure that all samples were truly equilibrated.

The volumetric swelling is characterized by the parameter Q , defined as the final swollen volume divided by the initial unswollen volume. To help better interpret the results to be shown below, Fig. 1 illustrates the reproducibility of data for swelling in a series of propanol-benzene mixtures. It can be seen that the swelling ratio deviation is generally below ± 0.02 , with only one exception visible in the concentration range from 10 to 20 mol% of propanol. One other occurrence of a larger uncertainty was observed in the case of benzene-NMP mixture (not shown here) that showed comparably large variation at a concentration of about 40 mol% of NMP.

3. Results and discussion

3.1. Pre-prepared binary mixture composition based analysis

Figs. 2–4 give changes in swelling ratios as a function of the molar compositions of the pre-prepared solvent mixtures. These figures show that the highest swelling capacities obtained in binary mixtures are not much greater than the maximum swelling ratio in the neighborhood of 1.4–1.45 obtained with the pure, high EDN solvents such as pyridine, NMP and propylamine. No synergistic effects of solvent pairs that resulting in an increase in maximum

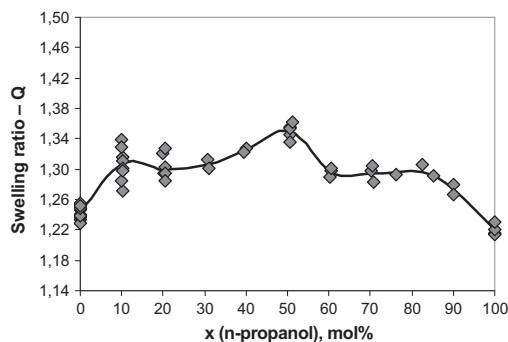


Fig. 1. Illustration of the reproducibility of swelling of kukersite oil shale kerogen in binary benzene-propanol mixtures. The curve is drawn through average swelling values at each composition.

swelling were seen. However, in some solvent pairs swelling ratios higher than those in the individual solvents were observed.

With respect to the following discussion, it is to be emphasized that Figs. 2–4 were constructed using average swelling ratios obtained at each binary mixture composition and assuming that the mixed solvent is taken up in the same proportions as exist in the liquid phase (so called “pseudo-solvent” or “uniform liquid” approximation [23]). While this might be true for simple systems, such as poly-isoprene swelling in a benzene–cyclohexane mixture [22] or cross-linked copolymer polyester urethane in a dioctylsebacate–diethylphthalate mixture [23], it is not generally valid for mixtures containing specifically interacting solvents that can break non-covalent cross-links and involve selective uptake of mixture components [24,25,27,30]. Hence, the reported liquid phase composition is not necessarily reflective of the ratio of absorbed components.

Fig. 2 illustrates swelling in benzene-based mixtures. The benzene can be viewed as a non-specifically interacting solvent. It is also known to be a good solvent for kukersite oil shale derived organic materials. Low fractions (<10 mol% for NMP and propylamine; <20 mol% for pyridine) of high EDN solvent or specifically interacting solvent in mixture with benzene are sufficient to in-

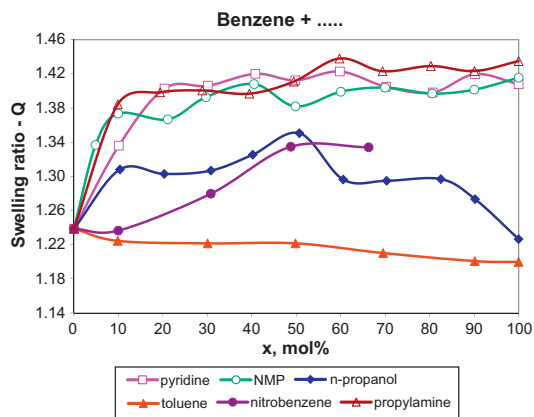


Fig. 2. Swelling of kukersite kerogen in benzene-based binary mixtures. Open points correspond to benzene mixed with high EDN solvents and solid points to benzene mixed with low to medium EDN solvents. The parameter x refers to the mol% of the solvent indicated in the legend.

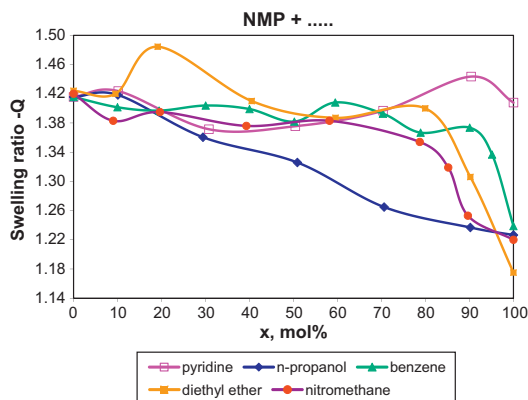


Fig. 3. Swelling of kukersite kerogen in NMP-based binary mixtures. Open points correspond to NMP mixed with high EDN solvent and solid points to NMP mixed with low to medium EDN solvents. The parameter x refers to the mol percentage of the solvent indicated in the legend.

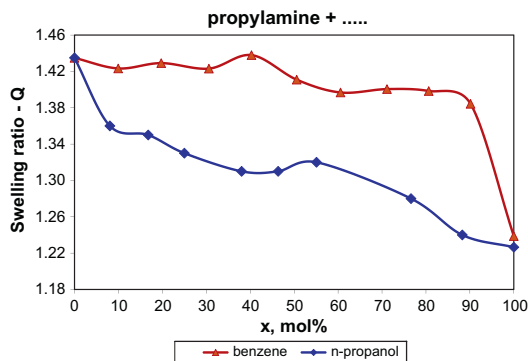


Fig. 4. Swelling of kukersite kerogen in propylamine-based binary mixtures. The parameter x refers to the mol% of the solvent indicated in the legend.

crease swelling to approximately the same levels observed for the pure, high EDN solvents. Increase in high EDN solvent concentration beyond these 10–20% values does not cause significant change in the extent of swelling, though there is some scatter in the results that might mask subtle trends. The results differ from a roughly linear trend with volume fraction of pyridine observed in Australian brown coal (low rank coal) swelling in benzene–pyridine mixture [31]. However, these results exhibit a trend consistent to that reported by Green and Larsen [25] for swelling of coals with mixtures of electron donor solvents (such as pyridine) and non-specifically interacting solvents (such as chlorobenzene). It is believed that the same process is involved here, namely, that a small amount of specifically interacting electron donor dissociates cross-links in the kerogen, permitting the non-specifically interacting solvent to more effectively swell the structure. Green and Larsen actually measured the amount of electron donor uptake (small uptakes had a significant impact). The present experimental results are different, in that the effects of the electron donors are being plotted as functions of their liquid phase concentrations. These concentrations will of course be related to the chemical potentials of the components in solution. There must exist a correlation between the electron donor liquid phase concentration and its absorption uptake by the kerogen, reflecting an equilibrium

uptake isotherm (that is determined through equality of chemical potential in the solvent mixture and in the kerogen phase). The electron donor uptake by the kerogen is expected to increase with increasing liquid phase concentration, until such a point at which the specific interaction sites in the kerogen are all satisfied, and the thermodynamic favorability of selective absorption abruptly decreases. Hence the present results are in accord with the behavior seen by Green and Larsen in their coal system.

Fig. 2 also shows that the weaker electron donor, n-propanol, gives similar behavior to that of the stronger electron donors, but apparently cannot dissociate cross-links to as great an extent as do the higher EDN solvents. If it could the same maximum extent of swelling would be expected. The fact that the weaker electron donor cannot disrupt as many non-covalent cross-links does not come as a surprise. There is expected to exist a distribution of non-covalent bond strengths in the kerogen, and the thermodynamics of disruption of some of these by n-propanol is simply unfavorable. When n-propanol concentration in benzene gets very high (that is, the mixture approaches pure n-propanol), then the solubility parameter mismatch between the relatively polar alcohol and non-polar kerogen begins to influence the results, and kerogen swellability sharply decreases. This demonstrates that the role of benzene is critical, and that this solvent actually has the better solubility parameter match with the kerogen.

Fig. 2 shows that mixtures of similar non-specifically interacting solvents (such as benzene and toluene) are no more effective for swelling the kerogen than are these pure solvents alone. The benzene–nitrobenzene results give a trend more like those for benzene–propanol. The nitrobenzene is a fairly weak electron donor (though stronger than benzene and toluene), and a stronger electron acceptor. It is seen that the shape of the curve of swelling as a function of solvent composition is much different for benzene–nitrobenzene than those for the stronger electron donors. Hence, it is concluded that nitrobenzene's interactions with the kerogen are of a different nature than are those involving stronger electron donors.

Fig. 3 presents swelling in NMP-based mixtures. NMP as the high EDN solvent in mixture with low EDN solvent nitromethane and medium EDN solvent diethyl ether shows similar behavior to NMP–benzene mixture seen in Fig. 2. However, Fig. 3 shows a different trend when kukersite kerogen is swollen in propanol–NMP mixtures. Pure n-propanol gives comparable swelling to that in lower EDN pure benzene and nitromethane or in the similar EDN solvent diethyl ether (see 100% solvent values for both solvents in Fig. 3). In NMP–propanol mixtures, swelling values decrease proportionally with increasing concentration of n-propanol (Fig. 3) and in propylamine–propanol mixtures, the same general trend is observed (Fig. 4). The observed proportionality does not simply reflect a substitution of the smaller n-propanol molecules for the larger electron donors in the kerogen structure, since the slope did not correspond to the relative molar volumes.

It has already been established above that the n-propanol can disrupt some non-covalent cross-links in the structure, but this is likely to not be of particular importance in the NMP–propanol solvent pair. At low n-propanol concentrations in NMP, the electron donating properties of the latter stronger electron donor dominate, and the non-covalent cross-links in the kerogen should mostly be opened. As the n-propanol concentration in the mixtures increases, the bond-disrupting properties of the NMP are somehow “lost”, despite the fact that there remains a significant amount of NMP in the solution. The most likely reason why this happens is that the chemical potential of the NMP is decreased with increasing n-propanol concentration, such that NMP transfer from solution into bond-disrupting interactions with kerogen non-covalent cross-links becomes thermodynamically progressively less favorable. The reasons for this may be understood by considering the properties of these solvents.

The n-propanol has a considerably higher electron acceptor number (EAN) than EDN which is opposite the nature of NMP, pyridine and propylamine, all of which are much stronger electron donors than acceptors (see Table 1). The n-propanol results in Figs. 3 and 4 may be interpreted as indicating that n-propanol is acting in the role of an electron acceptor relative to the electron donor solvents in these mixtures, thus effectively weakening the electron donor's strength. This does not happen in mixtures with benzene, because the latter has no electron donor strength. Compositional information on the absorbed solvents would have been useful for further evaluation of this possibility, but this was not done in the present experiments.

Fig. 3 also displays swelling data for NMP–pyridine mixtures (both similarly high EDN solvents). Though there might be some subtle variations in swelling with solvent composition, there are no significant trends visible. The strong EDN solvents thus swell the kerogen to an extent that is relatively independent of the identity of the solvent (this despite the somewhat higher molar volume of NMP as compared with pyridine – see Table 1). The data for NMP–benzene mixtures, also shown for comparison purposes in Fig. 3, display a third type of behavior. These data are the same as those for the NMP–benzene mixture shown in Fig. 2, and thus have been discussed above. The same explanation is true of the propylamine–benzene results shown in Fig. 4, which again show a behavior very distinct from that for propylamine–propanol.

3.2. Pre-prepared binary mixture solubility parameter based analysis

Fig. 5 offers a different way of plotting all of the binary mixture data shown in Figs. 2–4. Here, swelling ratios are shown as a function of the mixture total solubility parameter. The solubility parameters were calculated for the binary mixtures using the following: $\delta_{mix} = \sum(\theta_i \delta_i)$, where δ_{mix} is solubility parameter of the solvent mixture and δ_i and θ_i are the solubility parameters and the volume fraction of the solvents in the mixture, respectively. This type of plot is a solvent-swelling based method used to determine solubility parameters of cross-linked polymers under assumptions of classical thermodynamic swelling theories. Classic thermodynamic swelling theories require for maximum swelling of a network structure that the solubility parameter of the macromolecular network and of the solvent (or of the solvent mixture) should be close to equal. In the other words, the solvent and macromolecular structure should have energetic similarity. It is known from polymer swelling studies [23] that combination of solvents with lower and higher solubility parameters than that of the macromolecular network can result

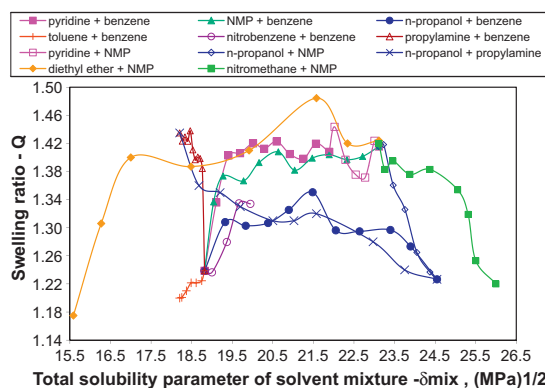


Fig. 5. Swelling of kukersite kerogen in solvent mixtures as a function of total solubility parameter for the mixture, calculated as described in the text.

in a swelling maximum. On the other hand, polymer results [23] also indicate that swelling in binary solvent mixtures that have net solubility parameters lower or higher than the macromolecular network do not show swelling maxima. However, it has also been indicated in polymer studies that swelling in mixed solvents, that can exhibit solvent–solvent associative behavior, the expected maxima may not be observed. For example swelling maximum was seen in swelling of PVC in toluene–methanol mixture, but not in swelling in n-butylacetate and nitromethane mixture [28]. Association between solvents or macromolecule and solvent can result in deviations from the regular solution behavior [30,31].

For comparison, it should also be noted that in coal swelling studies [24,26,27] swelling maxima in mixtures were in certain cases higher than were the swelling ratios in the individual solvents of the mixture. Unlike the polymer cases above, these results were accompanied by compositional differences between imbibed solvent in the swollen matrix, as compared with the applied solvent mixture; hence these experiments were characterized by selective solvent uptake. Similar behavior was also earlier observed by Green and Larsen [25].

The effects of solubility parameter on the behavior of this kerogen network will be discussed below. Fig. 5 again shows that the kukersite kerogen swellability is greatest in the high EDN solvents, though here the method of plotting the results does not make reference to EDN. The results in Fig. 5 show for the mixtures with high EDN solvent high values of swelling ratios over a very broad solubility parameter range, from $\delta \approx 17 \text{ MPa}^{1/2}$ (that for 20% NMP in diehtyl-ether) to $\delta \approx 25 \text{ MPa}^{1/2}$ (that for 20% NMP in nitromethane), something that is normally not the case in swelling of macromolecular networks in non-specifically interacting solvents (where the swellability generally shows a fairly clear maximum at a particular value of solubility parameter). In other words, there is another factor, not captured by the solubility parameter, which dominates the swelling behavior in the high EDN mixtures. This comes as no surprise, since it was already concluded that specific interactions involving electron donors play a key role, due to the influence of non-covalent cross-links.

The results for pyridine–benzene do not seem to show an influence of solubility parameter. Instead it again appears that the interactions driving the process are associated with what appears (from Fig. 2) to be a “titration” of a finite number of strong interaction sites. Once the chemical potential of the pyridine in solution exceeds a critical value, all specific interaction sites are involved, and the swelling no longer depends upon pyridine concentration (and hence, an increase in its chemical potential). Fig. 4 showed a similar threshold concentration for propylamine in benzene.

However, it is difficult to interpret the results of Fig. 5 purely on the basis of EDN alone. There is a considerable complexity displayed, and there is, at least in some cases, an indication of the importance of solubility parameter or something that correlates with it. One can expect that oil shale kerogen consists of many different types of chemical structures, distributed in some fashion (perhaps randomly, perhaps with some underlying order), with the different structures being energetically favorable to interactions with different solvents or solvent mixtures. Therefore, the different maxima and minima seen in the curves may be a result of subtle differences in the nature of possible interactions, as a function of the variation in chemical potential. Again, the uncertainty in the data shown in Fig. 1 warns about over-interpretation of the curves. Where the data are relatively free of concerns regarding specific interactions of strong electron donors (i.e., benzene–toluene, nitrobenzene–benzene), they clearly point towards a characteristic solubility parameter for the kerogen that is greater than about $20 \text{ MPa}^{1/2}$, since the curve of swellability in these solvents rises monotonically to that point.

The data on the n-propanol–benzene mixtures appear to have some character that is consistent with a solubility parameter matching, though at the same time, the propanol is an electron donor as well, and the behavior might be a composite of the two effects. The n-propanol–propylamine mixtures showed a monotonic decrease in swelling with increase in mixture solubility parameter. Again, the explanation is that the electron acceptor alcohol is influencing electron donor strength in the mixture, rather than making its influence felt through solubility parameter alone.

4. Conclusions

The present results show the important role of specific interactions in swelling of kukersite oil shale kerogen by solvents. It is the disruption of non-covalent cross-links that results in a roughly twofold increase in swellability, as compared with non-specifically interacting solvents.

The study establishes that the role of solvent solubility parameter (Hildebrand solubility parameter) is of secondary importance in determining the swellability of this kerogen. The mixtures with high donor number solvent (such as pyridine, propylamine, NMP) show the highest values of swelling ratios over a very broad solubility parameter range, from $17 \text{ MPa}^{1/2}$ to $25 \text{ MPa}^{1/2}$.

These results confirm that the highest swelling values for kukersite kerogens can be observed in high donor number solvents and these solvents determine the upper limit of swelling in mixtures of solvents. This upper limit cannot be significantly increased by the use of mixed solvents; the strong electron donor solvents give the highest swelling, though their effect can be decreased in mixture with non-specifically interacting solvents.

Acknowledgements

The authors gratefully acknowledge financial support provided by Estonian Science Foundation, under Grants G7222 and G9297, and by Estonian Minister of Education and Research, under target financing SF0140022s10.

References

- [1] Barton AFM. CRC handbook of polymer–liquid intercalation parameters and solubility parameters. CRC Press; 1990.
- [2] Barr-Howell BD, Peppas NA. Importance of junction functionality in highly crosslinked polymers. *Polym Bull* 1985;13:91–6.
- [3] Larsen JW, Li S. Solvent swelling studies of green river kerogen. *Energy Fuels* 1994;8:932–6.
- [4] Ballice L. Solvent swelling studies of Göynük (kerogen type-I) and Beypazari oil shale (kerogen type-II). *Fuel* 2003;82:1317–21.
- [5] Lucht LM, Peppas NA. Crosslinked macromolecular structures in bituminous coals: theoretical and experimental considerations. *AIP Conf Proc* 1981;70:28–48.
- [6] Suuberg EM, Otake Y, Langner MJ, Leung KT, Miloslajevic I. Coal macromolecular network structure analysis: solvent swelling thermodynamics and its implication. *Energy Fuels* 1994;8:1247–62.
- [7] Larsen JW, Parikh HM, Michels R, Raoult N, Pradier B. Kerogen macromolecular structure. *Prepr Symp Am Chem Soc Div Fuel Chem* 2000;45:211–5.
- [8] Larsen JW, Li S. An initial comparison of the interactions of type I and III kerogens with organic liquids. *Org Geochem* 1997;26:305–9.
- [9] Ertaz D, Kelemen SR, Halsey TC. Petroleum expulsion. Part 1. Theory of kerogen swelling in multicomponent solvents. *Energy Fuels* 2006;20:295–300.
- [10] Cooper WJ, Krasicky PD, Rodriguez FJ. Dissolution rates of poly(methyl methacrylate) films in mixed solvents. *J Appl Polym Sci* 1986;31:65–73.
- [11] Manjkow J, Papanu JS, Soong DS, Hess SW, Bell AT. An in situ study of dissolution and swelling behavior of poly(methyl methacrylate) thin films in solvent/nonsolvent binary mixtures. *J Appl Phys* 1987;62:682–8.
- [12] Savest N, Oja V, Kaevand T, Lille Ü. Interaction of Estonian kukersite with organic solvents: a volumetric swelling and molecular simulation study. *Fuel* 2007;86:17–21.
- [13] Savest N, Hruļjova J, Oja V. Characterization of thermally pretreated kukersite oil shale using the solvent-swelling technique. *Energy Fuels* 2009;23:5972–7.
- [14] Koch PR, Kirret OG, Oamer PE, Ahelik VP, Kõrts AV. Studies on the flotation process of Estonian kukersite. Thesis of all-union conference on the

- benefication of oil shales. Moscow: Academy of Sciences SSSR; 1973. p. 115–22 [in Russian].
- [15] Lille Ü. Current knowledge on the origin and structure of Estonian kukersite kerogen. *Oil Shale* 2003;20:253–63.
- [16] Karger BR, Snyder LR, Eon C. An expanded solubility parameter treatment for classification and use of chromatographic solvents and adsorbents. Parameters for dispersion, dipole and hydrogen bonding interactions. *J Chromatogr* 1976;125:71–88.
- [17] Belmares M, Blanco M, Goddard WA, Ross RB, Caldwell G, Chou SH, et al. Hildebrand and Hansen solubility parameters from molecular dynamics with applications to electronic nose polymer sensors. *J Comput Chem* 2004;25:1814–26.
- [18] Behbehani GR, Hamed M, Rajabi FH. The solvation of urea, tetramethylurea, TMU, in some organic solvents. *Int J Vib Spec*. 2001;5(6):5. <<http://www.ijvs.com/volume5/edition6/section3.html>> [09.01.12].
- [19] Malavolta L, Oliveira E, Cilli EM, Nakaie CR. Solvation of polymers as model for solvent effect investigation: proposition of a novel polarity scale. *Tetrahedron* 2002;58:4383–94.
- [20] Bistac S, Brogly M. Effect of polymer/solvent acid–base interactions: relevance to the aggregation of PMMA. In: Wypych G, editor. *Handbook of solvents*. Toronto: ChemTec Publishing; 2001. p. 570–83.
- [21] Hansen CM. *Hansen solubility parameters: a user's handbook*. CRC Press; 2000.
- [22] Schlick S, Gao Z, Matsukawa S, Ando I, Fead E, Rossi G. Swelling and transport in polyisoprene networks exposed to benzene-cyclohexane mixtures: a case study in multicomponent diffusion. *Macromolecules* 1998;31:8124–33.
- [23] Tereshatov VV, Senichev VY, Denisyuk EY. Equilibrium swelling in binary solvents. In: Wypych G, editor. *Handbook of solvents*. Toronto: ChemTec Publishing; 2001. p. 318–27.
- [24] Amemiya K, Kodama M, Esumi K, Meguro K, Honda H. Coal swelling using binary mixtures containing TQF. *Energy Fuels* 1989;3:55–9.
- [25] Green TK, Larsen JW. Coal swelling in binary solvent mixtures: pyridine-chlorobenzene and N,N-dimethylaniline-alcohol. *Fuel* 1984;63:1538–43.
- [26] Aida T, Shimoura Y, Yamawaki N, Fujii M, Squires TG, Yoshihara M, et al. Coal gel chemistry 1. An aspects of synergetic effects on the solvent swelling of coal. *ASC Div Fuel Chem Prep* 1988;33:968–71.
- [27] Aida T, Suzuki E, Yamanishi I, Sakai M. Synergetic effect on solvent swelling of coal. *ASC Div Fuel Chem Prep* 1999;44:623–6.
- [28] Froehling PE, Koenhen DM, Bantjes A, Smolders CA. Swelling of linear polymers in mixed swelling agents: predictability by means of solubility parameters. *Polymer* 1976;17:835–6.
- [29] Koel M, Ljovin S, Hollis K, Rubib J. Using neoteric solvents in oil shale studies. *Pure Appl Chem* 2011;73:153–9.
- [30] Westerbook PA, French RN. Elastomer swelling in mixed solvents. *Rubber Chem Technol* 1999;72:74–90.
- [31] Westerbook PA, French RN. Elastomer swelling in mixed associative solvents. *Polym Eng Sci* 2007;47:1554–68.

ARTICLE IV

Hruljova, J.; Järvik, O.; Oja, V. (2014) Application of differential scanning calorimetry to study solvent swelling of Kukersite oil shale macromolecular organic matter: A comparison with the fine-grained sample volumetric swelling method. – *Energy & Fuels*, 28 (2), 840–847.

Application of Differential Scanning Calorimetry to Study Solvent Swelling of Kukersite Oil Shale Macromolecular Organic Matter: A Comparison with the Fine-Grained Sample Volumetric Swelling Method

Jelena Hruļjova, Oliver Järvik, and Vahur Oja*

Department of Chemical Engineering, Tallinn University of Technology, Ehitajate Road 5, 19086 Tallinn, Estonia

ABSTRACT: A comparison of results of Estonian kukersite oil shale kerogen (i.e., the cross-linked macromolecular organic matter of oil shale) solvent swelling from two different methods is shown. Solvent uptakes calculated from differential scanning calorimetry (DSC) experiments are higher than those obtained by a widely used test-tube-type volumetric solvent swelling technique of fine-grained samples with swollen sample centrifugation. Solvent swelling of the kerogen sample was performed in a test tube in accordance with the common volumetric technique. Then, the swollen sample was introduced into a DSC apparatus, cooled to $-120\text{ }^{\circ}\text{C}$, and heated at a rate of $10\text{ }^{\circ}\text{C}/\text{min}$. The energy of fusion of the freezable part of the solvent was used to calculate the amount of nonfreezable bound solvent that is present inside the kerogen particles and that causes swelling. The data suggest that caution should be exercised in applying the test tube volumetric method because of a possible swollen sample compaction effect.

1. INTRODUCTION

Oil shale is a sedimentary rock that consists of mineral and organic matter. Kerogen, the dominating component of the oil shale organic matter, is a highly cross-linked macromolecular material insoluble in common organic solvents at room temperature. The data on the chemical structure and origin of kukersite oil shale (Estonian Middle-Upper Ordovician oil shale¹) organic matter is summarized in ref 2, and a two-dimensional model of kukersite kerogen is proposed in ref 3.

The solvent swelling technique is widely applied in solid fossil fuel research. Data obtained from swelling experiments is used to characterize the organic macromolecular structure of solid fossil fuels, estimate their solubility parameters, and calculate the number-average molecular weight between cross-links in the macromolecular organic network structure.^{4–14} In the field of fossil fuel research, the most popular has become a simple and low-cost volumetric solvent swelling technique of a fine-grained sample placed in a test tube. The method was first invented by Liotta et al.¹⁵ and presented in comparison with gravimetric swelling measurements by Green et al. in 1984.¹⁶ Since then, more than 50 research papers have been published based on this method (described in detail by Green et al.¹⁶). In brief, a fine-grained solid fuel sample is placed in a constant diameter test tube, centrifuged, and the initial height of the dry sample is measured. The swelling agent is added in excess, the content of the test tube is thoroughly mixed and centrifuged again, and the final height of the swollen sample is measured. The volumetric swelling ratio is commonly used as a measure of the swelling extent or the swelling power of the solvent. In addition, other useful parameters to quantitatively describe swelling can be calculated from volumetric measurements: the macromolecular material volume fraction in the equilibrium swollen state calculated as the reciprocal of the volumetric swelling ratio (usually used for the calculation of the number-

average molecular weight between cross-links in the macromolecular organic network structure), the swelling power on a molar basis such as the solvent molar uptake,^{8,17,18} the swelling power on a mass basis such as the solvent mass uptake, and the equilibrium gravimetric swelling ratio.^{16,19}

From the test-tube-type volumetric swelling experiment of fine-grained samples with swollen sample centrifugation, the calculations of these swelling-describing parameters have been commonly performed under a silent assumption of a constant void volume fraction throughout the experiment. For example, the volumetric swelling ratio, often denoted as Q , is calculated as a ratio of final and initial volumes or from directly measured quantities as a ratio of final and initial heights (the latter holds for the constant-diameter tube). Table 1 presents some equations applied to analyze solvent swelling results, both in whole material (such as a compact block) and in fine-grained bulk material cases.

It can be seen from Table 1 that commonly used simplified equations in column 4 can actually be used for packed-bed-forming fine-grained samples only if the void volume fraction in the swollen sample (ε_s) is equal to that in the dry sample (ε_d), or in other words, if the packing density of the sample has not changed. It is to emphasize that the volumetric swelling experiments in a test tube, described above, do not provide any insight into the possible changes in the void volume fraction and, thus, using the directly measurable quantities (heights of dry and swollen samples) through the simplified equations (column 4) straightforwardly may result in unwanted inaccuracies. In addition to a warning of possible differences in the packing of dry and solvent-swollen samples,²⁰ there is

Received: September 20, 2013

Revised: November 27, 2013

Published: December 23, 2013

Table 1. Equations for Solvent Swelling Calculations Based on Volumetric Measurements. See section 2.5 for symbols explanation

	solid material as a block	fine-grained material in a packed bed	fine-grained material in a packed bed, $\epsilon_f = \epsilon_i$
swelling ratio, Q	$Q = \frac{V_{\text{swollen material}}}{V_{\text{dry material}}} = \frac{V_f}{V_i}$	$Q_{\epsilon_f \neq \epsilon_i} = \frac{V_f(1 - \epsilon_f)}{V_i(1 - \epsilon_i)}$	$Q_{\epsilon_f = \epsilon_i} = \frac{V_f}{V_i} = \frac{h_f}{h_i}$
solvent mass uptake, S [g _s /g _m]	$S = (Q - 1) \frac{\rho_s}{\rho_m} = \left(\frac{V_f}{V_i} - 1 \right) \frac{\rho_s}{\rho_m}$	$S_{\epsilon_f \neq \epsilon_i} = \left(\frac{V_f(1 - \epsilon_f)}{V_i(1 - \epsilon_i)} - 1 \right) \frac{\rho_s}{\rho_m}$	$S_{\epsilon_f = \epsilon_i} = \left(\frac{V_f}{V_i} - 1 \right) \frac{\rho_s}{\rho_m}$
solvent molar uptake, S' [mol _s /g _m]	$S' = \frac{(Q - 1)}{V_{M,s} \rho_m} = \left(\frac{V_f}{V_i} - 1 \right) \frac{1}{V_{M,s} \rho_m}$	$S'_{\epsilon_f \neq \epsilon_i} = \left(\frac{V_f(1 - \epsilon_f)}{V_i(1 - \epsilon_i)} - 1 \right) \frac{1}{V_{M,s} \rho_m}$	$S'_{\epsilon_f = \epsilon_i} = \left(\frac{V_f}{V_i} - 1 \right) \frac{1}{V_{M,s} \rho_m}$

Table 2. Properties of the Solvents Used

no.	solvent	molar mass, g/mol	density (22 °C), g/cm ³	molar volume, cm ³ /mol	total solubility parameter, ^{34–36} MPa ^{1/2}	DN ^{37–39} , unitless	AN ^{37–39} , unitless	melting point ⁴⁰ , °C
1	acetonitrile	41.1	0.780	52.6	24.3	14.1	19.3	−45
2	aniline	93.1	1.020	91.3	21.1	33.3	28.8	−6
3	benzene	78.1	0.877	89.1	18.8	0.1	8.2	5.5
4	benzyl alcohol	108.1	1.044	103.6	24.8	23.0	36.8	−16
5	diethylamine	73.1	0.702	104.2	16.4	50.0	9.4	−50
6	DMF ^a	73.1	0.949	77.0	24.5	26.6	16.0	−60
7	NMP ^b	99.1	1.031	96.2	23.1	27.3	13.3	−24
8	<i>o</i> -xylene	106.2	0.878	120.9	18.0	4.8 ^c	2.4 ^c	−25
9	propylamine	59.1	0.714	82.8	18.2	55.5 ^d	4.8 ^d	−83
10	pyridine	79.1	0.981	80.6	21.9	33.1	14.2	−41
11	tetralin	132.2	0.967	136.7	19.4			−35

^aDMF is *N,N*-dimethylformamide. ^bNMP is *N*-methyl-2-pyrrolidone. ^cCalculated values for mixture of xylene isomers. ^dEthylamine DN and AN values are used for propylamine.

also some indirect experimental evidence indicating compressive changes in packing density found in literature. The shrinking of samples in some solvents (i.e., the final height of the samples in a test tube is lower than the initial height) has been observed in solvent swelling studies of Dictyonema oil shale¹³ and petroleum asphaltene²¹ for example. However, rearrangement of the kerogen structure under the action of the solvent has been proposed as a possible reason for this shrinking behavior in the former case. In the latter, the impression of asphaltene shrinking was withdrawn by the improvement of a compaction procedure for a dry sample.

In polymer science, solvent-swollen samples have often been investigated by using a differential scanning calorimeter (DSC). DSC has been used to describe qualitatively or quantitatively the state of solvent, freezable or nonfreezable, in polymer–solvent gels through studying the amount of solvent undergoing crystallization and melting processes.^{22–27} These studies have demonstrated the existence of some nonfreezable solvent that forms a homogeneous phase with a polymer structure.^{23,24} The nonfreezable solvent, also called “bound” solvent, is the result of an influence of the polymeric network that prevents solvent molecules from forming solvent crystals. As for the freezable solvent, depending on the specific solvent–macromolecule system, more or less complex interpretations can be found in literature. Various deviations relative to pure solvent melting peaks have been detected from DSC thermograms in some cases. The deviations include, for example, the following: the shift of melting temperature,²³ the tailing of melting peaks,²⁶ and the appearance of several peaks (from discrete to overlapping peaks).²² These deviations were used to indicate that at least some of the freezable solvent may differ from the bulk state of the pure solvent and could be by some means

under the influence of the polymeric network. DSC has been applied also in a few cases to investigate the physical state of solvent in swollen coals²⁸ and coal extracts.²⁹

The objective of the present study was to undertake a quantitative DSC-based analysis of solvent-swollen samples of kukersite oil shale kerogen. It was of particular interest to compare DSC data with results obtained by a widely used test-tube-type volumetric solvent swelling technique of fine-grained samples with swollen sample centrifugation.

2. EXPERIMENTAL SECTION

2.1. Kukersite Oil Shale Kerogen Sample. Kukersite oil shale (from Estonia) concentrated organic matter, or kerogen, was isolated from oil shale by a flotation technique³⁰ and had an organic matter content of 91%. Sample particle size was <100 μm. The samples were dried at 105–110 °C for 1 h in an air atmosphere and then cooled in an exsiccator shortly before the swelling experiments. As organic matter of kukersite oil shale is known to be practically insoluble in organic solvents at room temperature (extraction yield is no more than 1% of organic matter^{31,32}), no solvent extraction was performed before the experiments. It is assumed that one can neglect the influence of extractables (sol fraction) and consider solvent swelling of kukersite organic matter as the swelling of the cross-linked macromolecular network or kerogen.

The elemental composition of the organic matter of the concentrated kerogen sample was as follows (wt %): C, 73.3; H, 8.8; N, 1.6; O+S, 16.3 (by difference). The apparent density of the kerogen sample, determined by measuring the mass and volume of water displaced by the kerogen sample of the known mass,³³ was 1.23 g/cm³. This value of the apparent density, determined by the so-called pycnometer method, was conventionally used as the true density of the kerogen sample in this study.

2.2. Solvents. Solvent swelling of kukersite oil shale kerogen was performed with the 11 solvents listed in Table 2. All solvents were of

reagent grade and used without further purification. Solvent properties required for the research (molar mass, Gutmann electron donor and acceptor numbers, density, molar volume, solubility parameter, melting point) are presented in Table 2. Gutmann electron donor and acceptor numbers³⁷ were selected to describe quantitatively the electron donor and acceptor properties of solvents, as the Gutmann's scale is commonly used in the field of solvent swelling of solid fossil fuels. Another reason to prefer this scale was availability of data for the solvents used in the present work. Densities of the solvents used were verified with an Anton Paar DMA 5000 M density meter at 22 °C (mean ambient temperature in the laboratory). The molar volumes of the solvents were calculated as $V_M = M/\rho$, where M is the molar mass and ρ is the density of the solvent.

Solvents from two groups, hydrogen-bonding with high electron donor numbers and non-hydrogen-bonding solvents, were chosen for the present research. It was previously found¹¹ that there was a fundamental difference in the swelling power of these two groups of solvents: most of the hydrogen-bonding solvents were more effective in the swelling of the kukersite oil shale than non-hydrogen-bonding solvents. There were also additional restrictions concerning the selection of solvents associated with an experimental procedure. First, the density of a solvent should not be equal to or greater than the density of kerogen, otherwise it would be impossible to get a uniformly tight packed bed of kerogen in the centrifugation process. Second, as the next stage of the experiment is a DSC measurement, the lowest melting point of a solvent is set by parameters of a DSC cooling system. The melting point of a solvent should be high enough to ensure crystallization of the solvent during a DSC run.

2.3. Volumetric Solvent Swelling by Test-Tube Method. The volumetric solvent swelling procedure applied in this work is a modified Green's¹⁶ volumetric technique and it was reported in our previous paper.¹⁴ Shortly, 0.25 g of fine-grained kukersite kerogen sample was weighed into a test tube and fitted with a ground-glass stopper. The test tube had a flat bottom, a constant inside diameter of 5 mm and a length of 8 cm, excluding the cap region. The test tube was then centrifuged three times at 6000 rpm for 5 min each, with the test tube being rotated around its vertical axis for 100°–140° after each centrifugation period. The initial height of the dry sample (h_i) was measured with a vernier caliper after the third centrifugation. Solvent in excess was added into the test tube, and the content of the test tube was thoroughly mixed in order to achieve a complete wetting of the kerogen. The test tube was again centrifuged as described above, and the height of the swollen kerogen sample was measured after the third centrifugation. The height was remeasured after 24 h and reported as the final height of the swollen kerogen sample (h_f). All volumetric swelling experiments were conducted at room temperature. However, with reference to the DSC method to be explained in the next section, our previous experiments indicated that lower temperatures, up to -15 °C, had no effect on the extent of swelling.¹¹ The balance used for weighing samples in test tubes had a specified repeatability ± 0.02 mg.

2.4. Determination of Solvent Uptake by DSC Method. A differential scanning calorimeter NETZSCH DSC 204 HP Phoenix equipped with a CC200L liquid nitrogen cooling system was used to characterize the solvent melting behavior of both pure solvents and solvent-swollen samples. Thus, the swollen state characterized by DSC corresponds to the temperature of the solvent melting. Experiments were performed under atmospheric pressure with an inert gas (nitrogen) flow rate of 40 mL/min and using 40 μ L hermetically sealable standard aluminum DSC pans. Before each measurement, the DSC cell was purged with inert gas (nitrogen) for at least 10 min. Hermetically sealed samples were cooled to -120 °C at a rate of 10 °C/min, equilibrated at -120 °C for 10 min, and then heated to 40 °C at the same rate. The specified standard deviation for the balance used for weighing DSC samples was ± 0.2 μ g.

DSC measurements were performed on swollen kerogen samples obtained directly from test tube volumetric swelling experiments (see section 2.3). For this, a layer of excess solvent accumulated over the swollen kerogen bed was removed from the test tube. The test tube was then weighed in order to determine the mass of the solvent that

was present in the swollen kerogen bed. A total of 7–28 mg of sample from the swollen packed bed was transferred from the test tube into a preweighed aluminum pan, hermetically sealed, and then weighed. After the DSC run had been completed the pan lid was pierced and the pan was placed into a vacuum oven in order to determine the kerogen mass and the overall mass of the solvent in the DSC sample. The sample was dried at an absolute pressure of 13–16 kPa and a temperature of 110 °C until a constant weight was obtained (until the weight loss was less than 0.2% within 1 h). The overall mass of the solvent in the DSC sample was calculated as a difference between the initial mass of the DSC sample and the mass of dry kerogen. The mass of the solvent bound to the kerogen structure was calculated as a difference between solvent overall mass and free solvent mass. The free solvent mass was obtained from the melting peak area of the swollen sample assuming that enthalpy of fusion of the free solvent in the swollen kerogen sample is equal to that of pure solvent. Solvent mass uptake (S_{DSC}) was then calculated as a ratio of bound solvent mass to dry kerogen mass.

2.5. Equations Used to Analyze Experimental Results. This section summarizes equations used to analyze experimental results in this study. Equations 1–3 are for the test tube volumetric swelling method (see section 2.3), whereas eqs 1 and 2 are used only with the assumption of constant void volume fraction. Equations 4–6 are for DSC method (see section 2.4). To calculate the final void volume fraction in the swollen kerogen sample in a test tube, the DSC data and the data from test tube experiments were combined as shown in eq 7. The mass of free solvent per gram of kerogen, obtained directly from the DSC run, was not used in eq 7 because evaporation of highly volatile solvents (solvents between swollen particles in the packed bed) during the transfer of the sample from a test tube to a DSC pan was seen.

The swelling ratio from test tube volumetric swelling measurements (for $\epsilon_i = \epsilon_f$)

$$Q = h_f/h_i \quad (1)$$

The solvent mass uptake from test tube volumetric swelling measurements (for $\epsilon_i = \epsilon_f$)

$$S_Q = (Q - 1) \frac{\rho_s}{\rho_m} \quad (2)$$

The initial void volume fraction in the centrifuged dry kerogen sample in a test tube

$$\epsilon_i = 1 - \frac{\rho_{\text{bulk}}}{\rho_m} = 1 - \frac{m_m/V_i}{\rho_m} \quad (3)$$

The solvent mass uptake from DSC measurements

$$S_{DSC} = \frac{m_{S_bound,1}}{m_{k,1}} = \frac{m_{S_all,1} - m_{S_free,1}}{m_{k,1}} = \frac{m_{S_all,1} - \frac{A_1}{A_2/m_2}}{m_{k,1}} \quad (4)$$

The solvent molar uptake from DSC measurements

$$S'_{DSC} = S_{DSC}/M_S \quad (5)$$

The volumetric swelling ratio from DSC measurements (corresponds also to volumetric swelling situation, where $\epsilon_i = \epsilon_f$)

$$Q_{DSC} = \frac{S_{DSC} \rho_m}{\rho_s} + 1 \quad (6)$$

The final void volume fraction in the swollen kerogen sample in a test tube, from combined DSC and test tube volumetric swelling data

$$\epsilon_f = \frac{V_{S_free}}{V_f} = \frac{m_{S_all} - m_{S_bound}}{\rho_s V_f} = \frac{m_{S_all} - S_{DSC} m_m}{\rho_s V_f} \quad (7)$$

Symbols used:

h_i [mm] is the initial height of the centrifuged dry kerogen sample in a test tube.

h_f [mm] is the final height of the centrifuged swollen kerogen sample in a test tube.

M_s [g/mol] is the molar mass of the solvent.

m_m [g] is the mass of macromolecular material (i.e., the mass of the kerogen sample in a test tube).

$m_{s,all}$ [g] is the overall mass of the solvent present in the swollen sample in a test tube.

$m_{s,bound}$ [g] is the mass of the solvent bound to the kerogen structure (in a test tube).

Q and Q_{DSC} are the volumetric swelling ratios determined by the test-tube method and by the DSC method, respectively.

S_Q and S_{DSC} [g of solvent/g of kerogen] are the solvent mass uptakes determined by the test-tube method and by the DSC method, respectively.

S'_{DSC} [mol of solvent/g of kerogen] is the solvent molar uptake determined by the DSC method.

V_i [cm³] is the initial volume of the centrifuged dry kerogen sample in a test tube.

V_f [cm³] is the final volume of the centrifuged swollen kerogen sample in a test tube.

$V_{s,free}$ [cm³] is the volume of the free solvent in the centrifuged swollen sample in a test tube.

$V_{M,s}$ [cm³/mol] is the molar volume of the solvent.

ϵ_i is the initial void volume fraction in the centrifuged dry kerogen sample in a test tube.

ϵ_f is the final void volume fraction in the centrifuged swollen kerogen sample in a test tube.

ρ_{bulk} [g/cm³] is the bulk density of the centrifuged dry kerogen sample.

ρ_m [g/cm³] is the true density of macromolecular material (i.e., the true density of the kerogen).

ρ_s [g/cm³] is the density of the solvent.

Symbols used in eq 4:

Index 1 refers to the DSC experiments with swollen kerogen samples.

$m_{k,1}$ [g] is the mass of kerogen (dry) in the DSC sample.

$m_{s,bound,1}$ [g] is the mass of the bound (nonfreezable) solvent in the DSC sample.

$m_{s,all,1}$ [g] is the overall mass of the solvent present in the DSC sample.

$m_{s,free,1}$ [g] is the mass of the free (bulk freezable) solvent in the DSC sample.

A_1 [J] is the melting peak area that corresponds to the melting of the free solvent between kerogen particles in the swollen kerogen sample (energy of fusion).

Index 2 refers to the DSC experiments with pure solvent samples.

A_2 [J] is the melting peak area obtained from the experiment with the pure solvent sample.

m_2 [g] is the mass of the pure solvent sample.

A_2/m_2 [J/g] is the solvent enthalpy of fusion.

3. RESULTS AND DISCUSSION

3.1. DSC Measurements. Figure 1 shows DSC thermograms of dimethylformamide (DMF) as an example of typical DSC thermograms of a pure solvent and a solvent-swollen kerogen sample. The thermogram for the DMF-swollen kerogen sample is shown as measured, whereas the pure DMF thermogram is rescaled to correspond to the total amount of solvent present in the swollen kerogen sample. If all the solvent present in the sample crystallized and then melted like pure bulk solvent, the melting peak area would be as shown in the figure (assuming constant enthalpy of fusion or enthalpy of fusion of the pure solvent). It can be seen that the peak area obtained from the actual experiment is smaller than the one of rescaled pure solvent, indicating that the amount of solvent undergoing the melting process is smaller than the total solvent

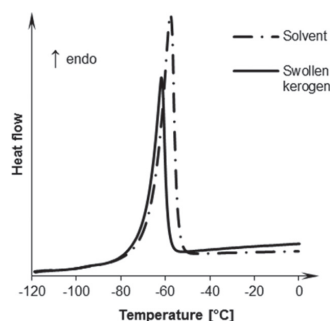


Figure 1. Typical normalized DSC thermograms for the pure solvent (dashed line) and the solvent-swollen kerogen sample (solid line). DMF thermograms are shown as an example.

amount in the DSC pan. Therefore, some amount of the solvent does not contribute to the crystallization and subsequent melting processes and is bound into macromolecule (kerogen). This phenomenon was seen for both hydrogen-bonding and nonpolar solvents. It is important to emphasize here that the swollen packed bed volume is the sum of the volume of swollen kerogen particles (consisting of kerogen and the solvent penetrated into the kerogen structure) and the volume of the solvent between them. Therefore, there are at least two types of solvent states present: the freezable solvent between swollen particles and the nonfreezable solvent bound into the swollen kerogen structure.

It is known from our early works¹¹ that hydrogen-bonding solvents with high electron donor numbers are more effective in kokersite swelling than other solvents. These former solvents are able to disrupt kerogen–kerogen specific interactions (such as hydrogen bonds) and participate in new solvent–kerogen specific interactions. However, regardless of the polarity of solvents, only two above-mentioned states of solvent were seen and no systematic differences were observed between thermograms of hydrogen-bonding solvents with high electron donor numbers and nonpolar solvents. In all cases, there was only one endotherm in the heating curve and one exotherm in the cooling curve in the present study. Neither overlapping peaks (recognized by unresolved shoulders) nor significant peak tailing were observed. There was also no significant difference in the position and the shape of the melting peak of the solvent in the mixture with kokersite kerogen as compared to that of the pure solvent. In most cases, the melting peak shift to lower temperatures was in the range of 0.1–1.3 K. The shift was somewhat more considerable in the case of DMF (2.5–4.2 K) and NMP (4.3–8.3 K). This effect may be also caused by more effective solvation of extractables from kokersite oil shale organic matter (shown to be not more than 1 wt % of organic matter^{31,32}), as some solvent color darkening was observed in test tube swelling in these solvents.

All data obtained, therefore, offer support for the view that the melting process detected by DSC corresponds to the melting of free bulk solvent present between the swollen kerogen particles. No considerably valid indications of existence of different types of solvent in the swollen kerogen particles (such as overlapping peaks, peak tailing) were seen. The decrease of the melting peak area relative to the area of the total solvent, existing in the swollen packed bed system, could therefore correspond to the nonfreezable bound solvent—to

Table 3. Results of Swelling Experiments Obtained by the Test-Tube Method and by the DSC Method As Described in Section 2

no.	solvent	swelling ratio		solvent mass uptake [$\frac{\text{g}_{\text{solvent}}}{\text{g}_{\text{ker}}}$]		free solvent [$\frac{\text{g}_{\text{solvent}}}{\text{g}_{\text{ker}}}$]	ratio of void fractions
		Q	Q _{DSC}	S _Q	S _{DSC}	S _{free}	ϵ_i / ϵ_f
1	acetonitrile	1.13	1.29	0.08	0.19	0.84	1.09
2	aniline	1.46	1.66	0.38	0.55	1.50	1.12
3	benzene	1.24	1.31	0.17	0.22	1.13	1.04
4	benzyl alcohol	1.45	1.53	0.38	0.45	1.54	1.05
5	diethylamine	1.41	1.70	0.24	0.40	0.93	1.12
6	DMF	1.31	1.89	0.24	0.69	0.95	1.44
7	NMP	1.48	2.02	0.40	0.85	1.22	1.39
8	o-xylene	1.11	1.27	0.08	0.19	0.92	1.15
9	propylamine	1.47	2.01	0.27	0.59	0.89	1.28
10	pyridine	1.45	1.79	0.36	0.63	1.39	1.19
11	tetralin	1.08	1.08	0.07	0.06	1.02	1.05

the solvent molecules causing swelling and, therefore, also quantitatively measurable by the test tube volumetric swelling technique. The outcomes of this observation to interpret the differences observed between DSC and volumetric methods are taken up in the next section.

3.2. Comparison of the Results Obtained by Volumetric and DSC Methods. Experimental results are summarized in Table 3 as the average data of at least two measurements. The volumetric swelling ratios determined by the test-tube method (calculated by eq 1, section 2.5) and by the DSC method (eq 6) are presented in columns 3 and 4, respectively. The solvent mass uptake, as grams of absorbed solvent per gram of dry kerogen, denoted as S_Q (in column 5) is calculated from the swelling ratio obtained by the test-tube method (eq 2). The solvent mass uptake denoted as S_{DSC} (in column 6) is calculated by eq 4 from the data of the DSC experiments as described in section 2.4. The void volume fractions for dry (ϵ_i) and swollen (ϵ_f) samples were calculated by eqs 3 and 7, respectively, on the basis of the data from test tube and DSC experiments. Corresponding ratios (ϵ_i / ϵ_f) are shown in column 8. The average void volume fraction in a dry centrifuged kerogen sample (ϵ_i) was 0.57 ± 0.01 . The amount of the solvent present between swollen kerogen particles in a test tube, or so-called free solvent, is shown in column 7 as the mass of the solvent per mass unit of kerogen (S_{free}).

It is evident from Table 3 that the results from test tube and DSC experiments (from columns 3–6) are not equal and that in almost all cases, with the exception of tetralin, the swelling extent determined by volumetric measurements is smaller than that of DSC measurements ($Q < Q_{DSC}$ and $S_Q < S_{DSC}$). In the case of tetralin, the difference between the solvent mass uptakes obtained by two different methods is within the limits of experimental error, and the swelling ratios are equal when expressed in rounded numbers.

Referring back to the discussion based on Table 1 (in section 1), it can be proposed that the difference between the results obtained by two different methods can be caused by the difference in packing density of the dry and the swollen sample. It is seen from column 8 in Table 3 that the void volume fraction in a packed bed of swollen kerogen (ϵ_f) is not equal to the void volume fraction in an initial packed bed of dry kerogen (ϵ_i). The results indicate that, when centrifuged, the swollen kerogen sample is packed more tightly than the initial dry sample and the void volume fraction decreases when a kerogen sample undergoes the swelling procedure described in section

2.3 ($\epsilon_i / \epsilon_f > 1$, see column 8 in Table 3). Figure 2 shows that the void volume fraction change correlates with the amount of

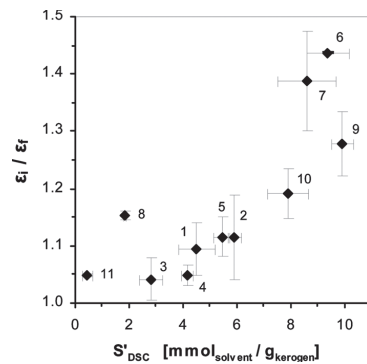


Figure 2. Ratio of initial and final void volume fractions as a function of solvent molar uptake.

solvent absorbed by kerogen. The increase of packing efficiency with the solvent molar uptake increase follows a roughly exponential trend. It seems plausible that the more solvent has been penetrated into a kerogen structure, the more plastic and soft the kerogen particles become, and as a result, the particles can be packed more tightly under centrifugation impact. In coal studies, increased flexibility of swollen macromolecular organic matter of coal samples in comparison with rigid dry samples was observed by Brenner.⁴¹ Similarly to Figure 2, ΔQ (the difference between swelling ratios that were obtained by two different techniques described in sections 2.3 and 2.4) correlates empirically with Q_{DSC} (swelling ratio from DSC method, calculated by eq 6) as seen in Figure 3.

It should be mentioned here that the present work should not be regarded as evidence against the suitability of the test-tube-type volumetric swelling technique generally. The outcomes of the present research could be characteristic for a specified combination between experimental procedure (see section 2.3) and material under study (kukersite oil shale kerogen). It is important to note that there is experimental evidence showing the validity of the simple volumetric test-tube method: Green et al. showed that volumetric and gravimetric (vapor sorption) methods gave close results in the case of

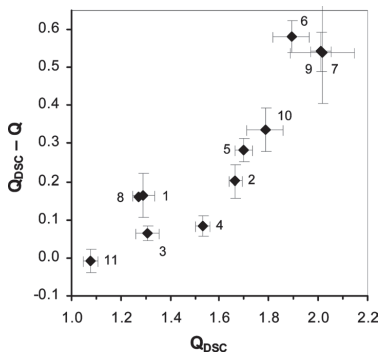


Figure 3. Difference between swelling ratios calculated from DSC data (Q_{DSC}) and obtained by the test-tube method (Q) as a function of swelling extent.

Bruceton and Illinois no. 6 coals;¹⁶ Gao et al. reported that the swelling results obtained by the volumetric test-tube method and by the orthogonal microscope image analysis method were comparable.⁴² Thus, the data presented show the importance of being careful when applying the test-tube-type volumetric swelling technique to different materials or modifying experimental procedures.

3.3. DSC Data Based Analysis of Swelling Behavior of Kukersite Kerogen.

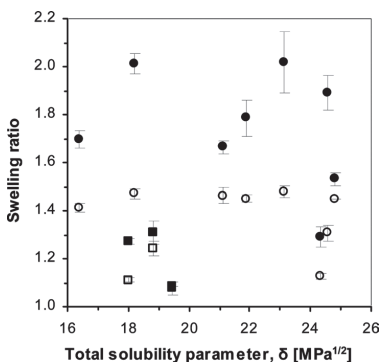


Figure 4. Swelling ratio as a function of the solvent total solubility parameter. Swelling ratios obtained by the test-tube method with H-bonding (\circ) and non-H-bonding (\square) solvents and calculated from DSC experiments with H-bonding (\bullet) and non-H-bonding (\blacksquare) solvents.

function of the total solubility parameter (δ) of applied solvents. Open points correspond to the results of the test-tube method (column 3, Table 3), and solid points to the results obtained by the DSC method (column 4, Table 3). The difference between the results is up to 1.5 times, and it varies depending on the solvent used as a swelling agent. The difference between the results obtained by two different methods when expressed in terms of solvent mass uptake is up to almost 3 times (see columns 5 and 6, Table 3). Otherwise, the data, from both techniques, qualitatively support the same conclusion and are consistent with the results of the previous studies on kukersite solvent swelling.^{11,14} Kukersite

kerogen swelling does not follow the regular solution theory that predicts a bell-shaped curve in the plot of swelling ratio vs solubility parameters of solvents. Scatter with relatively high swelling ratios is observed in a broad range of solubility parameter values, from 16 to 25 $\text{MPa}^{1/2}$, showing no clear relation between Q and δ . Therefore, the total solubility parameter (δ) is not a key property in determining swellability of kukersite kerogen.

In Figure 5, solvent molar uptake (mmoles of solvent absorbed by one gram of kerogen, calculated by eq 5) from the

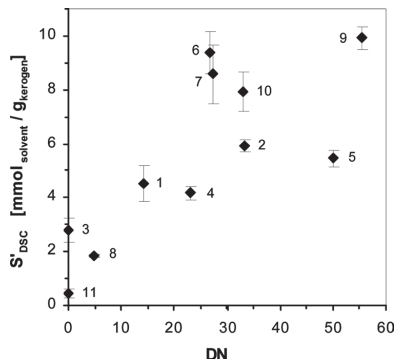


Figure 5. Solvent molar uptake obtained by the DSC method as a function of the solvent electron donor number. Tetralin DN is not available from the literature; the value of 0.1 for tetralin is predicted based on benzene and toluene data (0.1 for both solvents).

DSC experiments is displayed as a function of the solvent electron donor number. The main outcome is, again, qualitatively consistent with the previous test-tube-based volumetric studies,^{11,14} indicating the importance of specific interactions in the swelling of kukersite oil shale kerogen. It can be seen that solvents with a low electron donor number (such as tetralin, benzene, *o*-xylene, acetonitrile) are not efficient swelling agents for kukersite kerogen. Only solvents with high electron donor numbers (such as propylamine, pyridine, NMP, DMF) are able to show an extended swelling due to their ability to specifically interact with kerogen molecules (i.e., to disrupt kerogen–kerogen hydrogen bonds that serve as noncovalent cross-links and to form solvent–kerogen hydrogen bonds). The reduced cross-link density of macromolecule results in the increase of swellability. In addition to the main outcomes shown, the DSC data indicate one more underlying characteristic trend. As can be seen from Figure 6, the solvent molar uptake decreases with an increase of solvent molar volume. There are two groups of points highlighted separately in the plot: the points that correspond to the solvents with relatively high and low DN (see Table 1). The same rough tendency of influence of molar volume is seen within each group. Thus, a relatively large molar volume of solvent can be a limiting factor for the swelling process due to steric restrictions of the kerogen structure. The latter conclusion may also be proposed as a possible explanation for the relatively low diethylamine molar uptake seen in Figure 5.

4. CONCLUSION

Kukersite oil shale kerogen solvent swelling data, comparatively obtained by two different swelling techniques, show that

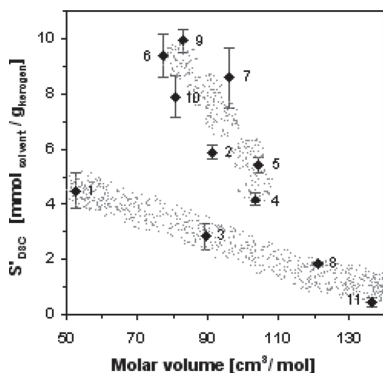


Figure 6. Solvent molar uptake obtained by the DSC method as a function of solvent molar volume.

solvent uptakes calculated from DSC experiments are higher than those obtained by the volumetric test-tube method of fine-grained samples with swollen sample centrifugation. Depending on the solvent used, the solvent mass uptake determined by DSC could be up to almost three times greater. The differences in determined swelling extent in these two cases were interpreted as follows: the swollen kukersite kerogen sample in the test tube was packed more tightly than the dry sample and the commonly accepted specified condition ($\epsilon_i = \epsilon_f$) was not met when the volumetric swelling procedure of this study was applied to kukersite kerogen.

The analysis performed indicated that DSC could be a valid technique for determining the swelling extent of kerogens. In a larger view, the DSC-based results supported conclusions reported in our previous publications on kukersite oil shale swelling: (1) the total solubility parameter was not a key parameter in determining the swellability of kukersite kerogen, (2) the swelling extent of kukersite kerogen depended mostly on solvent electron donor–acceptor properties. In addition, the DSC data also revealed one more underlying trend—molar volume of solvent could be a limiting factor.

The results of the present work should have an impact regarding the quantification of solvent uptake from volumetric test tube experiments, which are widely applied in fossil fuel science. It can be concluded that applying the test-tube-type volumetric swelling technique on different types of materials or modifying the experimental procedures should be done with caution.

AUTHOR INFORMATION

Corresponding Author

*V. Oja. E-mail: vahur.oja@ttu.ee. Phone: +372 620 2852. Fax: +372 620 2856.

Notes

The authors declare no competing financial interest.

ACKNOWLEDGMENTS

The authors gratefully acknowledge financial support provided by the Estonian Minister of Education and Research, under target financing SF0140022s10, and by the graduate school “Functional materials and technologies”, which received funding from the European Social Fund under project 1.2.0401.09-0079 in Estonia.

REFERENCES

- (1) Hints, O.; Nölvak, J.; Viira, V. *Oil Shale* **2007**, *24*, 527–533.
- (2) Lille, Ü. *Oil Shale* **2003**, *20*, 253–263.
- (3) Lille, Ü.; Heinmaa, I.; Pehk, T. *Fuel* **2003**, *82*, 799–804.
- (4) Lucht, L. M.; Peppas, N. A. *Fuel* **1987**, *66*, 803–809.
- (5) Larsen, J. W.; Li, S. *Energy Fuels* **1994**, *8*, 932–936.
- (6) Larsen, J. W.; Li, S. *Org. Geochem.* **1997**, *26*, 305–309.
- (7) Larsen, J. W.; Parikh, H.; Michels, R. *Org. Geochem.* **2002**, *33*, 1143–1152.
- (8) Suuberg, E. M.; Otake, Y.; Langer, M. J.; Leung, K. T.; Milosavljevic, I. *Energy Fuels* **1994**, *8*, 1247–1262.
- (9) Ballice, L. *Fuel* **2003**, *82*, 1317–1321.
- (10) Ballice, L. *Oil Shale* **2004**, *21*, 115–123.
- (11) Savest, N.; Oja, V.; Kaevand, T.; Lille, Ü. *Fuel* **2007**, *86*, 17–21.
- (12) Savest, N.; Hruļjova, J.; Oja, V. *Energy Fuels* **2009**, *23*, 5972–5977.
- (13) Kilk, K.; Savest, N.; Hruļjova, J.; Tearo, E.; Kamenev, S.; Oja, V. *Oil Shale* **2010**, *27*, 26–36.
- (14) Hruļjova, J.; Savest, N.; Oja, V.; Suuberg, E. M. *Fuel* **2013**, *105*, 77–82.
- (15) Liotta, R.; Brons, G.; Isaacs, J. *Fuel* **1983**, *62*, 781–791.
- (16) Green, T. K.; Kovac, J.; Larsen, J. W. *Fuel* **1984**, *63*, 935–938.
- (17) Green, T. K.; West, T. A. *Prepr. Pap. - Am. Chem. Soc., Div. Fuel Chem.* **1985**, *30*, 488–492.
- (18) Green, T. K.; West, T. A. *Fuel* **1986**, *65*, 298–299.
- (19) Shadle, L. J.; Khan, M. R. *Prepr. Pap. - Am. Chem. Soc., Div. Petroleum Chem.* **1989**, *34*, 55–61.
- (20) Turpin, M.; Rand, B.; Ellis, B. *Fuel* **1996**, *75*, 107–113.
- (21) Carbognani, L.; Rogel, E. *Energy Fuels* **2002**, *16*, 1348–1358.
- (22) Honiball, D.; Huson, M. G.; McGill, W. J. *J. Polym. Sci., Part B: Polym. Phys.* **1988**, *26*, 2413–2431.
- (23) Yang, H.; Nguyen, Q. T.; Ding, Y.; Long, Y.; Ping, Z. *J. Membr. Sci.* **2000**, *164*, 37–43.
- (24) Salmerón Sánchez, M.; Monleón Pradas, M.; Gómez Ribelles, J. L. *J. Non-Cryst. Solids* **2002**, *307–310*, 750–757.
- (25) Lue, S. J.; Yang, S. W. *J. Macromol. Sci., Part B: Phys.* **2005**, *44*, 711–725.
- (26) Wu, J.; McKenna, G. B. *J. Polym. Sci., Part B: Polym. Phys.* **2008**, *46*, 2779–2791.
- (27) Klein, M.; Guenet, J.-M. *Macromolecules* **1989**, *22*, 3716–3725.
- (28) Hall, P. J.; Larsen, J. W. *Energy Fuels* **1993**, *7*, 47–51.
- (29) Suzuki, M.; Norinaga, K.; Iino, M. *Fuel* **2004**, *83*, 2177–2182.
- (30) Koch, P. R.; Kirret, O. G.; Oamer, P. E.; Ahelik, V. P.; Körts, A. V. *Thesis of all-union conference on the beneficiation of oil shales*; Academy of Sciences USSR: Moscow, 1973; p 115–122 (in Russian).
- (31) Kogerman, P. N. Monograph, Bulletin No 3. From the Oil Shale Research Laboratory, University of Tartu, Estonia; Mattiesen: Tartu, 1931.
- (32) Koel, M.; Ljovin, S.; Hollis, K.; Rubin, J. *Pure Appl. Chem.* **2001**, *73*, 153–159.
- (33) Solid mineral fuel: Methods for determination of density. Standard: ГOCT 2160-92; Standards Publishing House: Moscow, 2002 (in Russian).
- (34) Belmares, M.; Blanco, M.; Goddard, W. A.; Ross, R. B.; Caldwell, G.; Chou, S. H.; Pham, J.; Olofson, P. M.; Thomas, C. J. *Comput. Chem.* **2004**, *25*, 1814–1826.
- (35) Karger, B. L.; Snyder, L. R.; Eon, C. *Anal. Chem.* **1978**, *50*, 2126–2136.
- (36) Zeng, W.; Du, Y.; Xue, Y.; Frisch, H. L. In *Physical properties of polymers handbook*; Mark, J. E., Ed.; Springer: New York, 2007; Chapter 16.
- (37) Gutmann, V. *The donor-acceptor approach to molecular interactions*; Plenum Press: New York, 1978; Chapter 2.
- (38) Linert, W. *Coord. Chem. Rev.* **2001**, *218*, 113–152.
- (39) Malavolta, L.; Oliveira, E.; Cilli, E. M.; Nakaie, C. R. *Tetrahedron* **2002**, *58*, 4383–4394.
- (40) NIST Standard Reference Database Number 69. <http://webbook.nist.gov/chemistry/> (accessed May 6, 2013).
- (41) Brenner, D. *Fuel* **1984**, *63*, 1324–1328.

(42) Gao, H.; Artok, L.; Kidena, K.; Murata, S.; Miura, M.; Nomura, M. *Energy Fuels* **1998**, *12*, 881–890.

ARTICLE V

Hruljova, J.; Savest, N.; Yanchilin, A.; Oja, V.; Suuberg, E. M. Kukersite oil shale macromolecular organic matter solvent swelling in binary mixtures: impact of specifically interacting solvents. – *Oil Shale. Submitted.*

KUKERSITE OIL SHALE MACROMOLECULAR ORGANIC MATTER SOLVENT SWELLING IN BINARY MIXTURES: IMPACT OF SPECIFICALLY INTERACTING SOLVENTS

JELENA HRULJOVA^(a), NATALJA SAVEST^(a), ALEXEY YANCHILIN^(a), VAHUR OJA^{(a)*}, ERIC M. SUUBERG^(b)

^(a) Department of Chemical Engineering, Tallinn University of Technology, Ehitajate Road 5, 19086 Tallinn, Estonia

^(b) Division of Engineering, Brown University, Providence, RI 02912, USA

Abstract. *The present work deals with volumetric solvent swelling of Estonian Kukersite oil shale cross-linked macromolecular organic matter (kerogen) in binary solvent mixtures. A two-step solvent swelling procedure was used in which swelling was performed first in one solvent followed by the addition of a second solvent. The results confirm the important role of specific interactions in determining the swelling behavior of this kerogen. The kerogen swells more in strong electron donor solvents that are able to break specific kerogen–kerogen interaction such as hydrogen bonds. When comparing the maximum swelling achieved, the binary solvent mixtures did not perform any better than strong electron donor solvents, regardless of how the experiments were conducted.*

Keywords: *oil shale, kerogen, Kukersite, solvent swelling, binary solvent mixture, electron donor number.*

1. Introduction

Solvent swelling is a simple and useful technique for determining the solubility parameters of cross-linked polymers, for characterizing solvent–polymer interactions, or, using suitable theoretical models, for calculating cross-link densities and molecular weights between cross-links of polymeric networks [1-3]. Volumetric solvent swelling has also been adapted for characterization of complex macromolecular organic structures from solid fossil fuels such as coals and oil shales (for oil shale [4-6]). These studies have been mostly aimed at improving the background knowledge of conversion of solid fossil fuels to liquid fuels and energy. While coal has been of continuous commercial interest over the past century, oil shale's development history has been quite chaotic (with the exception of a few locations such as Estonia, Brazil and China). However lately, due to the increasing search for alternative liquid fuel sources, commercial utilization of oil shale resources has gained more attention. Some general technical characteristics of oil shales and oils can be found from [7-11].

The organic matter of an oil shale consists primarily of a heterogeneous macromolecular structure (called kerogen) and is practically insoluble in organic solvents at room temperature. The yield of solubles, or non-macromolecular extractables, from Kukersite oil shale (the object of this study) in typical organic solvents does not exceed 1.5% of the organic matter [12]. Hence, while the extraction processes can influence the thermodynamics of swelling processes (by changing solvent activity), there is not an experimental measurement difficulty caused by significant mass loss during swelling of these materials, if the solvent is changed so as to keep the concentration of extractables low.

Although there have been a considerable number of experimental investigations on oil shale kerogen swelling in single solvents, there are few data found covering swelling

in binary solvent mixtures. This paper is an extension of the earlier work from this laboratory [13] and is aimed at giving further insights into the mechanism of solvent swelling of kukersite oil shale kerogen in binary mixtures. This experimental study has been extended to examine the swelling in binary mixtures in two-step swelling procedures – in which swelling was performed first in one solvent followed by the addition of a second solvent in order to obtain a desired solvent mixture composition in the swelling tube.

2. Experimental

2.1. Oil shale sample and solvents

The oil shale kerogen sample used was isolated from Kukersite oil shale by a flotation technique [14]. The concentrated sample had 91% organic matter content. The elemental composition of the organic matter was 73.3 wt.% C, 8.8 wt.% H, 1.6 wt.% N, 16.3 wt.% O+S (by difference), determined using an Exeter Analytical model CE440 elemental analyzer. The samples were ground to a particle size smaller than 100 μm . All samples were pre-dried 1 hour at 105–110°C in air (a standard oil shale drying procedure) before swelling measurements.

The solvents used in preparing the binary solvent mixtures were all reagent grade. Some solvent characteristics of interest in this study are shown in Table 1, including total (or Hildebrand) solubility parameter [15,16], Gutmann's electron donor (EDN) and electron acceptor (EAN) numbers [17,18], and molar volume [19]. The EDN and EAN are empirical parameters. For example, the EDN is experimentally determined as the negative ΔH -value for the 1:1 adduct formation between SbCl_5 (reference) and the solvent molecules in dilute solution of 1,2-dichloroethane [20].

2.2. Swelling Procedure

In this study a simple and widely used test-tube based procedure was used that involves solvent swelling of a powdered sample with swollen sample centrifugation. General details of the experimental procedure (test-tube dimensions, centrifugation conditions) are same that were applied previously for kukersite kerogen swelling in single solvents [21] or in prepared binary mixtures [13].

In the two-stage swelling procedure used in this study the kerogen sample (up to 0.25 g in the test tube) was first swollen to equilibrium in one solvent. The complete earlier described procedure for swelling in single solvents was followed (for details see [13]). Then, in a second stage, a different solvent was added in the amount needed to obtain the desired final solvent mixture composition. The following two different types of experiments were carried out at this second stage.

In the first, a large excess of the second solvent was added so that after the second stage both solvents were in considerable excess relative to the pure component swelling-related solvent uptake by the kerogen. For this, the solvent above the swollen kerogen sample, swollen to equilibrium in the first solvent, was removed from the tube with a syringe. The amount of solvent left in the swollen sample (between and inside the kerogen particles) was measured gravimetrically. After adding the second solvent the system was mixed well, centrifuged and allowed to swell to a new equilibrium state. The final height of the sample was then measured after allowing 48 hours of swelling in the solvent (for results see section 3.1). Due to experimental limitations (mainly the test tube volume limitation) these experiments were conducted only in the concentration range of about 20 mol% to 80 mol% of the second solvent.

In the second type of experiment, only a drop of the second solvent was added to the test tube after the first stage (using an automated pipet). The system was then mixed and centrifuged, and the swelling equilibrium was measured after 48 hours. Then the sequence was repeated until the second solvent concentration reached just slightly less than 5 mol% second solvent, on the basis of total solvents added to the system (for results see section 3.2).

The volumetric swelling was characterized by the usual experimental volumetric swelling extent parameter, the volumetric ratio Q_{exp} , defined as the final swollen volume (or swollen bed height after the second swelling step) divided by the initial un-swollen volume (or initial dry bed height) (see [13]). The accuracy of Q_{exp} for the two-step procedure used in this study was ± 0.03 .

The calculation of Q_{exp} from experimental data was based on a commonly accepted assumption of a constant void volume fraction i.e. the void volume fraction in the swollen sample was expected to be equal to that of initial dry sample. Our latest study on swelling in single solvents suggested that centrifugation caused the swollen sample to be packed more tightly and the actual or true swelling ratio was higher than the measured one by the test-tube method [22]. The study also indicated that the extent of compaction depended mostly on the amount of solvent absorbed by the kerogen, and the relationship between the actual swelling ratio and the difference (ΔQ) followed approximately an exponential trend. Therefore, the following empirical corrective equation is derived from the data of reference [22]: $Q_{cor} - Q_{exp} = 0.0011 \cdot e^{3.1021 \cdot Q_{cor}}$. The Q_{cor} stands for a corrected, or actual, swelling ratio. In order to get the most reliable fit suitable for the present study, the constants in the equation were obtained by forcing the exponential fit curve to go specifically through the data-points for benzene and NMP. Due to the considerable scope of error, the Q_{cor} values are shown mainly as an illustration of the consequence of sample compression during centrifugation.

3. Results and discussion

In previous studies [21-23] on Kukersite oil shale kerogen swelling in single solvents it was observed that the maximum swelling occurred in high electron donor number (EDN) solvents such as propylamine and 1-methyl-2-pyrrolidinone (NMP). The molar solvent uptake by Kukersite kerogen is shown in Figure 1 as a function of the EDN of solvents used in this study. The value of solvent molar uptake was calculated from Q_{exp} as $(Q_{exp} - 1)/V_M$, where V_M is the solvent molar volume (for values see Table 1). The figure shows the same general trend observed previously for Kukersite oil shale swelling in 22 pure solvents [21] and emphasizes that high EDN solvents are effective in breaking kerogen-kerogen non-covalent bond interactions (such as hydrogen bonds), resulting in maximum swellability. It also shows that there is a limiting molar uptake of high EDN solvents by the kerogen macromolecular structure (see [24]).

3.1. Swelling in binary mixtures over the whole concentration range

Figures 2 to 4 compare the results from the two-stage swelling experiments with the results obtained from the earlier reported binary mixture experiments involving direct single step exposure to pre-prepared binary solvent mixtures (for details see [13]). Open points correspond to experimental Q values (noted as Q_{exp}) measured using the test-tube method and, for illustrative purposes, the solid points show corrected Q values as discussed above (noted as Q_{cor}). Three solvent mixtures (benzene and n-propanol; benzene and NMP; n-propanol and NMP) were selected here because these result in

different kerogen swelling behaviors in pre-prepared mixtures, as seen and interpreted in our previous paper [13]. The following is a brief summary of interpretations given in that study [13]: in the case of the pre-prepared benzene–NMP mixture, a small amount of high EDN solvent NMP (less than 10 mol% of NMP) increases swelling to approximately the level of pure NMP due to the NMP's ability to reduce apparent cross-link density involving dissociating kerogen–kerogen non-covalent cross-links (i.e. hydrogen bonds); in the case of the pre-prepared benzene–propanol mixture, the swelling behavior can be explained as an interplay between the ability of the weaker (than NMP) donor n-propanol to disrupt kerogen–kerogen non-covalent cross-links and a mixture solubility parameter mismatch (according to classic thermodynamic swelling theories, the maximum swelling occurs when values of the solubility parameters of the macromolecule and of the solvent mixture do match); in the case of propanol–NMP mixture, the swelling behavior is believed to be influenced by the ability of n-propanol to act in the role of an electron acceptor (EAN=37.7; EDN=19.8) relative to the strong electron donor solvent NMP in the mixture. Again, the pre-prepared mixture swelling experiments were done by the method previously described [13], whereas in the two-stage swelling procedure of interest of this study, the swelling was performed first in one solvent followed by addition of a desired amount of a second solvent achieving a desired solvent mixture composition in the swelling tube. For the two-stage swelling, in the case of benzene–n-propanol and benzene–NMP mixtures, benzene was the first solvent added to the tube, and in the case of the n-propanol–NMP mixtures, the n-propanol was the first added solvent.

Figures 2 to 4 show similarities in the trends in the results from both types of experiments: for the same solvent pairs the kerogen's swelling behavior follows quite similar trends as a function of solvent composition (composition based on solvents added to the test tube). Also, the maximum extent of swelling is comparable, regardless of how the experiments are conducted, though the absolute values are often clearly different from the two types of experiments. Although the differences seen are modest in extent (keeping in mind the ± 0.03 deviation for two-step swelling and ± 0.02 for pre-prepared mixture swelling), these results might still be significant in terms of signaling a possible path dependence of the swelling process. For example, Figure 2 shows that when the n-propanol is added after the kerogen has first been swollen in benzene, low concentrations (<40%) of n-propanol are not particularly effective in increasing the swelling to values above those for benzene by itself, while above 50 mol% equivalent in the final mixture of the sequential experiment, the swelling is always comparable to that from the experiment in which the two solvents are added at the same time. This could reflect the fact that the n-propanol cannot be readily absorbed by the benzene-swollen kerogen matrix, until the chemical potential of the propanol exceeds a critical value. There is a large solubility parameter mismatch between these two solvents (see Table 1), though they are miscible. The observed behavior, in which the kerogen is more effectively swollen by an equimolar solvent mixture than in the sequential exposure experiments, mirrors other results obtained by swelling coal with methylnaphthalene (a non-specifically interacting solvent, like benzene) and methanol (a specifically interacting solvent, like n-propanol). In these latter experiments, immediate exposure to the mixed solvent resulted in a higher asymptotic swelling than sequential exposure, regardless of which solvent was used for the initial swelling [25]. Such path-dependent swelling behavior is not unique to the cross-linked organic matter of fossil fuels. Such hysteresis-like behavior has been observed in the swelling of cross-linked polystyrene resins in binary solvents [26]. It should be kept in mind that we believe that the results shown in Figure 2 are not kinetically determined, in that enough time has been allowed for the system to reach apparent equilibrium.

On the other hand, it is important to note, that due to kerogen's capabilities to selectively uptake solvent from the solvent mixture [13], it cannot be unequivocally claimed that the solvent compositions shown in Figures 2 to 4 for the two different experiments are identical, insofar as the actual liquid concentrations were not measured here. For example, in one preliminary experiment we determined directly the change in solvent concentration during kukersite swelling in pre-prepared binary mixtures of propanol:benzene (at 10:90) by gas chromatography. The experiment showed that the solvent mixture concentration above the swollen kukersite changed by about 2% (from 10:90 of propanol:benzene to 8:92), indicating that estimated solvent composition contained within the swollen network was about 20:80, thereby confirming existence of selective uptake, even in the case of solvents with weaker donor strength such as propanol (EDN=19.8). Thus it is likely that some of differences between the two different types of experiments in Figures 2 through 4 are attributable to differences in uptake of the two components, despite plotting of the points from the two different experiments at the same nominal concentrations. Still, the similarity of the trends with composition are so striking that it is unlikely that differences in amounts of uptake in the two experiments can explain the observed absolute differences.

3.2. Drop based swelling experiments

Figure 5 presents the results of experiments in which the second solvent was added by sequential drops to a pre-swollen sample. These experiments are similar to those performed by Larsen et al. on coals [27]. Like the coal studies, Figure 5 shows swelling ratio profiles where the swelling ratio data are plotted as a function of millimoles of second solvent added per gram of dry kerogen. The non-polar (non-specifically interacting) solvent toluene was chosen as the base solvent, i.e., as the solvent for the first swelling stage. Two different strong EDN solvents, NMP (EDN = 27.3) and propylamine (EDN = 55.5), were used as swelling-promoting solvents in the second stage. While in the first series of experiments described in the previous section, following the second swelling stage both solvents were in excess relative to their kerogen uptake capacities, then here the second solvent, that added dropwise, can be in deficit relative to the capability of the kerogen to imbibe it.

The two experimental swelling ratio profiles (open squares for NMP and open circles for propylamine as the second solvent) in Figure 5 show similar trends to each other and also qualitatively similar trends to that described by Larsen et al. [27] for coals – addition of small amounts of high EDN solvents can result in increased swelling of a network that was previously in equilibrium with respect to a non-specifically interacting solvent. In the earlier coal studies, this increase of the swelling ratio upon addition of high EDN solvent was explained by the solvent's ability to act as a hydrogen bond (or other strong electron donor-acceptor) breaker. This led to reducing macromolecule–macromolecule physical interactions, reducing effective network cross-links, and rendering the structure more elastic. In this way, the entropic favorability of solvent imbibition manifests itself, as there is no longer as large an enthalpic penalty for swelling the network structure by greater solvent uptake. The same phenomenon is likely responsible in the system in this study.

Moreover, in the earlier coal studies it was also determined, by gas-chromatographic measurements, that all the added high EDN solvent was completely absorbed into the coal macromolecular swollen structure, up to some specific limiting concentration (measured in millimole of high EDN solvent per gram of coal), with the specific concentration depending on the coal used. Assuming that the complete absorption of high EDN solvent can occur also in kukersite kerogen swelling, then the lines in Figure 5 correspond to

“hypothetical swelling increase” that could be caused only by absorption of all drop-wise added strong electron donor solvent (NMP solid line, propylamine dashed line). It can be seen from Figure 5 that initially (below 1 mmol of solvent added per gram of kerogen) the increase in swelling ratio (Q_{exp}) is clearly larger than could be accounted for by uptake of the swelling promoting solvent alone. Again, the open points (Q_{exp}) are the experimentally measured values, and the corresponding lines correspond to a system where no compaction occurs during swollen sample centrifugation. Therefore, for illustrative purposes, the corrected swelling ratios for NMP as a second solvent are also shown as solid points in Figure 5. This comparison illustrates the consequence of the greater elasticity of the swollen network right away at the smallest amounts of added second solvent, as it is network elasticity that also results in greater compaction.

4. Conclusions

The observation that significant extents of swelling of Kukersite kerogen macromolecular organic matter is achievable only in the presence of strong electron donor number (EDN) solvents, which are able to disrupt kerogen–kerogen specific interactions (such as hydrogen bonds), is supported by the results of this investigation.

Small amounts of specifically interacting high EDN solvents, such as NMP and propylamine, can act as promoters for increased swelling when added to pre-swollen samples in the non-polar (non-specifically interacting) solvent such as toluene. This is consistent with observations from earlier studies on coal macromolecular networks.

Over the whole concentration range, regardless of how the binary mixture based solvent swelling experiments were conducted (using pre-prepared mixtures or the two-step swelling procedure), the swelling behavior and the maximum extents of swelling obtained were comparable. In terms of maximizing the swelling, the binary solvent mixtures did not perform any better than pure strong electron donor solvents (such as NMP or propylamine).

Acknowledgement

The authors gratefully acknowledge financial support provided by the Estonian Minister of Education and Research, under target financing SF0140022s10, and by the graduate school „Functional materials and technologies“, which received funding from the European Social Fund under project 1.2.0401.09-0079 in Estonia.

REFERENCES

1. Flory, P. J. *Principles of polymer chemistry*. Cornell University Press, New York, 1953.
2. Kovac, J. Modified Gaussian Model for Rubber Elasticity. *Macromolecules*, 1978, **11**(2), 362–365.
3. Barr-Howell, B. D., Peppas, N. A. Importance of junction functionality in highly crosslinked polymers. *Polymer Bulletin*, 1985, **13**(2), 91–96.
4. Larsen, J. W., Li, S. Solvent swelling studies of Green River kerogen. *Energy Fuels*, 1994, **8**(4), 932–936.
5. Ballice, L. Solvent swelling studies of Göynük (Kerogen Type-I) and Beypazari oil shales (Kerogen Type-II). *Fuel*, 2003, **82**(11), 1317–1321.
6. Kilk, K., Savest, N., Hruljova, J., Tearo, E., Kamenev, S., Oja, V. Solvent Swelling of Dictyonema Oil Shale. *Oil Shale*, 2010, **27**(1), 26–36.

7. Oja, V., Suuberg, E. M. Oil shale processing, chemistry and technology. In: *Fossil Energy, Selected Entries from the Encyclopedia of Sustainability Science and Technology* (Malhotra, R.). Springer Science+Business Media, New York, 2013, 99–148.
8. Oja, V. Characterization of tars from Estonian kukersite oil shale based on their volatility. *J. Anal. Appl. Pyrolysis*, 2005, **74**(1–2), 55–60.
9. Oja, V., Elenurm, A., Rohtla, I., Tali, E., Tearo, E., Yanchilin, A. Comparison of oil shales from different deposits: Oil shale pyrolysis and co-pyrolysis with ash. *Oil Shale*, 2007, **24**(2), 101–108.
10. Urov, K., Sumberg, A. Characteristic of oil shales and shale-like rocks of known deposits and outcrops. *Oil Shale*, 1999, **16**(3 special: monograph), 1–64.
11. Kelemen, S. R., Afeworki, M., Gorbaty, M. L., Sansone, M., Kwiatek, P. J., Walters, C. C., Freund, H., Siskin, M., Bence, A. E., Curry, D. J., Solum, M., Pugmire, R. J., Vandenbroucke, M., Leblond, M., Behar, F. Direct characterization of kerogen by X-ray and solid-state ¹³C nuclear magnetic resonance methods. *Energy Fuels*, 2007, **21**(3), 1548–1561.
12. Koel, M., Ljovin, S., Hollis, K., Rubin, J. Using neoteric solvents in oil shale studies. *Pure Appl. Chem.*, 2001, **73**(1), 153–159.
13. Hruljova, J., Savest, N., Oja, V., Suuberg, E. M. Kukersite oil shale kerogen solvent swelling in binary mixtures. *Fuel*, 2013, **105**, 77–82.
14. Koch, P. R., Kirret, O. G., Oamer, P. E., Ahelik, V. P., Kõrts, A. V. Studies on the flotation process of Estonian kukersite. In: *All-union conference on the beneficiation of oil shales*. Academy of Sciences USSR, Moscow, 1973, 115–122 (in Russian).
15. Karger, B. L., Snyder, L. R., Eon, C. An expanded solubility parameter treatment for classification and use of chromatographic solvents and adsorbents. Parameters for dispersion, dipole and hydrogen bonding interactions. *J. Chromatogr. A*, 1976, **125**(1), 71–88.
16. Belmares, M., Blanco, M., Goddard, W. A., Ross, R. B., Caldwell, G., Chou, S. H., Pham, J., Olofson, P. M., Thomas, C. Hildebrand and Hansen solubility parameters from molecular dynamics with applications to electronic nose polymer sensors. *J. Comput. Chem.*, 2004, **25**(15), 1814–1826.
17. Behbehani, G. R., Hamed, M., Rajabi, F. H. The solvation of urea, tetramethylurea, TMU, in some organic solvents. *The Internet Journal of Vibrational Spectroscopy*, 2001, **5**(6) [<http://www.ijvs.com/volume5/edition6/section3.html>].
18. Malavolta, L., Oliveira, E., Cilli, E. M., Nakaie, C. R. Solvation of polymers as model for solvent effect investigation: proposition of a novel polarity scale. *Tetrahedron*, 2002, **58**(22), 4383–4394.
19. Hansen, C. M. *Hansen Solubility Parameters: a User's Handbook*. CRC Press, 2000.
20. Mayer, U., Gutmann, V., Gerger, W. The acceptor number - A quantitative empirical parameter for the electrophilic properties of solvents. *Monatshefte Für Chemie*, 1975, **106**(6), 1235–1257.
21. Savest, N., Hruljova, J., Oja, V. Characterization of thermally pretreated kukersite oil shale using the solvent-swelling technique. *Energy Fuels*, 2009, **23**(12), 5972–5977.
22. Hruljova, J., Järvi, O., Oja, V. Application of differential scanning calorimetry to study solvent swelling of kukersite oil shale macromolecular organic matter: A

- comparison with the fine-grained sample volumetric swelling method. *Energy Fuels*, 2014, xxx, xxx-xxx. DOI: 10.1021/ef401895u
23. Savest, N., Oja, V., Kaevand, T., Lille, Ü. Interaction of Estonian kukersite with organic solvents: A volumetric swelling and molecular simulation study. *Fuel*, 2007, **86**(1-2), 17–21.
 24. Suuberg, E. M., Otake, Y., Langer, M. J., Leung, K. T., Milosavljevic, I. Coal macromolecular network structure analysis: solvent swelling thermodynamics and its implications. *Energy Fuels*, 1994, **8**(6), 1247–1262.
 25. Yun, Y., Suuberg, E. M. Cooperative effects in solvent swelling of a bituminous coal. *Energy Fuels*, 1998, **12**(4), 798–800.
 26. O'Kane, J. M., Sherrington, D. C. Hysteresis-like behavior in the swelling/deswelling of polystyrene cross-linked resins using binary solvent mixtures. *Macromolecules*, 1990, **23**(25), 5286–5291.
 27. Larsen, J. W., Gurevich, I., Glass, A. S., Stevenson, D. S. A method for counting the hydrogen-bond cross-links in coal. *Energy Fuels*, 1996, **10**(6), 1269–1272.

Table 1. Properties of the solvents used

Solvent	Solubility parameter δ , MPa ^{1/2}	EDN	EAN	Molar volume V_M , cm ³ /mol
Propylamine	18.2	55.5 ^a	4.8 ^a	83.0
NMP ^b	23.1	27.3	13.3	96.5
n-Propanol	24.5	19.8	37.7	75.2
Benzene	18.8	0.1	8.2	89.4
Toluene	18.2	0.1	3.3	106.8

^a Ethylamine EDN and EAN values were used for propylamine.

^b NMP stands for 1-methyl-2-pyrrolidinone.

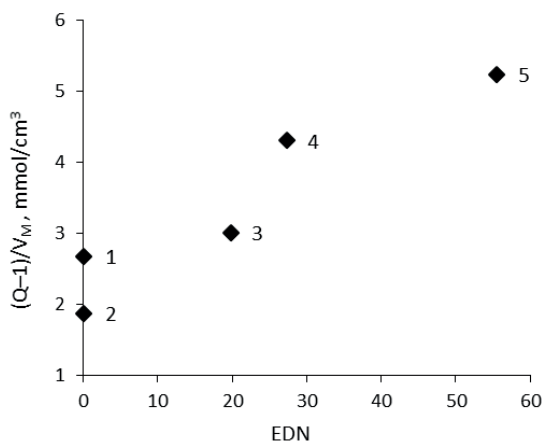


Fig. 1. Variation of solvent molar uptakes with Gutmann's electron donor number (EDN). (1) benzene; (2) toluene; (3) n-propanol; (4) NMP; (5) propylamine (EDN value in this case is taken to be the same as that for ethylamine). The parameter V_M is solvent molar volume, as given in Table 1.

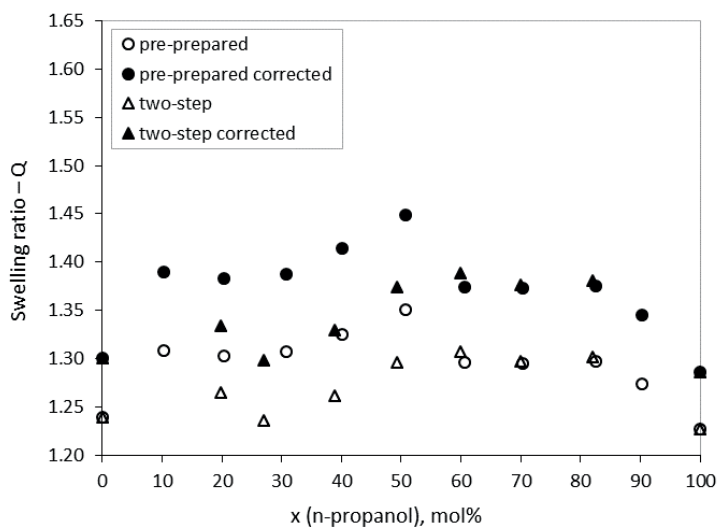


Fig. 2. Kukersite kerogen swelling in benzene and n-propanol mixtures. The open triangles correspond to results from the two-step swelling experiments with benzene as the first solvent. The open circles are for the comparative pre-prepared solvent mixture experiments. The solid points are corrected values for illustrative purposes.

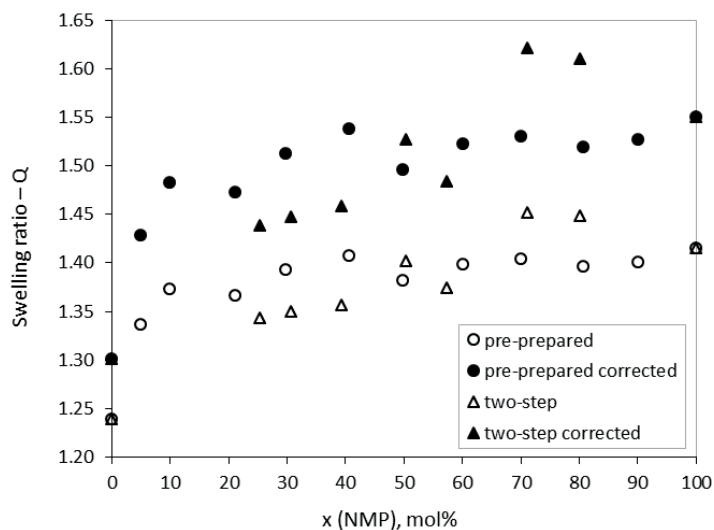


Fig. 3. Kukersite kerogen swelling in benzene and NMP mixtures. The open triangles correspond to the results from the two-step swelling experiments with benzene as the first solvent. The open circles are for the comparative pre-prepared solvent mixture experiments. The solid points are corrected values for illustrative purposes.

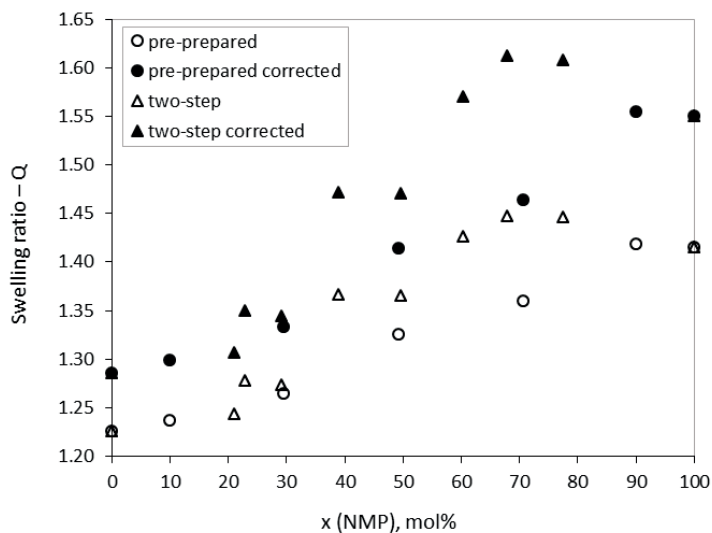


Fig. 4. Kukersite kerogen swelling in n-propanol and NMP mixtures. The open triangles correspond to the results of the two-step swelling experiments with n-propanol as the first solvent. The open circles are for the comparative pre-prepared solvent mixture experiments. The solid points are corrected values for illustrative purposes.

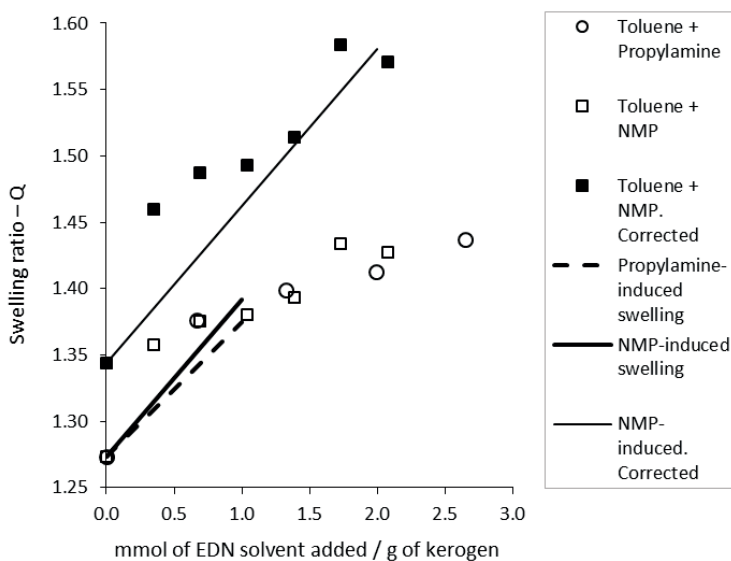


Fig. 5. Impact of small amounts of swelling promoting solvents on swelling of Kukersite kerogen pre-swollen in toluene. Lines indicate “hypothetical swelling increase” when only all dropwise added strong electron donor solvent (EDN solvent) is absorbed into kerogen structure and causes the extended swelling.

APPENDIX B
CURRICULUM VITAE

Elulookirjeldus

1. Isikuandmed

Ees- ja perekonnanimi Jelena Hruljova
Sünniaeg ja -koht 2. juuli 1986, Tallinn
Kodakondsus Eesti
E-posti aadress jelena.hruljova@ttu.ee

2. Hariduskäik

Õppeasutus (nimetus lõpetamise ajal)	Lõpetamise aeg	Haridus (eriala/kraad)
Tallinna Tehnikaülikool	2009	Keemia- ja keskkonnakaitse tehnoloogia eriala. Tehnikateaduse magistri kraad (<i>cum laude</i>)
Tallinna Tehnikaülikool	2007	Keemia- ja keskkonnakaitse tehnoloogia eriala. Tehnikateaduse bakalaureuse kraad (<i>cum laude</i>)
Tallinna Tõnismäe Reaalkool	2004	Keskharidus (hõbemedal)

3. Keelteoskus (alg-, kesk- või kõrgtase)

Keel	Tase
Vene keel	Kõrgtase (emakeel)
Eesti keel	Kõrgtase
Inglise keel	Keskstase

4. Täiendusõpe

Õppimise aeg	Täiendusõppe korraldaja nimetus
juuni 2013	Kreeka termoanalüüsi selts. Termoanalüüsi suvekool.
2010–2014	Tallinna Tehnikaülikool. Sisekoolitused.
2009–2014	TÜ ja TTÜ Doktorikool “Funktsionaalsed materjalid ja tehnoloogiad”.

5. Teenistuskäik

Töötamise aeg	Tööandja nimetus	Ametikoht
2009–...	Keemiatehnika instituut, Tallinna Tehnikaülikool	Assistent
2008–2009	Keemiatehnika instituut, Tallinna Tehnikaülikool	Insener

6. Teadustegevus

Kaitstud lõputöö: Põlevkivide pundumine lahustites: võrdlev uuring. Tehnikateaduse magistri kraad, 2009. Juhendaja prof Vahur Oja.

Teadustöö põhisuunad: Loodusteadused ja tehnika, Keemia ja keemiatehnika.

Osalus uurimisprojektides:

ETF9297. Hapnikurikaste vesiniksidemeid moodustavate ühendite ja nende komplekssete segude aurustumisparameetrid.

SF0140022s10. Keemiatehnilised aspektid keskkonnariskide hindamisel.

SF0142628s04. Kütused ja kütuse komponendid, nende termodünaamilis-füüsikalised omadused.

ETF7222. Termilise lagunemisega kaasnevate Eesti põlevkivi struktuuri ja soojusfüüsikaliste omaduste muutumiste uurimine.

Curriculum Vitae

1. Personal data

Name Jelena Hruljova
Date and place of birth 2nd July 1986, Tallinn
E-mail address jelena.hruljova@ttu.ee

2. Education

Educational institution	Graduation year	Education (field of study/degree)
Tallinn University of Technology	2009	Chemical and Environmental Technology. Master of Science in Engineering (cum laude)
Tallinn University of Technology	2007	Chemical and Environmental Technology. Bachelor of Science in Engineering (cum laude)
Tallinn Tõnismäe Science School	2004	High school education (silver medal)

3. Language competence/skills (fluent, average, basic skills)

Language	Level
Russian	Fluent
Estonian	Fluent
English	Average

4. Special courses

Period	Educational or other organisation
June 2013	Hellenic Society for Thermal Analysis. Summer Training School on Thermal Analysis.
2010–2014	Tallinn University of Technology. Special courses.
2009–2014	Graduate School „Functional Materials and Technologies“

5. Professional employment

Period	Organisation	Position
2009–...	Department of Chemical Engineering, Tallinn University of Technology	Teaching Assistant
2008–2009	Department of Chemical Engineering, Tallinn University of Technology	Engineer

6. Research activity

Defended thesis: Comparative study of oil shale solvent swelling. Master's Degree, 2009. Supervisor prof Vahur Oja.

Main field of research: Natural Sciences and Engineering, Chemistry and Chemical Technology

Participation in research projects:

ETF9297. Vaporization properties of heavier multi-functional oxygen-containing organic compounds with hydrogen bond capabilities and their ill-defined mixtures.

SF0140022s10. Chemical Engineering Aspects in Environmental Risk Assessment.

SF0142628s04. Thermodynamic and transport properties of fuels and fuel components.

ETF7222. Investigation of thermally induced changes in structure and thermal properties of Estonian oil-shales.

**DISSERTATIONS DEFENDED AT
TALLINN UNIVERSITY OF TECHNOLOGY ON
*CHEMISTRY AND CHEMICAL ENGINEERING***

1. **Endel Piiraja**. Oxidation and Destruction of Polyethylene. 1993.
2. **Meili Rei**. Lihatehnoloogia teaduslikud alused. Fundamentals of Food Technology. 1995.
3. **Meeme Põldme**. Phase Transformations in Hydrothermal Sintering Processing of Phosphate Rock. 1995.
4. **Kaia Tõnsuaadu**. Thermophosphates from Kovdor and Siilinjärvi Apatites. 1995.
5. **Anu Hamburg**. The Influence of Food Processing and Storage on the N-Nitrosamines Formation and Content in Some Estonian Foodstuffs. 1995.
6. **Ruth Kuldvee**. Computerized Sampling in Ion Chromatography and in Capillary Electrophoresis. 1999.
7. **Külliki Varvas**. Enzymatic Oxidation of Arachidonic Acid in the Coral *Gersemia fruticosa*. 1999.
8. **Marina Kudrjašova**. Application of Factor Analysis to Thermochromatography and Promotion Studies. 2000.
9. **Viia Lepane**. Characterization of Aquatic Humic Substances by Size Exclusion Chromatography and Capillary Electrophoresis. 2001.
10. **Andres Triikkel**. Estonian Calcareous Rocks and Oil Shale Ash as Sorbents for SO₂. 2001.
11. **Marina Kritševskaja**. Photocatalytic Oxidation of Organic Pollutants in Aqueous and Gaseous Phases. 2003.
12. **Inna Kamenev**. Aerobic Bio-Oxidation with Ozonation in Recalcitrant Wastewater Treatment. 2003.
13. **Janek Reinik**. Methods for Purification of Xylidine-Polluted Water. 2003.
14. **Andres Krumme**. Crystallisation Behaviour of High Density Polyethylene Blends with Bimodal Molar Mass Distribution. 2003.
15. **Anna Goi**. Advanced Oxidation Processes for Water Purification and Soil Remediation. 2005.
16. **Pille Meier**. Influence of Aqueous Solutions of Organic Substances on Structure and Properties of Pinewood (*Pinus sylvestris*). 2007.

17. **Kristjan Kruusement.** Water Conversion of Oil Shales and Biomass. 2007.
18. **Niina Kulik.** The Application of Fenton-Based Processes for Wastewater and Soil Treatment. 2008.
19. **Raul Järviste.** The Study of the Changes of Diesel Fuel Properties a its Long Term Storage. 2008.
20. **Mai Uibu.** Abatement of CO₂ Emissions in Estonian Oil Shale-Based Power Production. 2008.
21. **Valeri Gorkunov.** Calcium-Aluminothermal Production of Niobium and Utilization of Wastes. 2008.
22. **Elina Portjanskaja.** Photocatalytic Oxidation of Natural Polymers in Aqueous Solutions. 2009.
23. **Karin Reinhold.** Workplace Assessment: Determination of Hazards Profile using a Flexible Risk Assessment Method. 2009.
24. **Natalja Savest.** Solvent Swelling of Estonian Oil Shales: Low Temperature Thermochemical Conversion Caused Changes in Swelling. 2010.
25. **Triin Märtson.** Methodology and Equipment for Optical Studies of Fast Crystallizing Polymers. 2010.
26. **Deniss Klauson.** Aqueous Photocatalytic Oxidation of Non-Biodegradable Pollutants. 2010.
27. **Oliver Järvik.** Intensification of Activated Sludge Process – the Impact of Ozone and Activated Carbon. 2011.
28. **Triinu Poltimäe.** Thermal Analysis of Crystallization Behaviour of Polyethylene Copolymers and Their Blends. 2011.
29. **Mariliis Sihtmäe.** (Eco)toxicological Information on REACH-Relevant Chemicals: Contribution of Alternative Methods to *in vivo* Approaches. 2011.
30. **Olga Velts.** Oil Shale Ash as a Source of Calcium for Calcium Carbonate: Process Feasibility, Mechanism and Modeling. 2011.
31. **Svetlana Jõks.** Gas-Phase Photocatalytic Oxidation of Organic Air Pollutants. 2012.
32. **Aleksandr Dulov.** Advanced Oxidation Processes for the Treatment of Water and Wastewater Contaminated with Refractory Organic Compounds. 2012.
33. **Aleksei Zaidentsal.** Investigation of Estonian Oil Shale Thermo-bituminization in Open and Closed System. 2012.
34. **Dmitri Šumigin.** Composites of Low-Density Polyethylene and Poly(Lactic Acid) With Cellulose and Its Derivatives. 2014.

35. **Aleksandr Käkinen**. The Role of Physico-chemical Properties and Test Environment on Biological Effects of Copper and Silver Nanoparticles. 2014.

36. **Ada Traumann**. Improvement of Work Environment through Modelling the Prevention of Health Risks Focusing on Indoor Pollutants. 2014.

37. **Marika Viisimaa**. Peroxygen Compounds and New Integrated Processes for Chlorinated Hydrocarbons Degradation in Contaminated Soil. 2014.

38. **Olga Budarnaja**. Visible-light-sensitive Photocatalysts for Oxidation of Organic Pollutants and Hydrogen Generation. 2014.

